BLOWN FLAP NOISE

by

Martin Haas

June 1972

FTL Report 72-5

MIT

DEPARTMENT
OF
AERONAUTICS
&
ASTRONAUTICS

FLIGHT TRANSPORTATION
LABORATORY
Cambridge, Mass. 02139

MASSACHUSETTS INSTITUTE OF TECHNOLOGY

Flight Transportation Laboratory

Blown Flap Noise

by

Martin Haas

Report FTL 72-5

June 1972

BLOWN FLAP NOISE

ABSTRACT

This report is concerned with the noise generated by blown flaps of the type currently being developed for the short take off and landing aircraft. The majority of the report is an experimental study of the sound-radiation produced by a small scale externally blown double-slotted flap model. Tests were carried out with and without a forward velocity of 60 MPH for a basic engine-wing configuration and for a modified (Engine moved inboard) configuration. Noise radiation patterns and sound pressure level spectra were obtained for nozzle exhaust velocities between 100 and 500 ft/sec. In addition all model data was extrapolated to five fictional full scale STOL aircrafts.

The noise generated by the impingement of the jet on the externally blown flap is highly dependent on the jet velocity and the flap position. As the flap angle is increased the noise generated increases. At the 45° - 70° flap position the noise is more than 25db over that caused by the model jet alone. It is especially louder below the wing. The sound power level generated by the externally blown flap (at all positions) increased with the sixth power of the jet's blowing velocity. As the nozzle jet velocity is increased, the sound power level of the noise from the nozzle alone generally increased with the expected eighth power of the jet velocity. Therefore, the difference between the impingement noise and the noise of the nozzle alone decreased with increasing velocity. The noise radiation pattern becomes more directed below the wing as the flaps are lowered. The effect of forward velocity on the noise generated was neglible for a ratio of jet to forward velocity greater than 4.5. Results on tests made on the modified engine-wing configurations were similar to that of the basic configuration except for a slight reduction in overall sound pressure level (2 to 4 db) over all positions measured. An extrapolation to full scale indicated that the externally blown flap noise must be suppressed to meet STOL aircraft noise goals.

This work was performed under Contract DOT-TSC-93, DSR No. 73770, from the Transportation Systems Center, Department of Transportation, Cambridge, Massachusetts.

TABLE OF CONTENTS

LIST OF ILLUSTRATIONS

SYMBOLS

Sh	Strouhal number
f	Frequency (Hertz)
D	Reference length (usually nozzle diameter), ft.
V	Jet exhaust or blowing velocity (ft./sec.)
U	Tunnel speed (mph)
P_A	Acoustic radiated power (Watts)
PWL	Total sound power level (10 $\log_{10}$ $P_A/10^{-13}$ Watts)
R	Source-Microphone distance (ft)
P	Sound pressure (dyne/cm^2)
I	Sound intensity (Watts/cm^2)
SPL	Sound pressure level (10 $\log_{10}$ P/0.0002 microbar)
OASPL	Overall sound pressure level
θ	Angle relative to the jet axis in the horizontal plane (degree).
ϕ	Azimuthal angle (degree)
ρ	Atmospheric density (lb-sec^2/ft^4)
c	Sound speed (ft/sec)
	Subscripts
T	Total or overall
B	Background

CHAPTER I

INTRODUCTION

To achieve the requirement of taking off and landing on very short runways the STOL vehicle must have some form of lift augmentation. Three lift augmentation devices currently being studied are the augmentor wing ejector-flap, the internally blown flap and the externally blown flap (figure 1). The requirement of additional power for lift along with the fact that the STOL aircraft are to be designed to take off and land near heavily populated areas produce a serious noise annoyance problem. Noise reduction techniques must therefore be developed for the STOL aircraft in order that the noise they generate during take off and landing stay below acceptable limits. The noise restriction goal of a maximum perceived noise level of 95 PNdb at a 500 foot sideline has been set for the development of the STOL aircraft.

Both the augmentor wing ejector flap and the internally blown flap (commonly called a jet flap) are blown by air jets, from slot nozzles supplied by ducts located within the wing which inturn are supplied by a high by-pass engine. On the otherhand, the externally blown flap is immersed directly into the engine exhaust of the high by-pass engine, where the engine exhaust jet is deflected downward by the trailing edge flaps. The impingement and turning of the engine exhaust jet by the flap results in additional noise radiated by the aircraft. This additional noise may become the dominant noise source if a quiet engine is employed.

One high by-pass engine which is being considered for use in conjunction with these lift augmentation devices has been christen, Q-Fan standing for quiet turbofan engine (6). This engine is expected to produce twice the take off thrust per horse power of the present day turbofan engines and maintains its performance advantage at the partially throttled cruise condition. The

engine has very low fan pressure ratios (1.1 - 1.2) which means low fan and core exit velocities (400 - 500 feet/sec.) minimizing flap impingement and jet noise. For this reason the Q-Fan with its large mass flow and low efflux velocity seems to be particularly well suited to power the externally -- blown flap. The spreading tendency of the large fan flow provides greater spanwise immersion of the flaps for maximum lifting effectiveness during takeoff and landing while the lower fan and core velocities mean less interaction noise from the jet stream impinging on the deflected flaps.

The noise source from the blown flaps can be split into two categories. The first is produced by the nozzle jet wake. This noise is the result of free turbulence produced in the mixing region of the jet exhaust which can be modelled as an acoustic guadrupole. When aerodynamic scaling is used to predict the strength and frequency of the acoustic sources within the jet the noise generated is shown to increase in intensity according to the eight power of the exhaust velocity. This was originally derived by Lighthill (1) and is well confirmed experimentally both for real and model jet flows where the upstream flow is clean and the exit velocity is in the high subsonic range. The second noise source from the blown flap comes from the direct interaction of the jet turbulence with the solid flaps. The impinging jet turbulence produces fluctuating forces on the flap. Curle's extension of Lighthills arguments (2) suggest that fluctuating forces on solid boundaries can be modelled as acoustic dipoles. Such noise sources increase in intensity with the sixth power of the exhaust jet velocity. This agrees with the previous experimental work done on externally blown flaps (3), (4), (5). Since the jet-flap interaction noise intensity level goes like the sixth power of the velocity while the pure jet noise goes like the eight power of the velocity it can be concluded that the jet-flap interaction noise source will dominate the system.

In Curle's paper (2) a dimensional analysis was done which showed that the intensity of the sound generated by the dipoles should at large distance, R be of the general form:

$$1.1 \qquad I \alpha \rho V^6 c^{-3} L^2 R^{-2}$$

where V is the typical velocity of the flow which in this case is the mean jet velocity and L is a typical length of the body. L^2 would then represent a typical area. The magnitude of the sound pressure level is then proportional to an area, the jet velocity, and the inverse square of the distance. It has also been shown experimentally that the frequency of the noise spectrum and the jet velocity could be scaled by the Strouhal relationship.

$$1.2 \qquad Sh = fD/v$$

On the basis of these two arguments a scaling procedure was constructed by Robert Drosh, Eugene Krejsa, and William Olsen (3) to extrapolate laboratory data to geometrically similar full size configurations. This scaling procedure which was also used here can be summarized as follows; Model nozzle, nozzle location, and wing and flap dimensions were linearly scaled up to conform to the full scale nozzle exhaust area required at each exhaust velocity in order to obtain the specified engine thrust. The noise data measured at a given jet exhaust velocity and microphone position was then extrapolated by using the fact that the frequency of the 1/3 octave band spectrum could be scaled by the Strouhal reciprocal relationship between frequency and nozzle diameter. The magnitude of the sound pressure level at each frequency is then proportional to the nozzle area, the number of engines, and the inverse square of the distance. For sideline estimates the magnitude of the sound pressure level was adjusted to the azimuthal angle. The SPL being an experimentally know function of azimuthal angle. The preceived

noise level was then calculated from the resultant 1/3 octave spectra in the usual manner.

The investigation undertaken here is an extension of the blown flap noise research conducted at the NASA Lewis Research Center (3), (4). Far field noise data from a small scale externally blown flap for four flap position, and two engine - wing configurations are presented for nozzle exhaust velocities from 100 to 500 feet per second. All test configurations were made with and without a forward velocity of 60 mph and a comparison between the two are made. However, due to high tunnel background noise forward speed noise measurements were limited to a jet velocity to flight speed ratio of 4.5. Most noise measurements were taken at an azimuthal angle of 50.5°. In order to see the difference in the order of magnitude these measurements had from that in the horizontal plane azimuthal variation of noise about the nozzle centerline were also taken. Lift measurements were made for each model configuration and a correlation was made between the lift produced on a wing and the sound radiated by the wing.

The model data was then extrapolated using the established scaling laws to predict the noise for five different STOL aircraft having gross weights from 62,500 lbs (50 passengers) to 187,500 lbs (150 passengers). Computer programs were written to extrapolate the data and give flyover and sideline perceived noise level at 500 feet for the full scale aircraft as a function of the jet exhaust velocity. The input to the programs were the thrust need to accomplish a maneuver which is a function of the gross weight, wing loading and maneuver lengths (i.e. landing and takeoff field lengths.), the relevant dimensions of the model and the sound pressure level spectra of the model at the various jet exhaust velocities. For the extrapolations used here a field length of from 1,000 to 1,500 feet and a wing loading between 70 lb/ft^2 to 100 lb/ft^2 was assumed.

As part of the National Aeronautics and Space Administration's aeronautical research program at the Lewis Research Center, the noise generated by several STOL Lift-augmentation methods is being studied (3), (4), (5). All three types of blown flaps; augmentor-wing ejector - flap, conventional jet flap, and externally blown flap have been under acoustic investigation as reported in reference 3. The results of this report have shown that all three types exhibit similar trends in overall sound pressure levels. That is, the sound levels generally increase with an increase in nozzle size, nozzle pressure ratio (jet exhaust velocity) and flap deflection. At a given set of test parameters however, the relative magnitudes differ considerably for the three systems. Figure 2 taken from reference 3 is a plot of the overall sound pressure level as a function of the nozzle pressure ratio for the three lift augmentors, where the data has been normalized to the same nozzle area and jet turning or flap angle. A large variation in the overall sound pressure level for the different systems can be seen (about 15 db difference between the jet and externally blown flaps). This difference can be misleading since in practice the jet flap and augmentor wing must operate at higher nozzle pressure ratios than that of the externally blown flap to obtain the same lift. This tends to equalize the noise level radiated by a real aircraft using these lift augmentors at the same operating conditions. Noise radiation patterns show that all three types of blown flap assemblies redirect the noise source. The augmentor wing and the externally blown flap being the most serious since the noise is redirected downward while the jet flap redirects the noise upward and rearward. The noise spectra of the three systems were found to be broad band and could be scaled by the strouhal relationship;

$$1.2 \qquad Sh = fD/V$$

where the reference length, D, was taken to be the slot height or nozzle diameter depending on the system.

Reference (4) contains additional results on the investigation of the noise

generated by the small scale model of a double-slotted, externally blown flap used in reference 3. In addition to the test made in reference 3 several variations of the blown flap model were also tested. The jet was blown against a slotless metal wing and against a very large, flat board. Comparison of the noise radiation patterns with the basic configuration suggests that the noise is generated by jet impingement on the curved surfaces and by the jet wake leaving the wing. The frequency distributions of the noise generated by the model wing and the two variations were similar. Noise data was also taken for another group of variations which involved changes in the nozzle position relative to the wing and flap. All of these tests were made with a jet exit velocity of 950 feet per second and showed an increase in noise level which was probably due to the increase in impingement velocity.

In reference 5 noise tests were conducted with a large 1/2 scale externally blown flap model. The results are compared with the earlier small scale data in reference 3 and 4, and the validity of the scaling laws were established.

Hamilton Standard in cooperation with NASA Langley Research Center have been studying Prop-Fan-Externally Blown Flap configurations (7). Tests conducted extend the results found by NASA Lewis to include fan noise.

CHAPTER II

TEST APPARATUS

In this chapter the model configuration, airflow facility and hardware used in the experiments are described.

A. Model Configuration

A cross sectional view of the externally blown flap model configuration tested is shown in figure 3 in its fully retracted position. The externally blown flap configuration is a small scale model of a double-slotted external flow jet flap based on two externally blown flap models developed by the NASA Langley Research Center. (8, 9) The airfoil shape is a small scale of the wing developed in reference 8. The vane was extracted from reference 9 and placed in the airfoil such that the vane-flap configuration would comprise about 30% of the wing's chord. The flap used in reference 8 was then scaled and extended to make a correct wing-vane-flap configuration. The model as a whole was linearly scaled in proportion to a 2-inch jet nozzle diameter which was assumed to represent a high by-pass (order of ten) engine. Coordinates for the wing, vane, and flap are given in Table I.

The airfoil had a chord length of 9.7 inches (flaps retracted) and a 2 foot span. It was made out of mahogany and covered entirely by adhesive (contact) paper for protection. Solid steel shafts were run through the model (figure 3). These shafts served a dual purpose; first they increased the strength of the model, second they provide a means for the mounting of the wing to its end plates. The end plates which prevent any spanwise flow over the model consisted of a pair of thin rectangular plywood plates 18 inches long by 10 inches wide. The location of the mounts on the end plates determined the relative position of the wing, vane, and flap. The use of different plates then provided a simple means of achieving the four flap positions. Figure 4 is a picture of the test set

up with the model at a 10° - 20° vane-flap angle. Figure 5 gives the relative position of the wing, vane and flap for the four flap positions tested; 45° - 70°, 30° - 55°, 10° - 20°, and 0° (retracted) positions. (the flap angle notation 30° - 55° refers to a leading flap vane angle of 30° and a trailing flap angle of 55° down from the mean chord line of the wing).

A detailed sketch of the wing-engine arrangement for the basic and modified configuration is shown in figure 6. The flaps were blown by an air jet issuing from a 2 inch diameter steel pipe having a straight length of fourteen feet which extended upstream into the low velocity section of the wind tunnel. This long straight section insured that the flow at the exit section would be well extablished pipe flow so that the jet alone would exhibit quadrupole noise.

B. Flow Measurement

The mean velocity of the air flow within the pipe was measured by a single pitot-static like arrangement placed 5 feet from the exit plane of the pipe. A small, 3/32 inch, tube was located parallel to the flow at the center of the pipe which read the stagnation pressure, while two statics (3/32 inch holes) were placed on the pipe itself to read the undistrubed pressure. The difference of these two pressures, the dynamic pressure, can be directly related to the velocity of the air in the pipe. This pitot-static system was connected to a mercury manometer calibrated to read out this velocity in miles per hour.

C. Wind Tunnel

The wind tunnel used to simulate a forward velocity on the externally blown flap model was a modified closed circuit open test section wind tunnel with the test section located inside an anechoic chamber. The chamber is constructed of panels made up of 22 gauge galvanized steel sheets with perforations

in the front sheet of 3/32 inch diameter holes on 5/32 inch staggered centers. The panels are constructed of 2 inch thick, specially treated and specially packed acoustic material. The chamber was constructed by Barry Controls. In addition the tunnel itself is acoustically treated with turning vanes covered by fiberglass material held in place by perforated steel sheets. The background noise of the tunnel run at full speed is shown in figure 7.

Test section dimensions are 4 1/2 feet by 7 feet with a distance of 8 feet between the exit plane of the entrance cone to the beginning of the diffuser. The tunnel is capable of a maximum velocity of 115 feet/sec. A pitot-static tube connected to an alcohol monometer which reads velocity directly was used to measure the tunnel's speed.

D. Air-Flow Equipment

A Nash Hytor Vacuum Pump-Compressor size H-7 was used to supply the air flow. The pump is a water sealed compressor pump with a constant angular velocity of 1185 revolutions per minute, driven by a 150 horsepower General Electric induction motor model 85E38G1. The compressor was capable of supplying 900 standard cubic feet of air per minute at a pressure of 30 psia. The air output from this pump is connected to a network of valves. By changing the position of these valves the amount of air going to the experimental jet system could be controled.

Since the pump was run with water as a seal excess water was carried over with the air. The result being that the air became saturated with water. In order to remove this water, the saturated air was passed through the Lectro Dryer. The Lectro Dryer manufactured by the Pittsburg Lectro Dryer Corporation is a dryer consisting of two large steel cylinders filled with concentric iron tubing surrounded with flakes of a deliquescent nature. The wet air was forced into one cylinder where the deliquescent material absorbs the water while the air was passing through. (Each cylinder was good for eight hours.

of drying.) From the dryer the dry air was run to the jet system via a 4 inch diameter flexible mill (fire) hose.

E. Experimental Jet System

The air supply was conducted to the jet system via the 4 inch diameter flexible mill hose into a large radius conduit elbow and the into a 4 inch to 2 inch reducer. The jet pipe consisted of a 14 foot long straight section of 2 inch diameter steel pipe. Thus, at the exit plane fully developed pipe turbulence was established. The pipe ran down the middle of the wind tunnel connected to the conduit elbow in the "stilling" section of the wind tunnel. This minimizes the wake produced by the non parallel sections of pipe at the transition. To prevent direct radiation of internal noise transmitted through the pipe walls the flow system was wrapped in a thick layer of sound absorptive fiberglass. The air supply temperature at the exit of the jet was usually between 50° and 70°F.

F. Acoustic Instrumentation

A block diagram of the instrumentation used is shown in Figure 8. The noise data was measured using a 1/2 inch Brüel and Kjaer condensor microphone cartridge type 4133 with cathode follower type 2614. The microphone had a fairly flat frequency response over the range from 30HZ to 22 kHZ and a dynamic range from 20 db to 160 db (re. 0.0002 microbar). Temperature and pressure sensititives of the microphone were negligible in our working range. The microphone had a 2 db variance over a 15° angle from the center of the source. The microphone was pointed at the center of the exhaust nozzle. Before and after each test session the microphone was calibrated with a Brüel and Kjaer pistonphone type 4220. The pistonphone type 4220 produced a precision sound source having a puretone at 250HZ with a sound pressure level of 124 db. (r. m. s.) re. 0.0002 microbar. It has a calibration accuracy of $\pm$ 0.2 db. With a working

temperature range from -40°C to 60°c

The microphone signal was amplified by the Brüel and Kjaer audio frequency analyzer type 2107 which has a linear frequency response from 2 to 40,000 HZ. The amplifier is made so that external filters can be placed between amplifier sections. Both the high-pass filter and the Brüel and Kjaer band-pass filter set type 1612 were used in this way. The high-pass filter served to remove that part of the acoustic signal below 200 hertz, for which the test section's background noise level was higher than the signal. The Brüel and Kjaer band-pass filter set type 1612 has third octave and octave band-pass filters. Each filter has a flat pass-band giving the filter system a linear range from 22 to 45,000 HZ. When the filter set and the amplifier are combined with an external source such as a Brüel and Kjaer level recorder type 2305 automatic filter selection can be achieved. Sound pressure level spectra (referenced to 0.0002 Microbar) could then be obtained in the frequency range from 22 HZ to 22 KHZ.

Due to the lack of availability of the 1/3 octave band-pass filter set, the Brüel and Kjaer audio frequency analyzer type 2107 was used when the band-pass filter set was not available. The audio frequency analyzer is an A. C. operated constant precentage bandwidth frequency analyzer. It was designed especially as a narrow band sound analyzer but may be used for any kind of frequency analysis within the specified frequency range. Anyone or all of the frequency ranges can be selected. A built in mechanical device similar to that in the band-pass filter enables automatic turning from an external motor such that from the Brüel and Kjaer level recorder. When the frequency analyzer was used the data was corrected too 1/3 octave bandwidth by the usual method (10).

G. Lift Measurement

Lift measurements were carried out on a three component force balance modified for lift measurements only. Figure 9 is a picture of the externally blown flap hung from the balance. Flexures for this balance were made out of tool steel one and half inches long with a rectangular cross section 1/2 inch by 1/4 inch. Four A-18 strain gages having a gage factor of 1.8 and a resolution of 120 ohms were placed on each flexure. Two on top of the flexure and two on the bottom. Each gage then acted as an arm of the wheatstone bridge circuit. The effect of placement of these gages was to quadruple the bridge output from that of just one strain gage thus increasing the strain sensitivity. In addidion since the number of strain gages were even and felt the same temperature changes the system was self temperature compensating. Each flexure was calibrated up to 50 lbs.

The model was hung upside down from a point close to the wing's center of lift (quarterchord) with 0.02 inch piano (steel) wire. Since the attachment point could not be put exactly at the center of lift, the wing had a pitching moment due to the uneven distribution of lift around the point at which the wing was hung. A 2 foot sting was therefore attached to the wing and hung from another flexure. Additional wire secured the wing in the drag direction without interfering with that of the lift direction.

CHAPTER III

EXPERIMENTAL PROCEUDRE

The objective of this study was to investigate the sound pressure level spectra, overall sound pressure levels, and sound power radiated from an externally blown flap model which has various jet exhaust velocities, with and without a forward flow, with two different wing-engine configurations. The sound radiated was also evaluated on the basis of the lift produced under each condition tested. In this chapter a discription of the experimental techniques used to achieve our objectives is given.

Fifteen microphone locations were chosen in a 40 inch circle whose center was the center of jet exhaust plane and was at angle of 50.5 degrees from the horizontal plane which passed through the nozzle centerline. The microphone was located at intervals of 25 degrees around this circle at an equal distance from the jet. This set of positions was chosen in order that the microphones would at no time be immersed in the wind stream of the tunnel. In order to see how this noise data differed from that in the horizontal plane which passes through the nozzle centerline microphones were also positioned at 20 degree intervals from that plane to direct sideline (Actually do to the end plates a maximum of 80 degrees could only be obtained). In this way the aximuthal, ϕ variation was obtained. Figure 10 is a sketch of the microphone geometry used.

The apparatus was set up in the tunnel test section as described earlier and a study of the background noise (spectra and overall sound pressure levels) with and without a tunnel speed of 60 mph was made at each microphone position to be used in the tests. Background values were needed for the data reduction.

After all background noise data was specified the wing was removed and the model jet was examined. With zero tunnel speed noise spectra and overall sound pressure levels were measured at each microphone location for jet

exhaust velocities ranging from 200 to 700 feet per second. This insured the noise of the jet alone agreed with previous results.

The wing was then fixed relative to the jet to approximate the basic configuration. Sound pressure level spectra and overall sound pressure levels were measured at each microphone locations for each flap configuration; 45° - 70°, 30° - 55°, 10° - 20°, and 0° (cruise), at blowing velocities from 100 feet per second to 500 feet per second (with the except of the cruise position where velocities were varied between 200 and 700 feet per second). This set of experiments was carried out with and without a tunnel speed of 60 mph.

The jet was then moved relative to the wing such that it simulated the modified configuration (figure 6). Far field noise measurements were again taken at each microphone location for the 10° - 20°, 30° - 55°, and 45° - 70° flap configurations for the full range of jet exhaust velocities.

The three component force balance was then set up and the model was hung upside and in a position relative to the jet to represent the basic configuration. Lift measurements were then taken for the three flap configurations at each jet exhaust velocity for a forward flight speed of 60 mph. In order to compare the blown flap with the conventional flap system additional lift measurement were taken without blowing at each flap position. The jet was then moved relative to the wing to its modified configuration and the tests were repeated.

CHAPTER IV

DATA REDUCTION

Power levels directional patterns, and sound pressure spectra and their variations with flap angle, jet exhaust velocity, forward speed, and engine-wing configuration are of particular interest in this study. In this chapter the data reduction techniques used in this report are presented.

A. Spectra and Overall Sound Pressure Levels

The level recorder output consisted of a trace representing the sound pressure level of the total noise signal. This was not always a true representation of the source spectrum since under certain conditions the background noise level was within 10 decibels of the total signal. In order to get the source spectrum for those cases the background noise spectrum had to be subtracted out of the total signal's spectrum. The method for doing this was taken from chapter 3 of reference 10 and produced the following equation which gives the sound pressure level of the source for a particular frequency:

$$4.2 \quad SPL = 20 \log_{10} \left(\sqrt{10^{SPL_T/10}} - \sqrt{10^{SPL_B/10}} \right)$$

The overall sound pressure levels were obtained from the reduced one-third octave band spectra with a frequency range from 200 to 20,000 hertz. The mean sound pressure levels in each band were then added with the aid of the nomograph in reference 10 to give the overall sound pressure level. This was then checked with the value of overall sound pressure level measured by the instrumentation corrected for background noise.

B. Total Power Measurements

The measurement of total radiated sound power, although easy to envision in theory, in practice is considerably complicated by the three-

dimensional character and directive nature of the radiation field. The "free-field" method is used here to measure total radiated sound power and it is only limited by the completeness with which the microphone can survey the radiation field. The anechoic chamber is ideally suited to such measurements, removing the ground-plane effect normally present in outside measurements. Sound pressure measurements in a 360 degree circle around the model were used to define the radiation field. Computation of the total radiated sound power from the free-field measurements then involved a weight or spatial integration of the form;

$$4.2 \quad P_A = \frac{\pi R^2}{\rho c} \int_0^{2\pi} \overline{P^2} \sin\theta \, d\theta$$

Here $\overline{P^2}$ is the mean square sound pressure measured at $\phi = 0°$ (total signal-background). The integration was performed numerically on MIT's 360 IBM computer. It must be noted that the above formula is theoretically only valid for an axisymmetric sound source such as a jet and does not give the total power for the blown flap noise. The power found by this formula for the flap noise is therefore called the nominal power. It is used to compare these results with previous experiments and to obtain in a qualitative fashion the variation of acoustic power with jet velocity.

C. Directivity

The directivity of the noise from blown flap would be expected to be that of two dipoles at right angles; one caused by the fluctuating lift forces and other due to fluctuating drag forces. The directivity would therefore be the sum of two, three-dimensional dipoles at right angles to each other. The directivity for such an arrangement is given by:

$$4.3 \quad D \sim d \cos\phi \cos\theta - \ell \cos\phi / \sin\theta$$

where ℓ and d are the dipole strengths of the lift and drag dipoles respectively.

In order to keep the microphone out of the tunnel's wind stream, the acutal acoustic measurements were taken at an angle ϕ of 50.5° from the horizontal plane. (see figure 10.) In order to extrapolate this data to the horizontal plane the decrease in overall sound pressure level from its value at $\phi = 0°$ was measured as a function of ϕ for $\theta = 90°$ for each test. (e.g. figure 25). This result was then used to correct the acoustic measurements to the horizontal plane for all values of θ. This basically assumes that the directivity of the sound radiation from the fluctuating drag forces is the same as the directivity of the sound radiated by the fluctuating lift forces as measured at $\theta = 90°$. It was found that at most there was only a four decibel difference in sound pressure level between $\phi = 0°$ and $\phi = 50.5°$ (this is confirmed for other jet angles, θ in reference 4). The data obtained in previous works indicates that the error in this problem is experimentally neglible.

CHAPTER V

PRESENTATION OF RESULTS

A. The Plain Jet System

In order for the results presented here to be comparable with other data, the acoustic characteristics of the jet must be specified. The sound power level radiated from the unspoiled jet pipe flow (wing not present) is shown in figure 11 as a function of the exit - plane velocity of the jet. The results are compared with the experimental data obtained in reference 11 on a similar jet as well as the theoretical prediction (solid line). The results demonstrate a high order of repeatability for such types of experiments. The plain pipe radiation shows a sixth-power of velocity dependence at the lower velocities changing into an eight power dependence at the higher velocities. This eighth power dependence is identified with the free-jet turbulence and agrees closely with the theoretical prediction.

The sound directivity pattern at a 72.5 inch radius and an azimuthal angle of 45° for the free jet is shown in figure 12. The overall sound pressure level is given as a function of angle θ, for jet exhaust velocities from 200 feet per second to 700 feet per second. The data shows that the shape of the directivity pattern is similar over all jet exhaust velocities and there is a strong increase in OASPL as the velocity is increased.

One-third octave sound pressure level spectra measured at a microphone radius of 72.5 inches and at $\theta = 25°$, $\phi = 0°$, for each jet exhaust velocity is shown in figure 13. The spectra are broadband with the frequency at which the maximum sound pressure level occurs increasing with increasing velocity. The strong increase in sound pressure level with exhaust velocity is again readily apparent.

B. Externally Blown Flap

In this section an analysis of the results for the externally blown flap with its basic wing-engine configuration is presented. STOL aricraft are expected to steeply ascend from or descend to small airports near populated areas. Consequently the important noise level measurements are those below the aircraft. The sound directivity patterns for the various flap configurations at a 63.5 inch radius for the externally blown flap model is shown in figure 14 for a jet exhaust velocity of 400 feet per second. The OASPL is plotted as a function of angle, θ for flap deflections of 45° - 70°, 30° - 55°, 10° - 20° and 0° (fully retracted). The data for the free-jet corrected to the above conditions is included for ready comparison. The noise level clearly increases with flap angle, with large increases in the OASPL below and forward of the wing. The noise from the 0° (flap retracted) position is about 10 decibels greater than the noise generated by the nozzle alone for most angles of θ. This means that the noise caused by the nozzle alone contributes less than 1/2 a decibel to the total noise level caused by the jet scrubbing on the wing.

The effect of jet exhaust velocity on the overall sound pressure level is shown in figures 15-18 for the 45° - 70°, 30° - 55°, 10° - 20°, and 0° flap deflections respectively. The OASPL is represented in polar plots at a 63.5 inch radius and are given for jet exhaust velocities from 100 feet per second to 500 feet per second with the exception of the flaps retracted position where data was taken up to 700 feet per second. A strong increase in OASPL is observed for increases in jet exhaust velocities for each flap position. The noise is greatest under the wing and least above it. The shapes of the noise radiation patterns for each flap angle are fairly similar over the range of exhaust velocities tested.

The nominal sound power level (defined in Chapter IV) is shown as a

function of the jet exhaust velocity for the five test configurations in figure 19. Although this definition does not take into account the lack of spherical symmetry of the sound field, the nominal sound power level is useful because it shows the trends with velocity and flap angle. Included in figure 19 are the data points obtained with and without a 60 mph forward speed. A comparison of these data points indicate a neglible (one or two db) difference in the power radiated from the model externally blown flap in the static condition from that with forward speed. This means that the jet impingment on the externally blown flap is not affected by forward velocity. It must be noted that due to the tunnel background noise the source signal could only be extracted for a ratio of jet velocity to flight speed greater than 4.5. It is therefore not known how the forward velocity effects an externally blown flap with a lower jet velocity. Also included in the figure is the experimental data found in reference 3 on a similar model. A comparison shows good agreement.

It can be seen that the nominal sound power level increases with the 6th power of the velocity for the four flap positions in contrast to the nozzle alone (free-jet) which follows the well established 8th power law at subsonic velocities. The interaction noise due to the model can be seen to be much louder than the nozzle jet noise. Even at the fully retracted flap position the noise is as much as 10 db greater than that of the nozzle at a jet exhaust velocity of 500 feet per second. The interaction noise then completely dominates the sound field.

One-third octave spectra measured at 63.5 inches from the nozzle centerline at an angle of $\theta = 90°$ in the plane perpendicular to the wing are presented in figures 20-23 for each flap configuration and jet velocity tested. The spectra are broad band and for each flap angle are generally similar in shape. The strong increase in sound pressure level as the nozzle exhaust velocity is increased is again apparent for all flap configurations. A comparison of

typical one-third octave sound pressure level spectra for the five different externally blown flap, flap configurations are presented in Figure 24. The 0° flap case is nearly equivalent to the CTOL, conventional takeoff and landing, aircraft configuration for an engine pod mounted below an aircraft wing where the interaction noise is due to the scrubbing of the jet on the bottom surface. As the flaps are deflected down a strong increase in sound pressure level can be observed. At the maximum flap setting (45° - 70° flap angle) there is an increase of about 20 decibels measured below the wing (θ = 90°) over that for the flaps retracted position. Thus a significant increase in noise would result below the wing of an externally-blown-flap STOL aircraft in comparison with that of a CTOL aircraft.

As mentioned previously the sound field is asymmetrical. In order to evaluate sideline noise (in comparison to flyover noise below the wing) the microphone was positioned at several azimuthal angular positions and noise measurements were made at intervals of 20° up to an angle of ϕ = 80°. The difference between the OASPL at ϕ = 0° and the OASPL at various other values of ϕ for a microphone angle of θ = 90° from the jet axis is shown in figure 25. The figure presents curves of the difference ((OASPL atϕ = 0°) - (OASPL at ϕ)) for each flap configuration at a nozzle exhaust velocity of 400 feet per second. The noise was found to decrease linearly with azimuthal angle indicating that the flap system is much quieter when viewed directly from the side. If the fluctuating lift and drag forces on the flaps could be modelled as simple point acoustic dipoles, the directivity of the acoustic field would be given by equation 4.3. This means that the directivity as a function of ϕ at ϕ = 90° would not vary with flap angle or forward speed. The experimental results in figure 25, indicate a more directional acoustic field, probably due to the distributed character of the sources and the presence of the solid-wing reflecting surface. (12)

It is well known that the spectra of the noise from subsonic nozzles of circular cross section can be correlated by a normalized sound pressure level spectrum as a function of strouhal number, fD/V. Figure 26 is such a plot for our jet where the normalized 1/3 octave sound pressure level spectrum, NSSD, is defined as;

$$5.1 \quad NSSD = SPL_{1/3\ octave} - OASPL$$

Where SPL is the sound pressure level at the center frequency of the one-third octave band width, Δf. The data seems to correlate very well, with the peak of the noise spectrum occurring at a strouhal frequency of .2.

A similar correlation was made for the interaction noise generated by the externally blown flap at each flap position. Figures 27-30 are strouhal plots for the different flap configurations at the five different jet exhaust velocities tested. Excellent data correlation is shown.

C. Modified Externally Blown Flap

A variation on the basic configuration was made in order to gain some insight in estimating the effects of such changes on the blown flap noise. The modified externally blown flap consists of moving the nozzle rearward along the jet axis towards the flaps so that its exit plane is three inches behind the leading edge of the wing (see figure 6).

The sound power radiated by the modified externally blown flap for the three flap positions tested are compared with that of the basic configuration in figures 31-33. In each case there is a 3 or 4 db drop in the power radiated over all velocities. The power radiated by the modified configuration falls along the tradition V^6 slope for dipole sources.

The sound pressure radiation patterns for the modified externally blown flap at each of the three flap positions are presented in figures 34-36. The patterns were measured at a radius of 63.5 inches with a jet velocity of 400 feet per second. Directivities for the basic externally blown flap are

included for ready comparison. A two to four decibel drop in OASPL can be observed at most microphone locations. This decrease, which amounts to halfing the acoustic power level radiated, is probably due to the fact that the jet has less time for turbulent mixing with the ambient air before it hits the flap. Jet noise is caused by this turbulent mixing. Therefore a decrease in the amount of turbulent mixing means a decrease in the noise the flaps can redirect and amplify. It is noted here that in reference 4 a similar experiment with a much higher jet velocity (App. 950 feet per second) indicated a slight increase in the noise level over most angles. The rational for this result was the higher impingement velocity on the flap. The difference in the two results indicate that there are at least two variables present. At low jet velocities the amount of turbulence dominates while at higher velocities the impingement velocity dominates.

The effect of velocity on the overall sound pressure level radiated by the modified externally blown flap at its different flap positions is shown in figures 37-39. The OASPL at a 63.5 inch radius is plotted as a function of angle, θ, for nozzle exhaust velocities from 100 ft/sec to 500 ft/sec. At each flap position the shape of the directivity pattern remains practically constant over the full range of velocities tested. A strong increase in OASPL is noted as the nozzle exhaust velocity is increased.

Typical one-third octave sound pressure level spectra measured at a distance of 63.5 inches with $\theta = 90°$ in the plane of the wing are given in figures 40-42 for the three modified blown flap test configurations. Each plot contains spectra for the different jet exhaust velocities. An increase in the frequency at which the peak sound pressure level occurs as the velocity is increased is evident. Comparing these spectra with the basic configuration's spectra (figures 21-23) one sees a marked similarity. That is, both spectra are broad band and are generally similar in shape.

The normalized sound pressure level spectrum as a function of strouhal number for the different modified externally blown flap, flap configurations are plotted in figures 43-45. The data is well correlated. Included on these curves are the mean spectral curves for the basic configuration. Comparison of the curves show a shift to the left for the modified configuration spectral curves relative to that for the basic configuration. This is because the same impingement velocity and area was used in the making of the curves (namely velocity at the nozzle's exit plane and nozzle area) while in fact by moving the nozzle closer to the flaps there has been an increase in the impingement velocity and a decrease in the impingement area.

D. Aerodynamic Measurements

Since the purpose of the externally blown flap is to provide lift augmentation one is naturally interested in how the sound power radiated by the externally blown flap varies with the lift it can achieve. Lift coefficient, based on a 60 mph free stream velocity, as a function of blowing velocity for the different flap position is shown in figures 46-48. A comparison is made between the lift obtained by the basic and modified configurations, showing that the modified configuration gets slightly less lift than that of the basic configuration for a given jet blowing velocity. Comparing the curves of the different flap angle it can be seen that the amount of lift agumentation increases much more rapidly for the higher flap angles.

To shown the amount of lift augmentation obtained by the externally blown flap as compared to the conventional flap system a plot of the lift coefficient based on a free stream velocity of 60 mph obtained with and without a blowing jet of 500 feet per second, for the different flap angles is presented in figure 49. A significant increase in lift was obtained as the flaps are lowered for the blown flap as compared to the conventional

flap system.

A correlation between the non-dimensional lift and the sound power radiated is made in Figure 50. The data seems to correlate well. The lift coefficient is based on the free stream velocity. The lift seems to follow a straight line at high values of sound power with a slope varying with about the third powere of lift and then asymptotes out to a particular value of lift at lower sound power. For a slight increase of lift one obtains large penalties in the sound power radiated.

E. Extrapolation To Full Size Flap System

Blown flap noise estimates were made for five hypothetical 4 engine STOL aircrafts. The aircrafts had gross weights from 62,500 lbs (50 passengers) to 187,500 lbs (150 passengers) with thrust levels dependent both on field lengths and wing loading. Field lengths of from 1,000 to 1,500 feet and wing loadings from 70 lbs/ft^2 to 100 lbs/ft^2 were used. The maximum perceived noise level which would occur during a 500 foot flyover was calculated for both the take off and landing conditions. The results of these calculations are shown in figures 51-55 which give the perceive noise level as a function of jet blowing velocity. The take off condition was assumed to have 100 percent thrust, and a flap angle setting of 10°-20°. The landing conditions were assumed to have 80 percent thrust and either a 30°-55° flap angle or a 45°-70° flap angle. The 500 foot direct sideline percieve noise level was also estimated for each condition and is shown in figures 56-60. Comparing corresponding curves shows a 5 to 10 db reduction of perceived noise level at a 500 foot sideline. It has been assumed in the estimates that the rotating machinery noise has been suppressed leaving the jet exhaust mixing and flap interaction as the dominant noise sources.

The perceived noise levels are as much as 10 db above the 95 Pn db goal at a Q-Fan jet exhaust velocity (500 feet per second). The results of these test indicate flap noise suppression would be required to meet the 95 Pn db goal at 500 foot sideline.

CHAPTER VI

CONCLUSIONS

The full scale externally blown flap STOL aircraft noise estimates indicate that even with the proposed Q-Fan engine the aircraft cannot meet the goal of 95 Pn db at a 500 foot sideline. However at a lower exhaust velocity, 400 feet per second the perceived noise level falls below this STOL noise goal.

Noise directivities for the externally blown flap are seen to be noisier below the wing than above it with directivity patterns remaining similar in shape for different flap systems as the jet velocity is changed. It was found that the azimuthal directivity in overall sound pressure level was approximately linear in azimuthal angle for all flap positions tested and the direct sideline is less noisy then that below the wing.

The nominal sound power level of the externally blown flap for all configurations increased with the sixth power of the jet velocity as opposed to the jet alone which increased with the eight power of the velocity.

Interaction noise from the flap system completely dominates the noise generated by the jet.

The sound power level radiated by the externally blown flap is seen to be uneffected by a forward speed for a ratio of jet velocity to flight speed greater than 4.5.

By moving the nozzle rearward, toward the flap system on the same jet axis a decrease in overall sound pressure level of three to four decibels can be obtained for jet velocities up to 500 ft/sec.

A correlation between the power radiated and the lift obtained by an externally blown flap can be made. For a slight increase in lift one obtains large penalties in the sound power radiated.

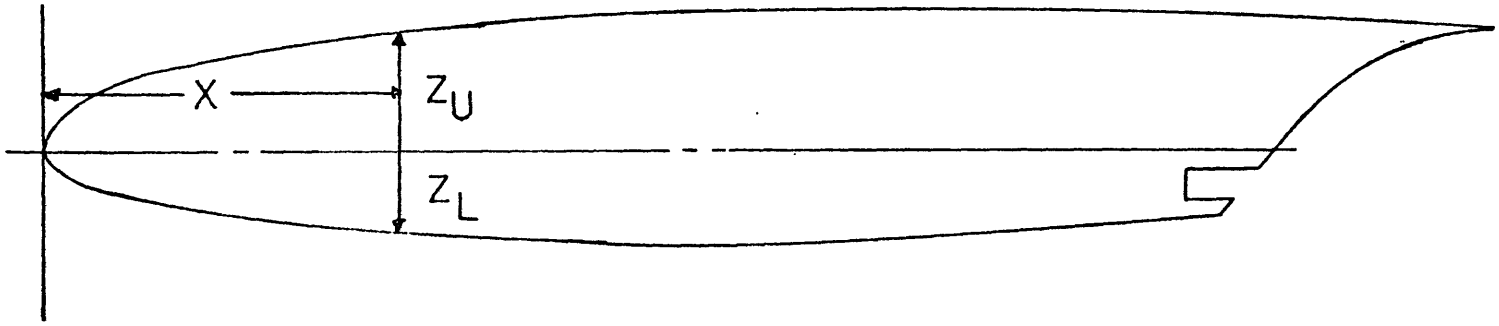

TABLE I

(A) WING

X (INCH)	Z_U (INCH)	Z_L (INCH)
0.012	0.054	0.048
0.036	0.097	0.078
0.060	0.128	0.097
0.093	0.165	0.118
0.180	0.233	0.155
0.480	0.355	0.250
0.955	0.459	0.354
1.910	0.582	0.477
2.870	0.640	0.540
3.820	0.665	0.557
4.825	0.652	0.530
5.750	0.605	0.461
6.700	0.527	0.357
7.650	0.412	0.034
8.630	0.246	0.108
9.650	0.012	0.012

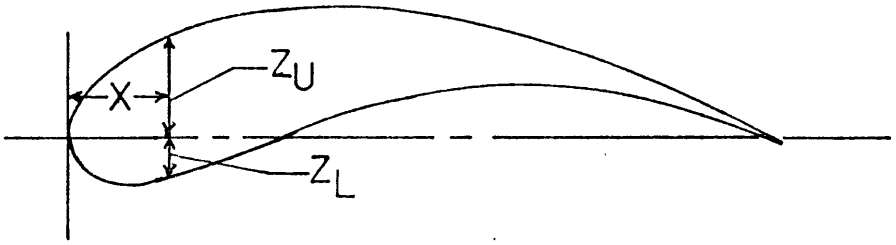

TABLE I

(B) VANE

X (INCH)	Z_U (INCH)	Z_L (INCH)
0	0	0
0.039	0.087	0.083
0.077	0.125	0.105
0.154	0.176	0.107
0.231	0.212	0.087
0.308	0.238	0.059
0.386	0.256	0.029
0.464	0.267	-0.015
0.618	0.279	-0.048
0.707	0.272	-0.087
0.926	0.246	-0.108
1.080	0.207	-0.113
1.232	0.105	-0.096
1.390	0.082	-0.054
1.542	0	0

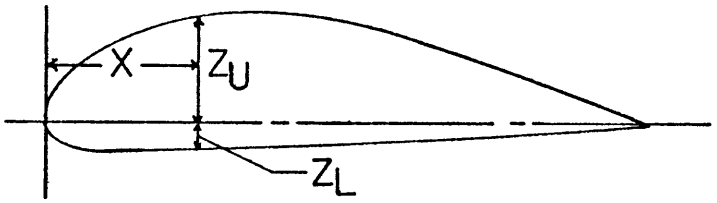

TABLE I

(C) FLAP

X (INCH)	Z_U (INCH)	Z_L (INCH)
0.112	0.220	0.112
0.224	0.312	0.102
0.336	0.378	0.092
0.448	0.410	0.088
0.560	0.470	0.078
0.662	0.475	0.075
0.890	0.490	0.065
1.125	0.470	0.051
1.345	0.420	0.037
1.700	0.400	0.027
1.790	0.310	0.017
2.150	0.200	0.014
2.240	0.180	0.010
2.400	0.120	0.004
2.600	0.060	0.002
2.700	0	0

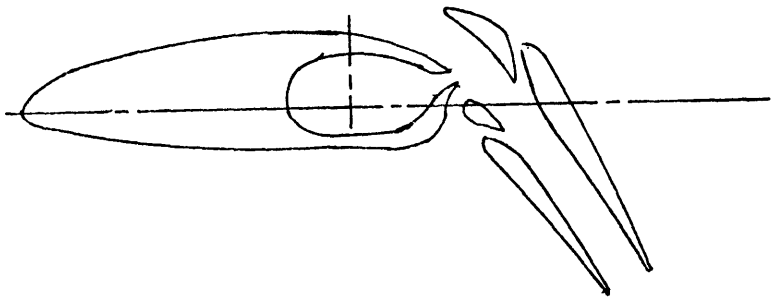

AUGMENTOR WING FLAP

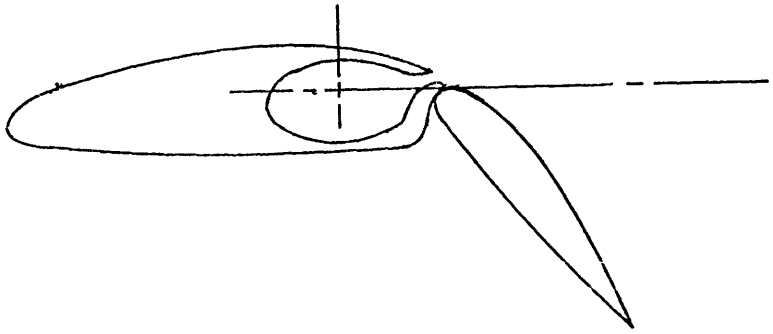

JET OR INTERNALLY BLOWN FLAP

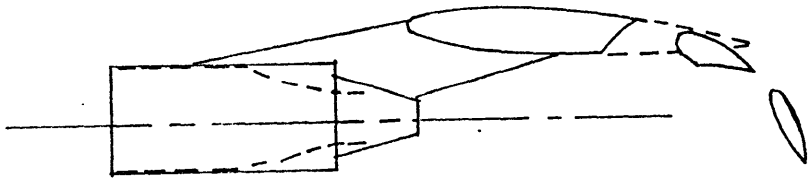

EXTERNALLY BLOWN FLAP

FIGURE]. Blown Flap Noise Test Configuration

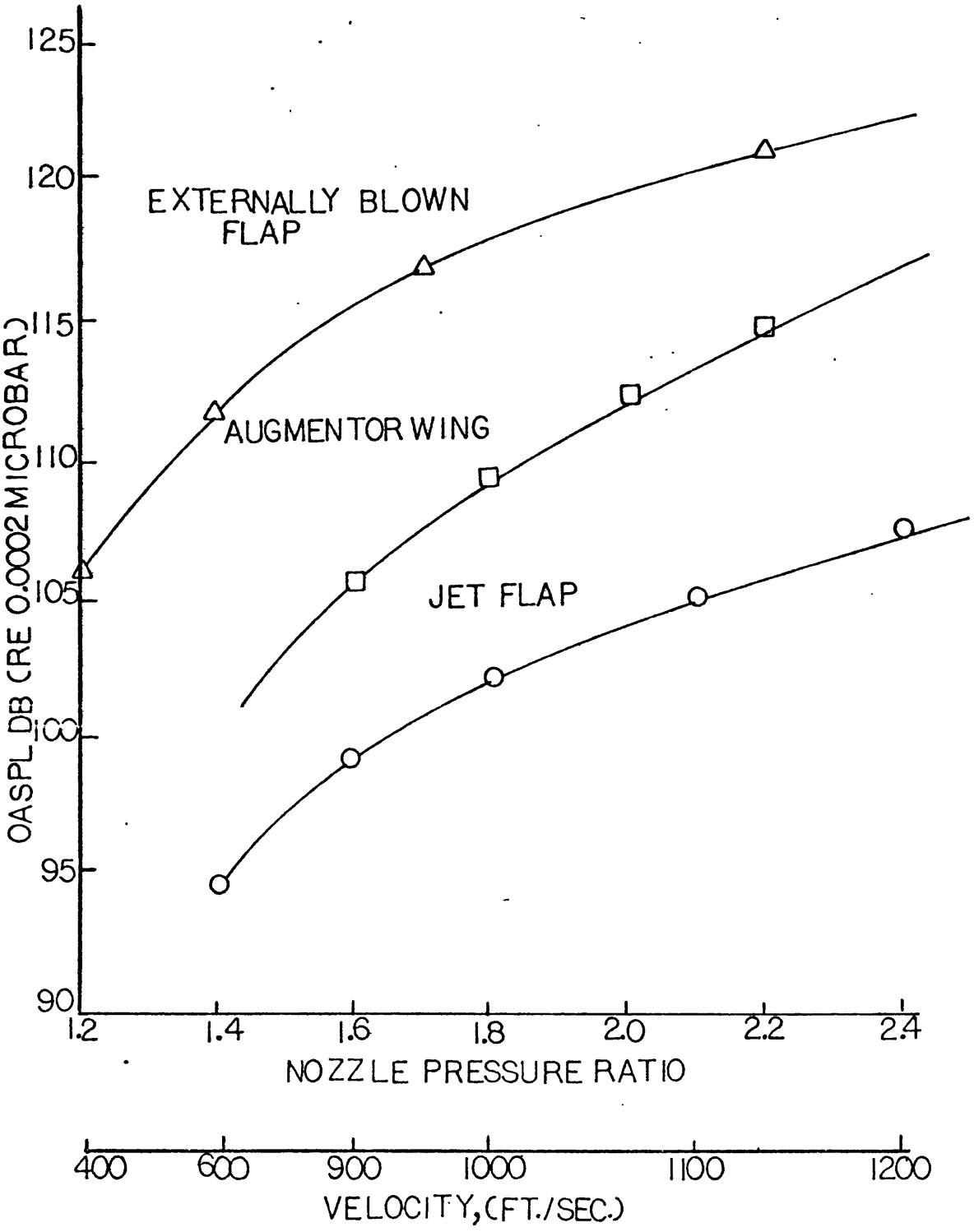

FIGURE 2. Comparison of the Three Types of Blown Flaps taken from Reference 3. Data Normalized to Flap Turning Angle, 50°, Microphone Distance 10 feet, Nozzle Area, 3.45 inches^2.

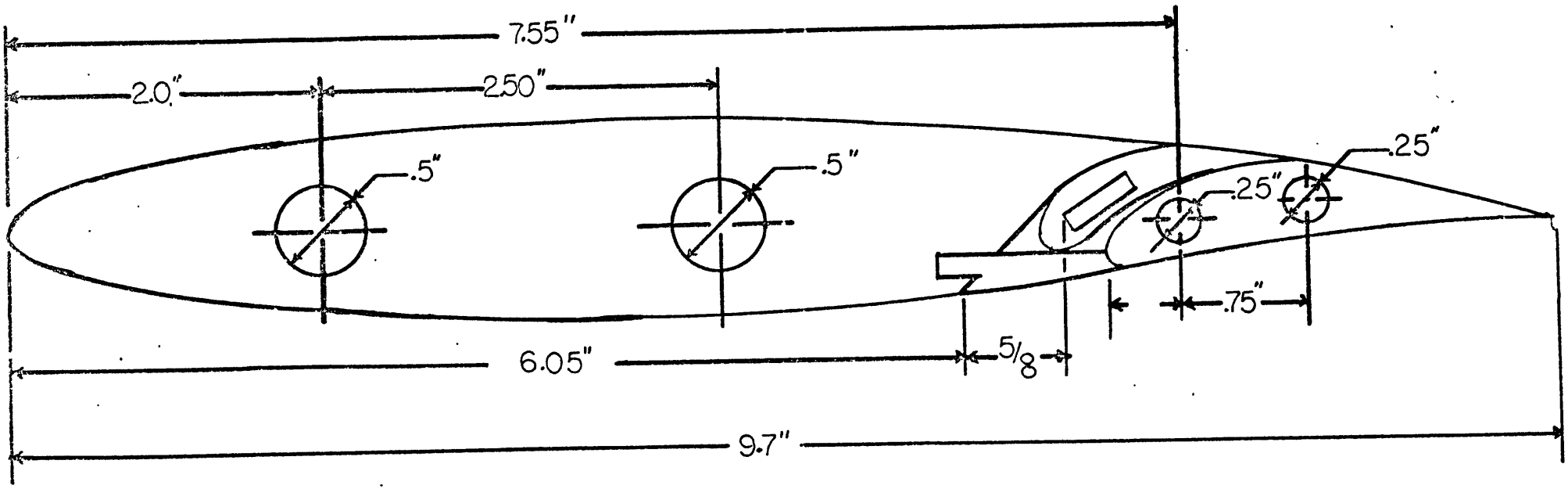

FIGURE 3. Externally Blown Flap Model Tested

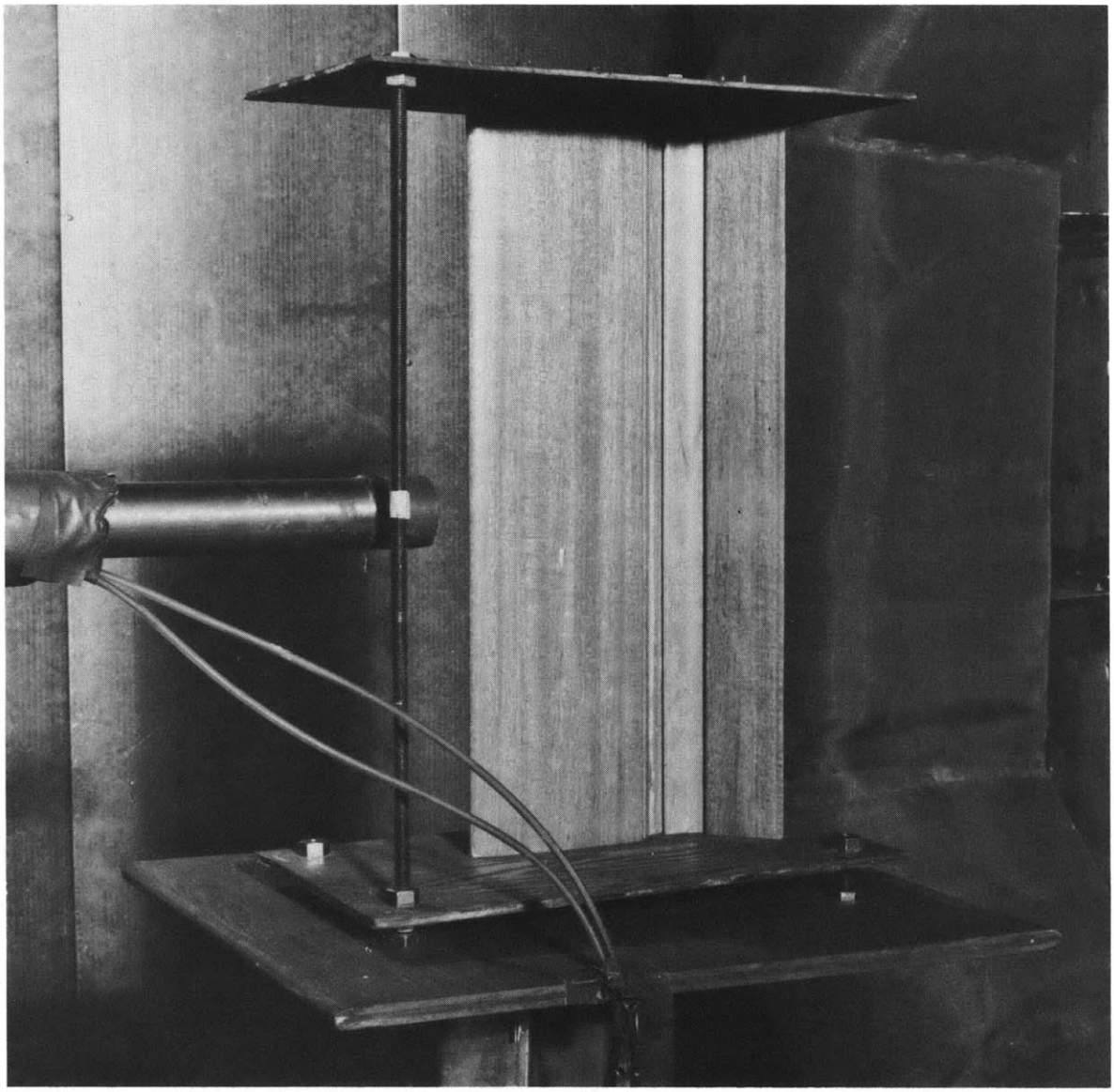

FIGURE 4. Externally Blown Flap Test Configuration.

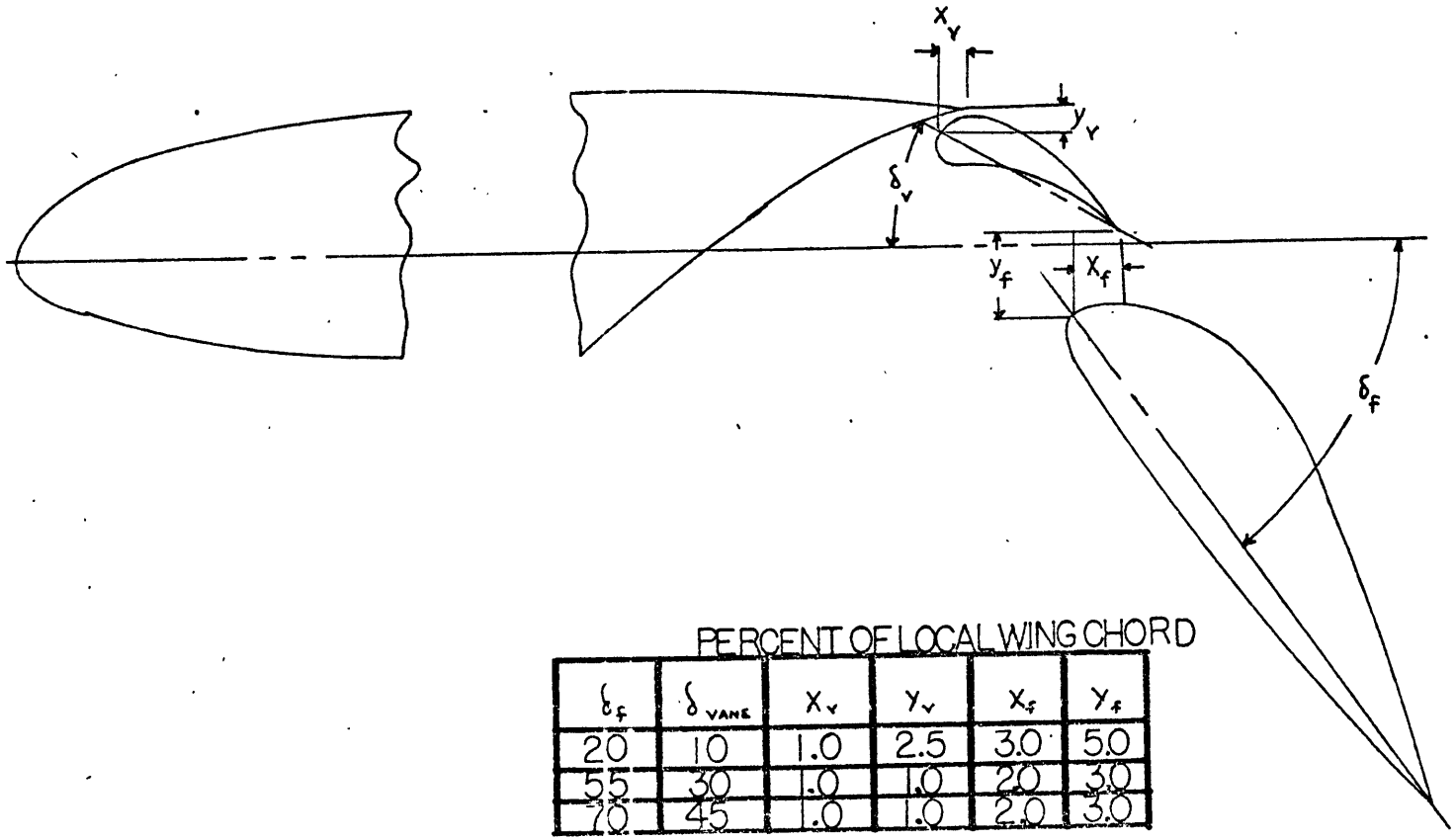

PERCENT OF LOCAL WING CHORD

δ_f	δ_{VANE}	X_v	y_v	X_f	y_f
20	10	1.0	2.5	3.0	5.0
55	30	1.0	1.0	2.0	3.0
70	45	1.0	1.0	2.0	3.0

FIGURE 5. Flap Configurations

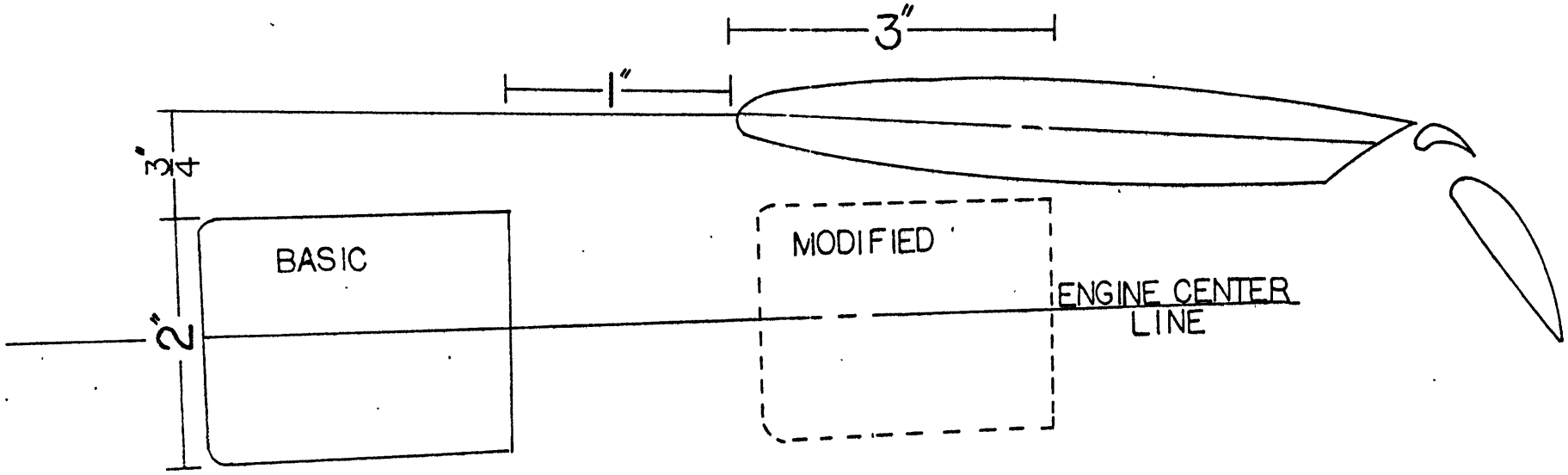

FIGURE 6. Wing-Nacelle Assembly for the Basic and Modified Externally Blown Flap Configurations

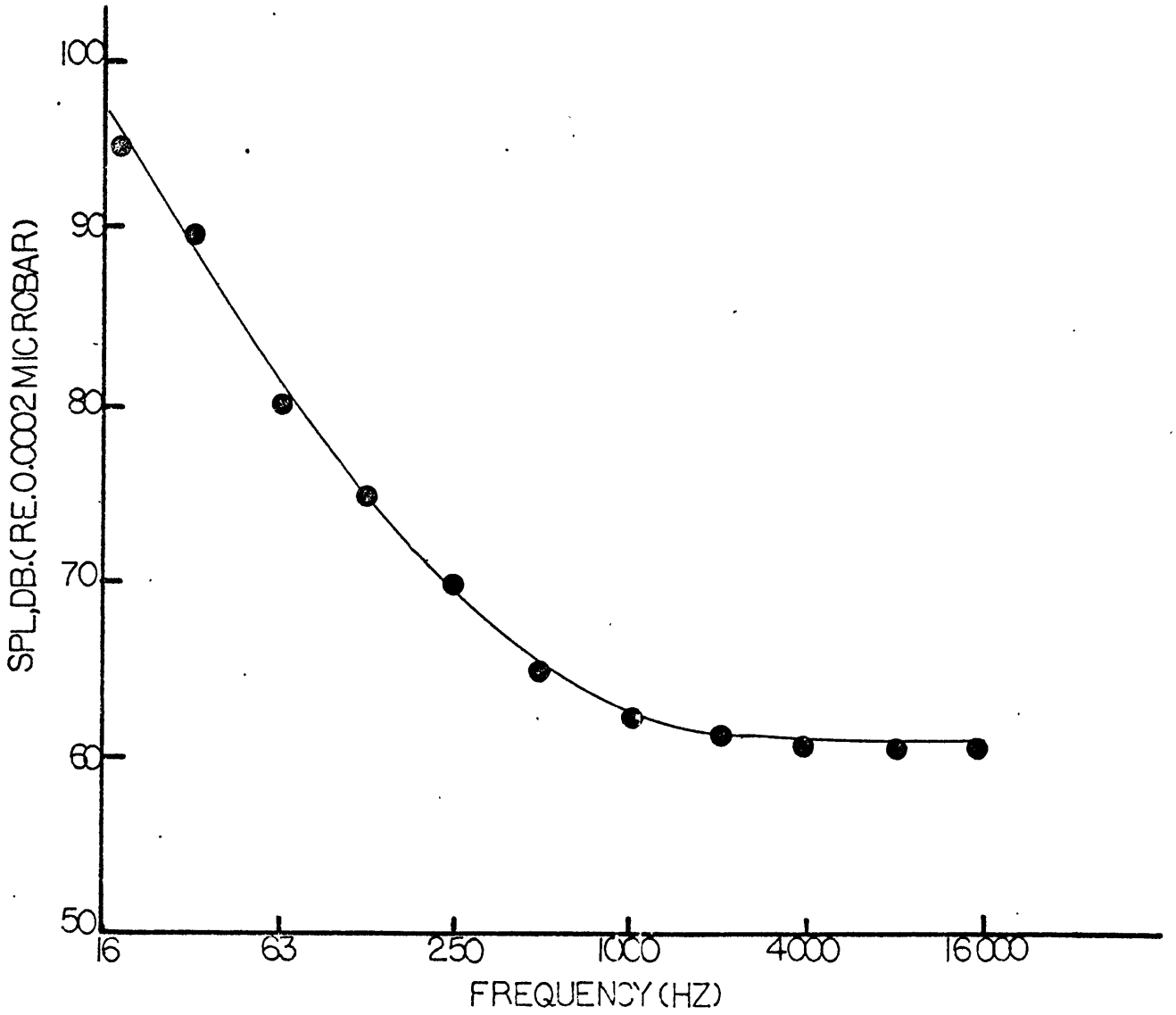

FIGURE 7. Frequency analysis of Tunnel's Background Noise at 10 feet from the Center-line, corrected to one-third Octave Band. Tunnel Speed, 70 MPH

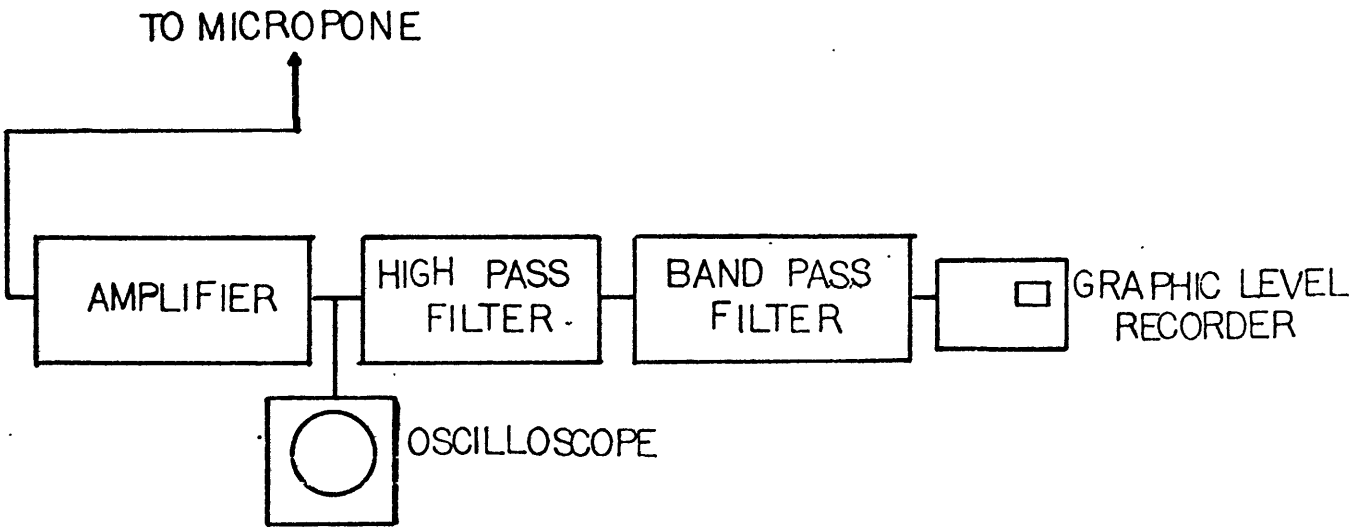

FIGURE 8. Instrumentation Schematic

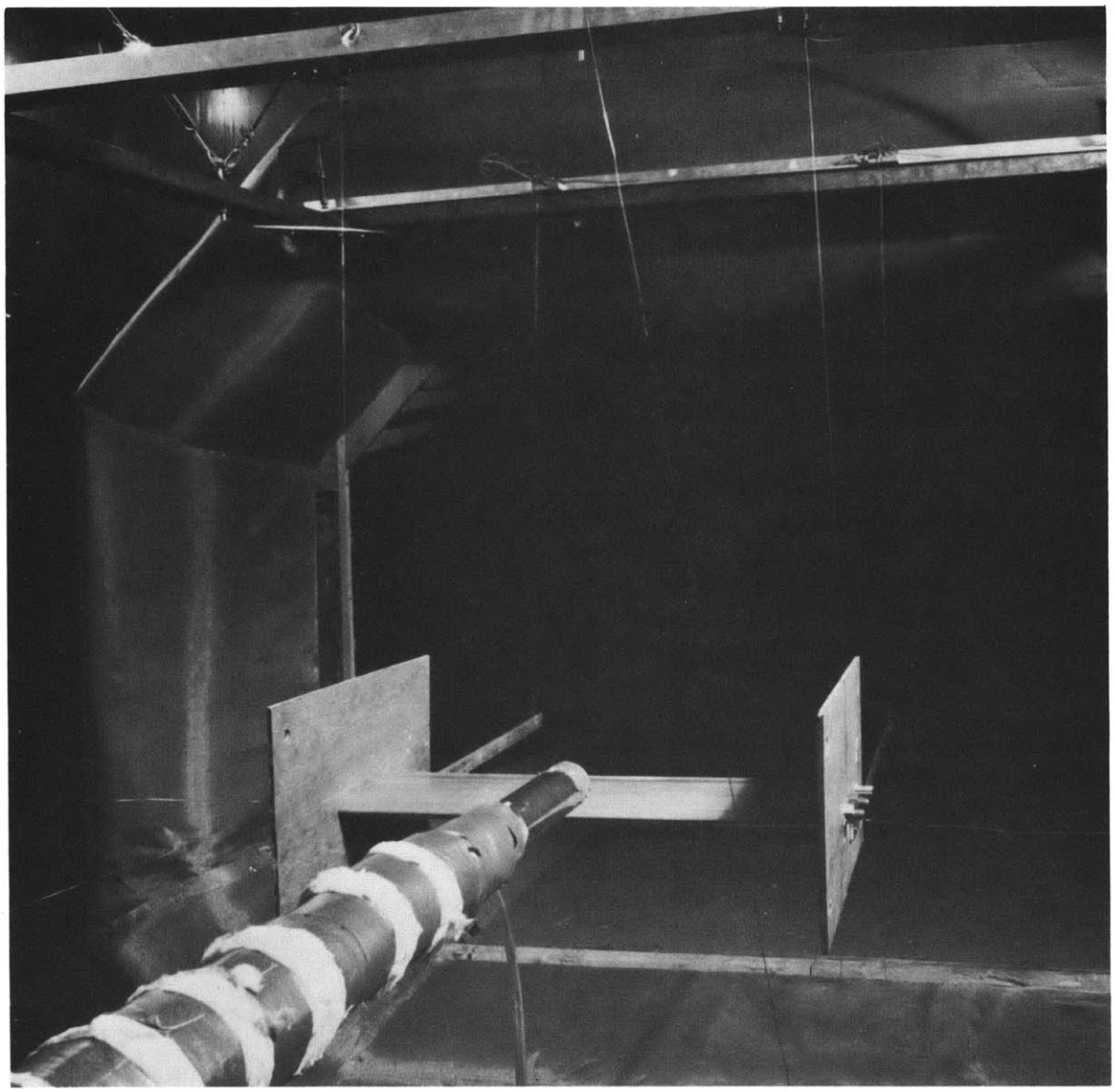

FIGURE 9. Lift Measurements.

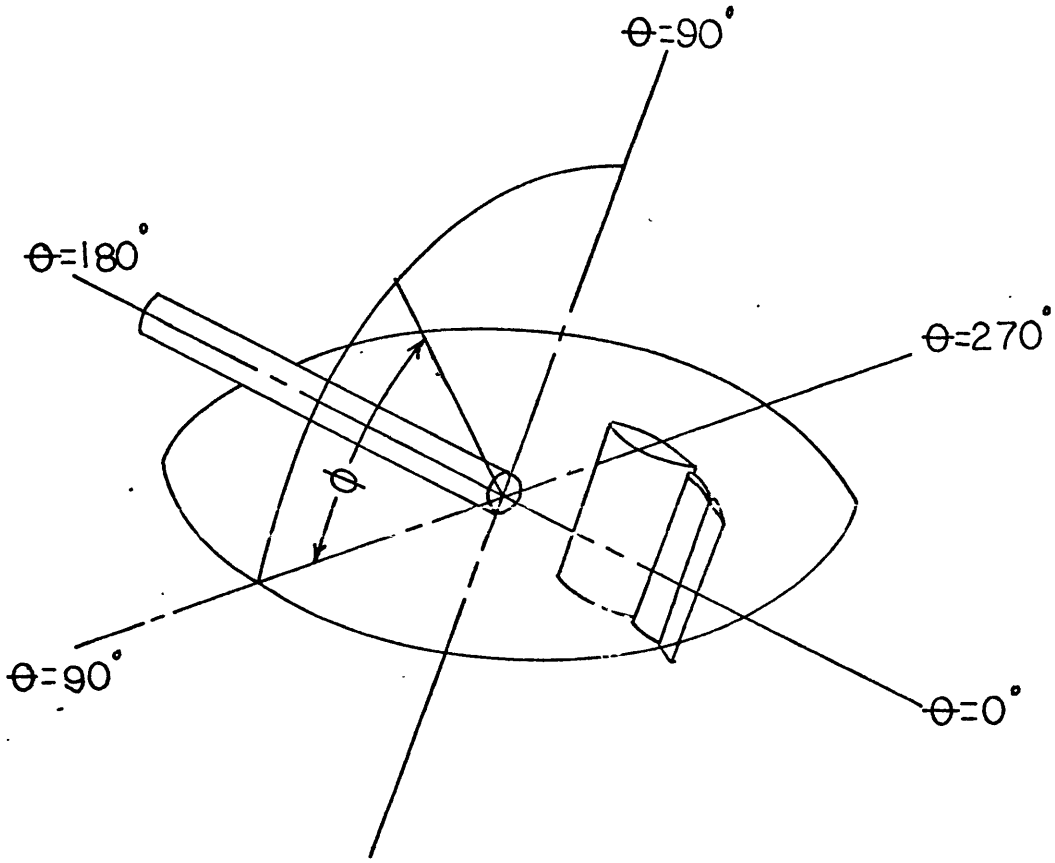

FIGURE 10. Microphone Geometry

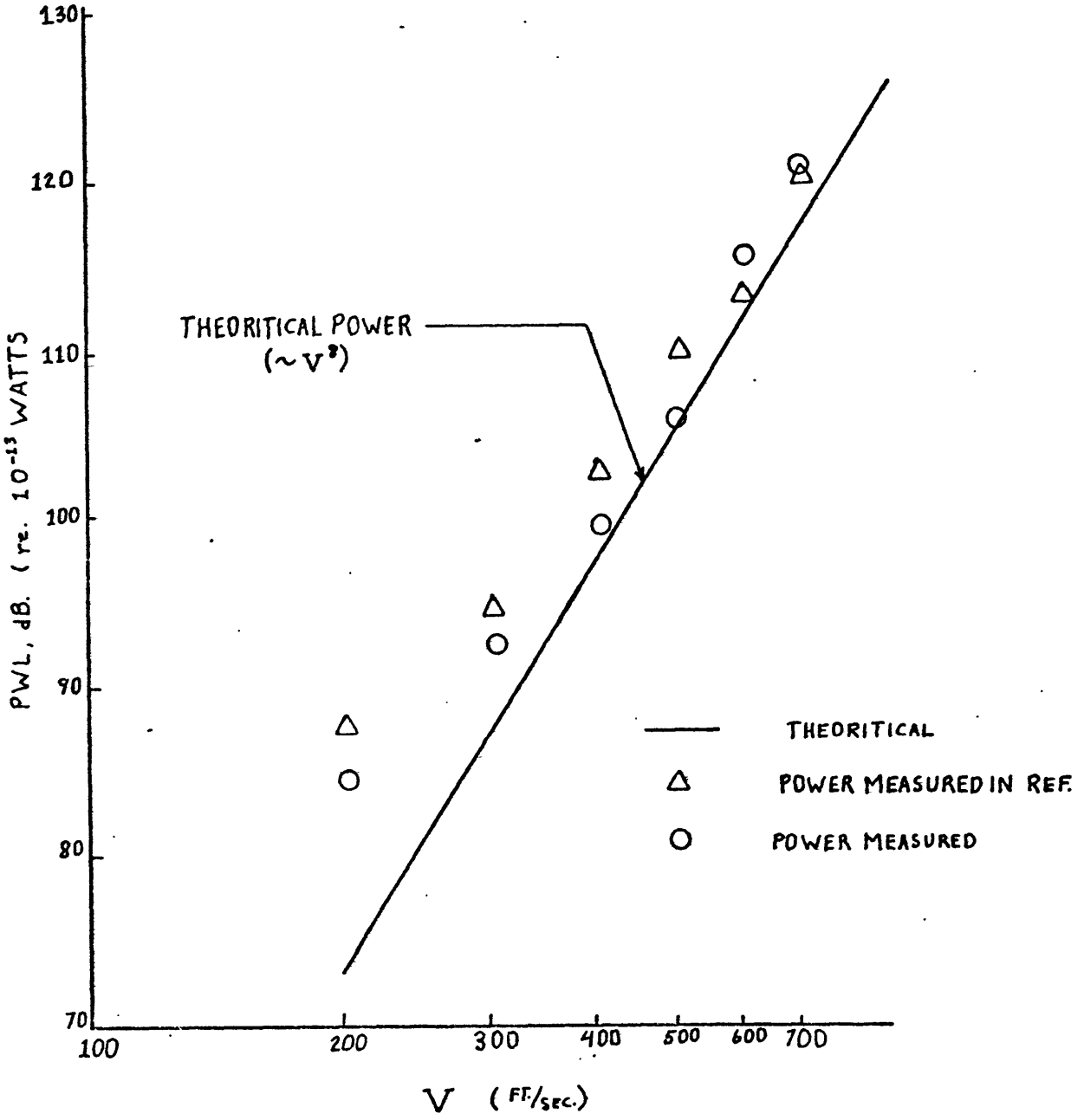

FIGURE]]. Sound Pressure Level Radiated by the Unspoiled Jet as a Function of Exit-Plane Velocity

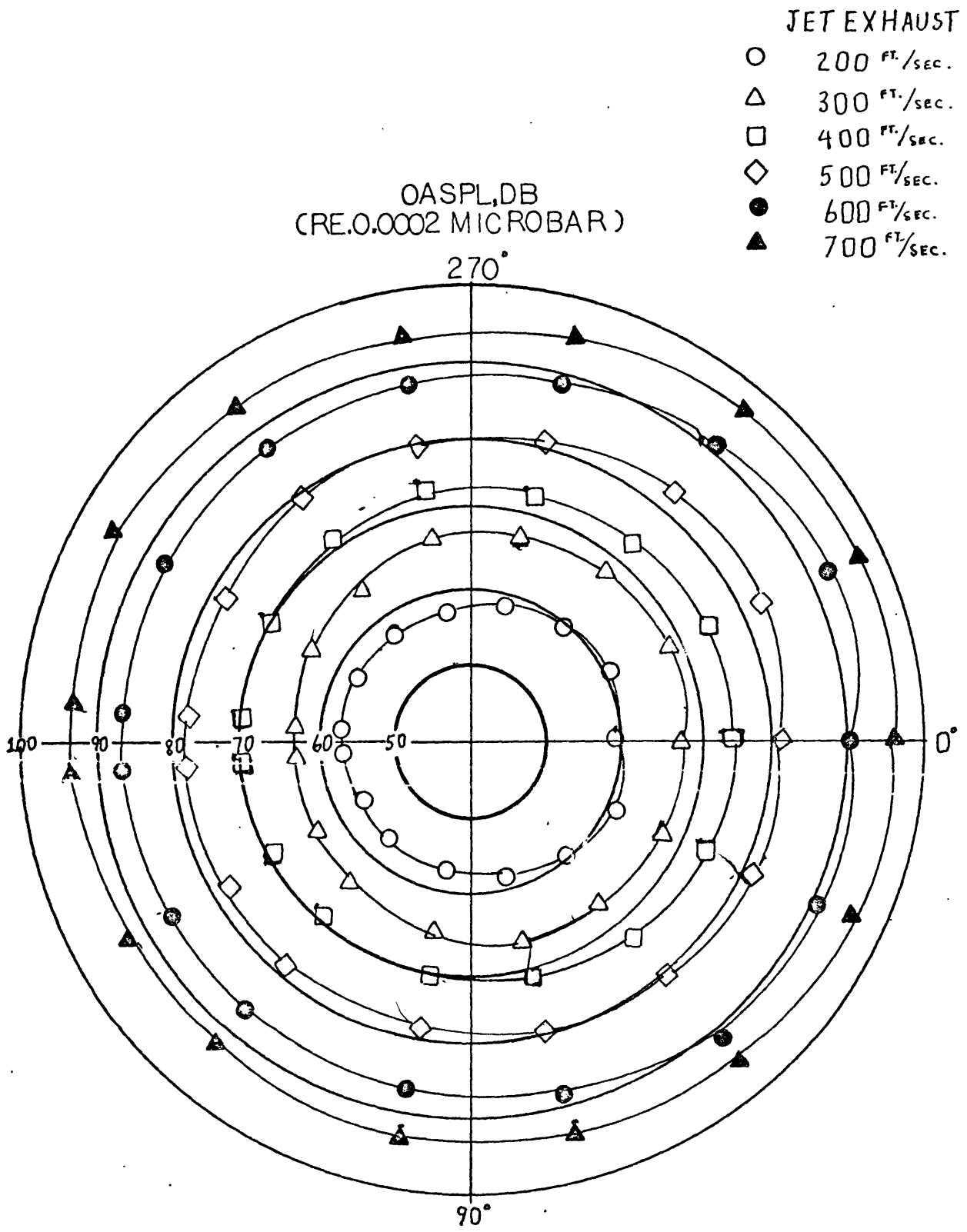

FIGURE 12. Jet Noise Directivity Pattern . Microphone Radius, 72 inches.

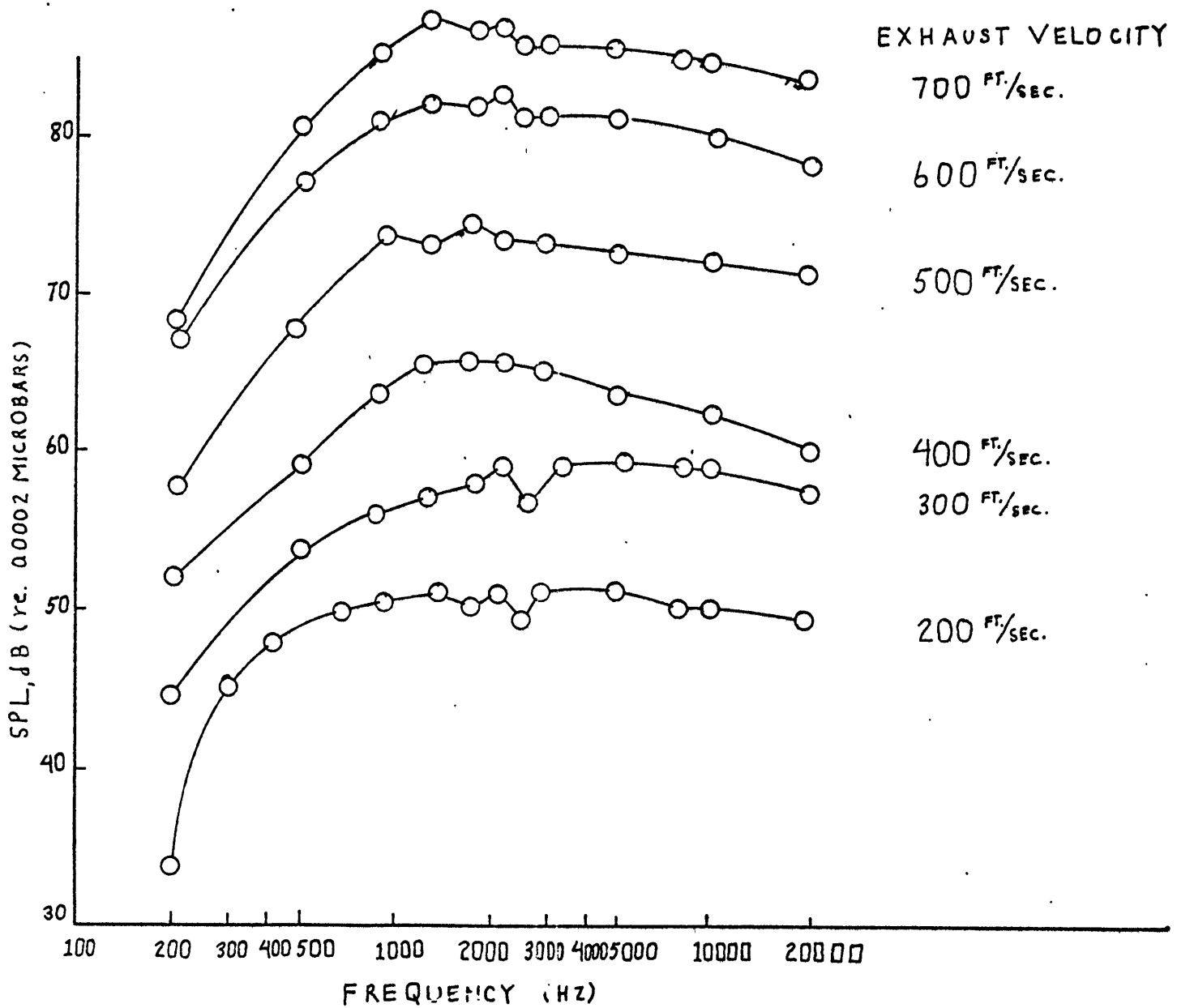

FIGURE 13. Comparison of NOise Spectra of Jet Noise for Different Blowing Velocities. Microphone Position, θ=25°, R=72"

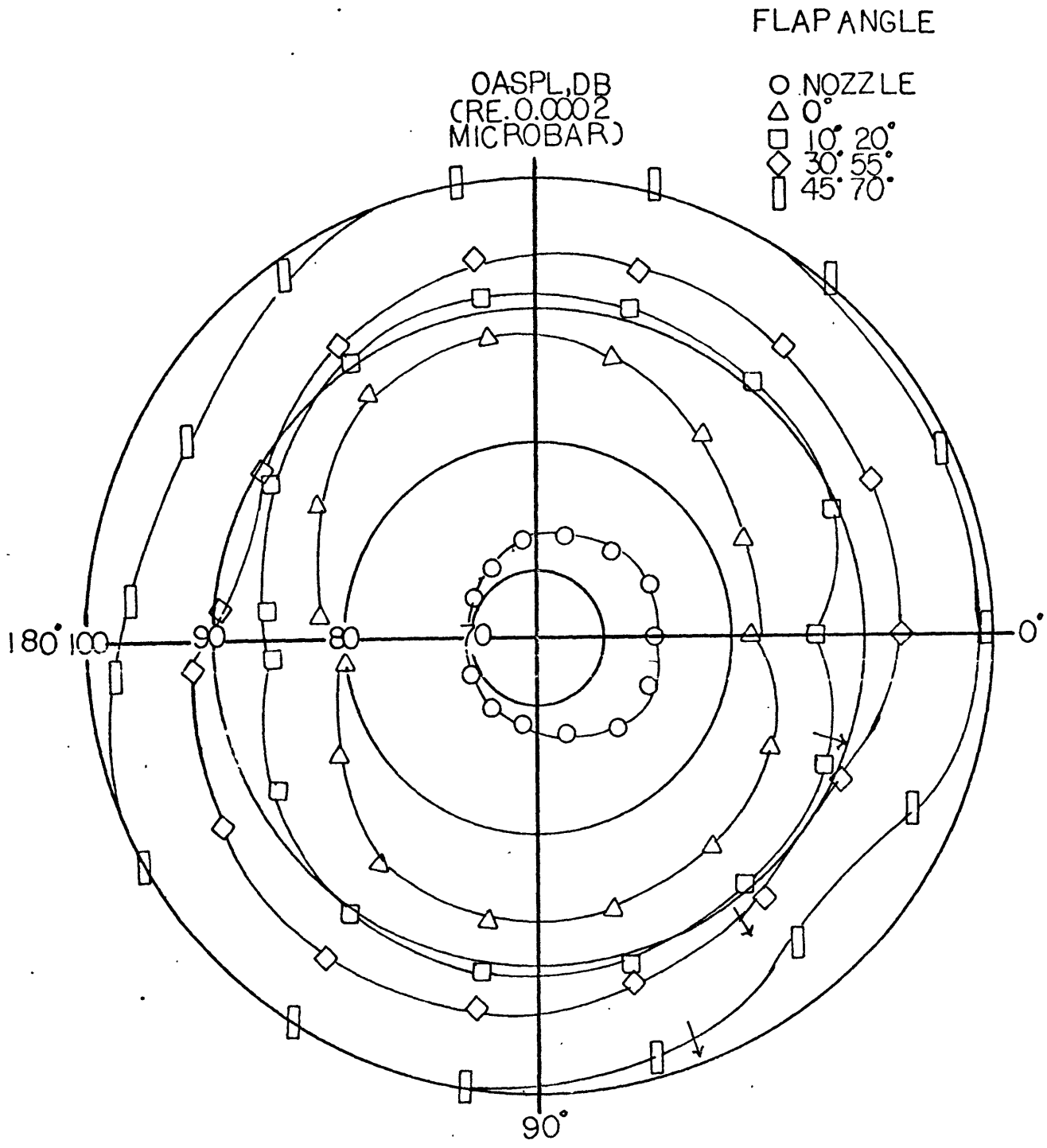

FIGURE 14. Comparison of Directional Patterns for the Various Flap Angles. Exhaust Velocity, 400 ft./sec. Microphone Position; R= 63.5 inches.

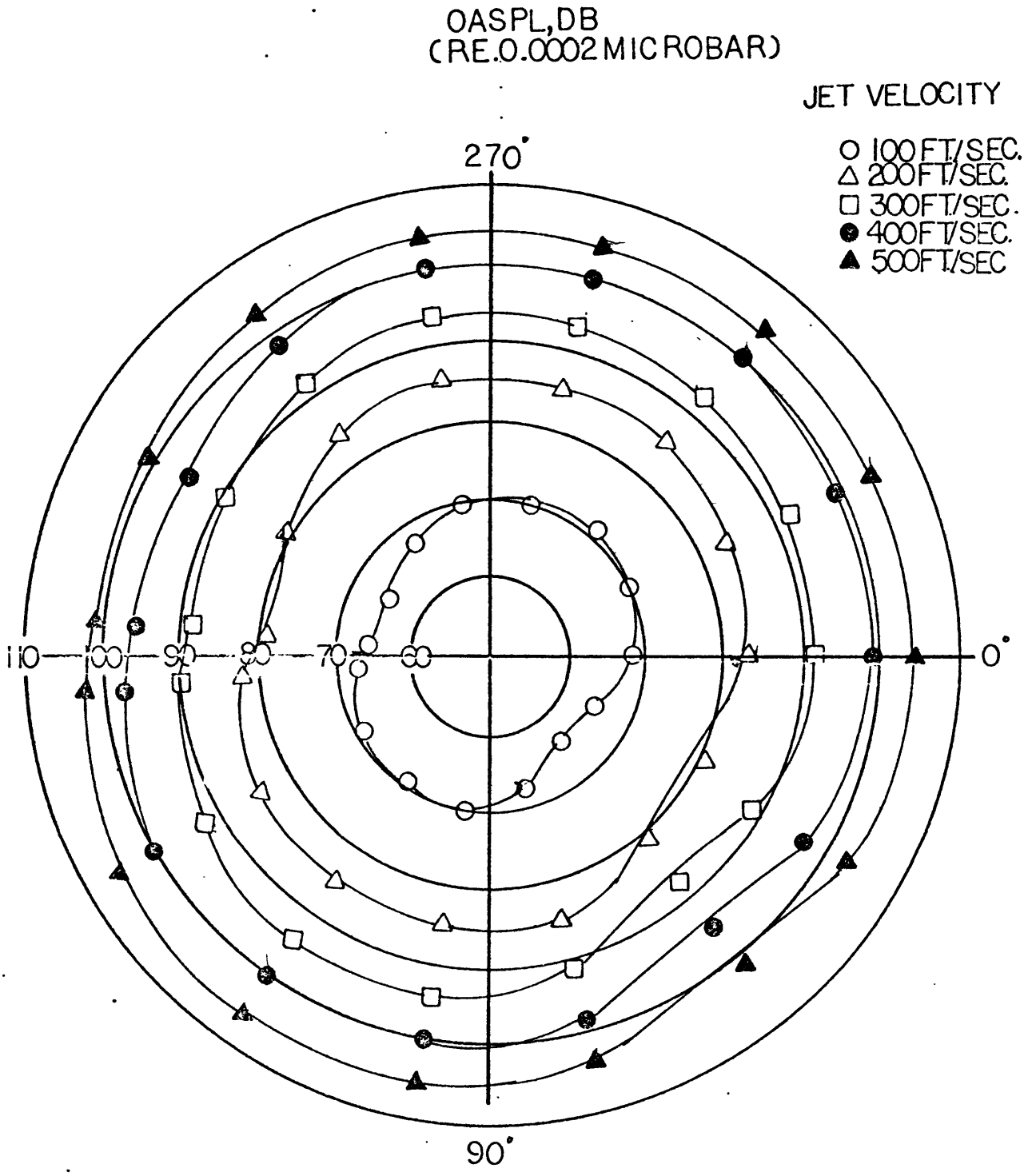

FIGURE 15. Directivity Pattern for an Externally Blown Flap at a 45°-70° Flap Angle. Microphone Radius, 63.5 inches.

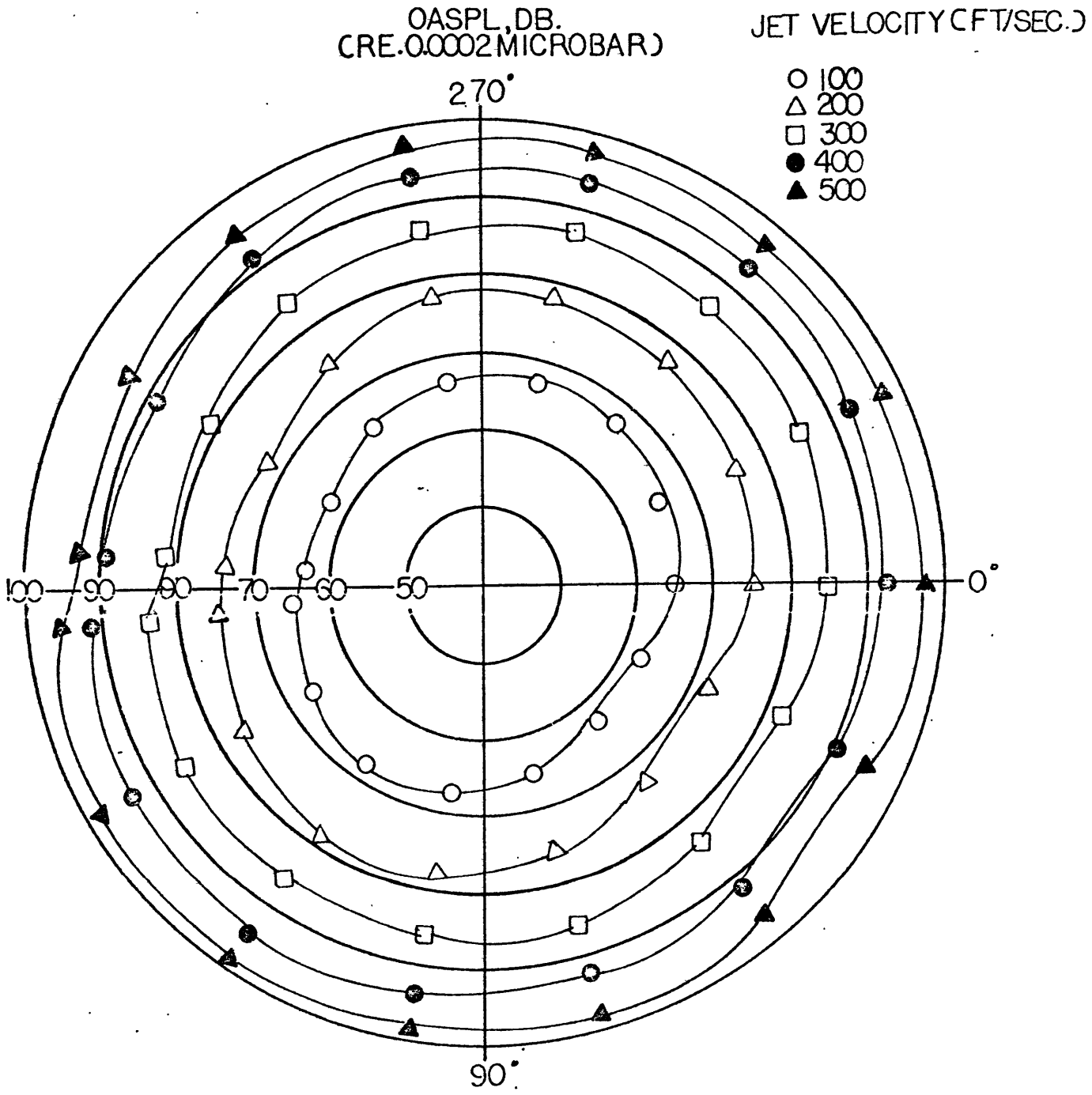

FIGURE 16. Directivity Pattern for an Externally Blown Flap at a 30°-55° Flap Angle. Microphone Radius 63.5 inches.

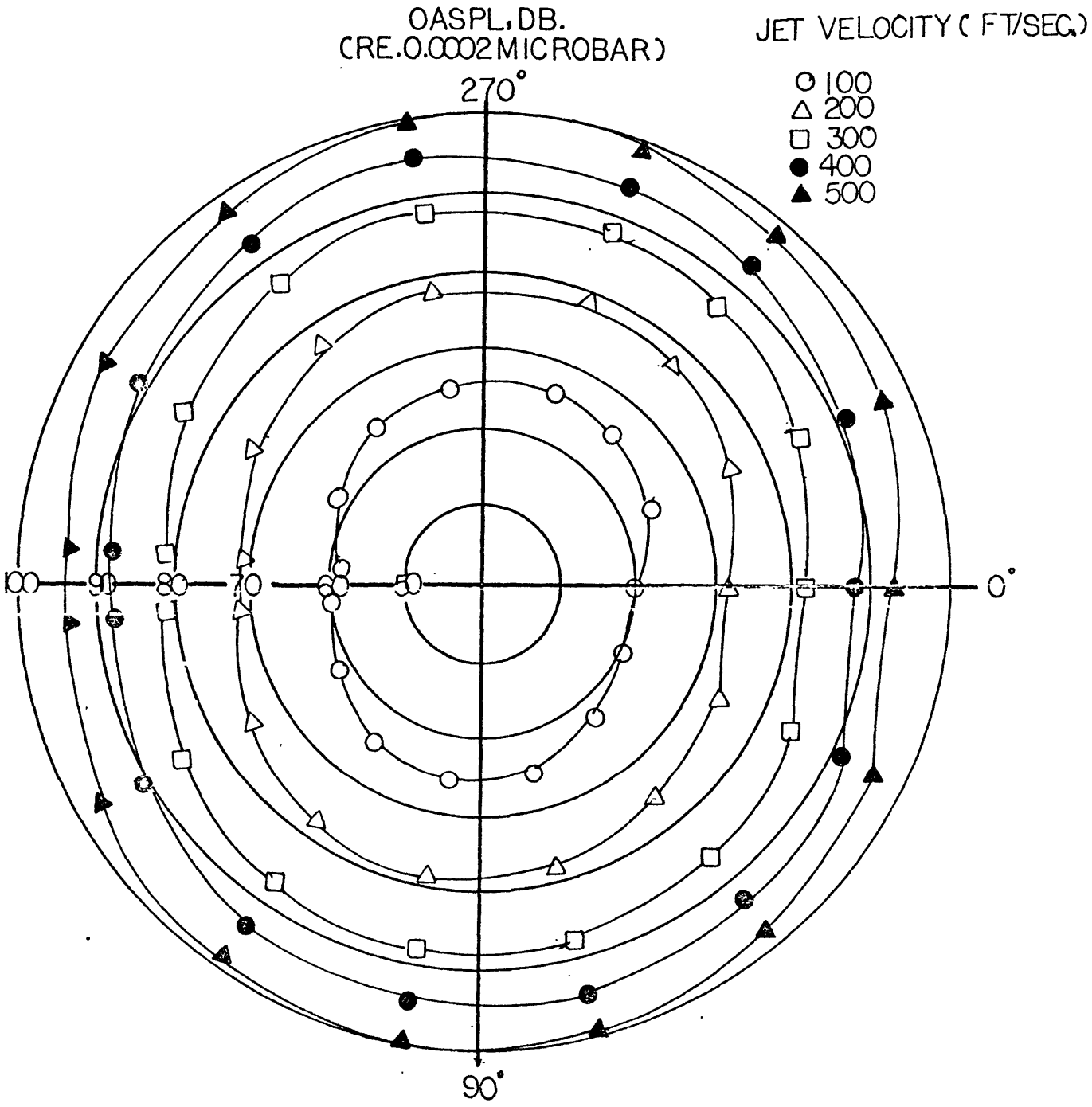

FIGURE 17. Directivity Pattern for an Externally Blown Flap at a 10°-20° Flap Angle. Microphone Radius, 63.5 inches.

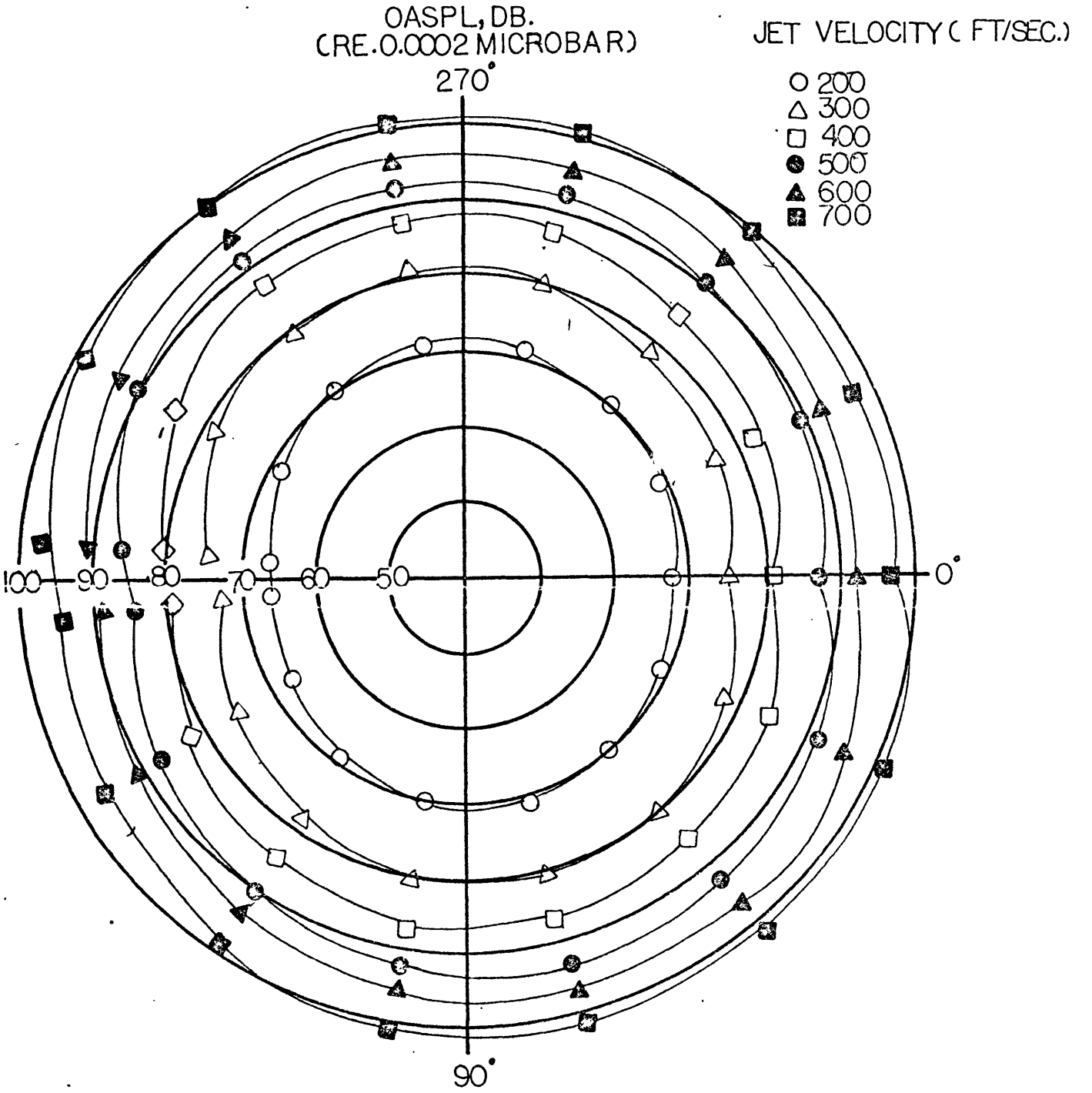

FIGURE 18. Directivity Pattern for an Externally Blown Flap at the Flaps Retracted Position. Microphone Radius, 63.5 inches.

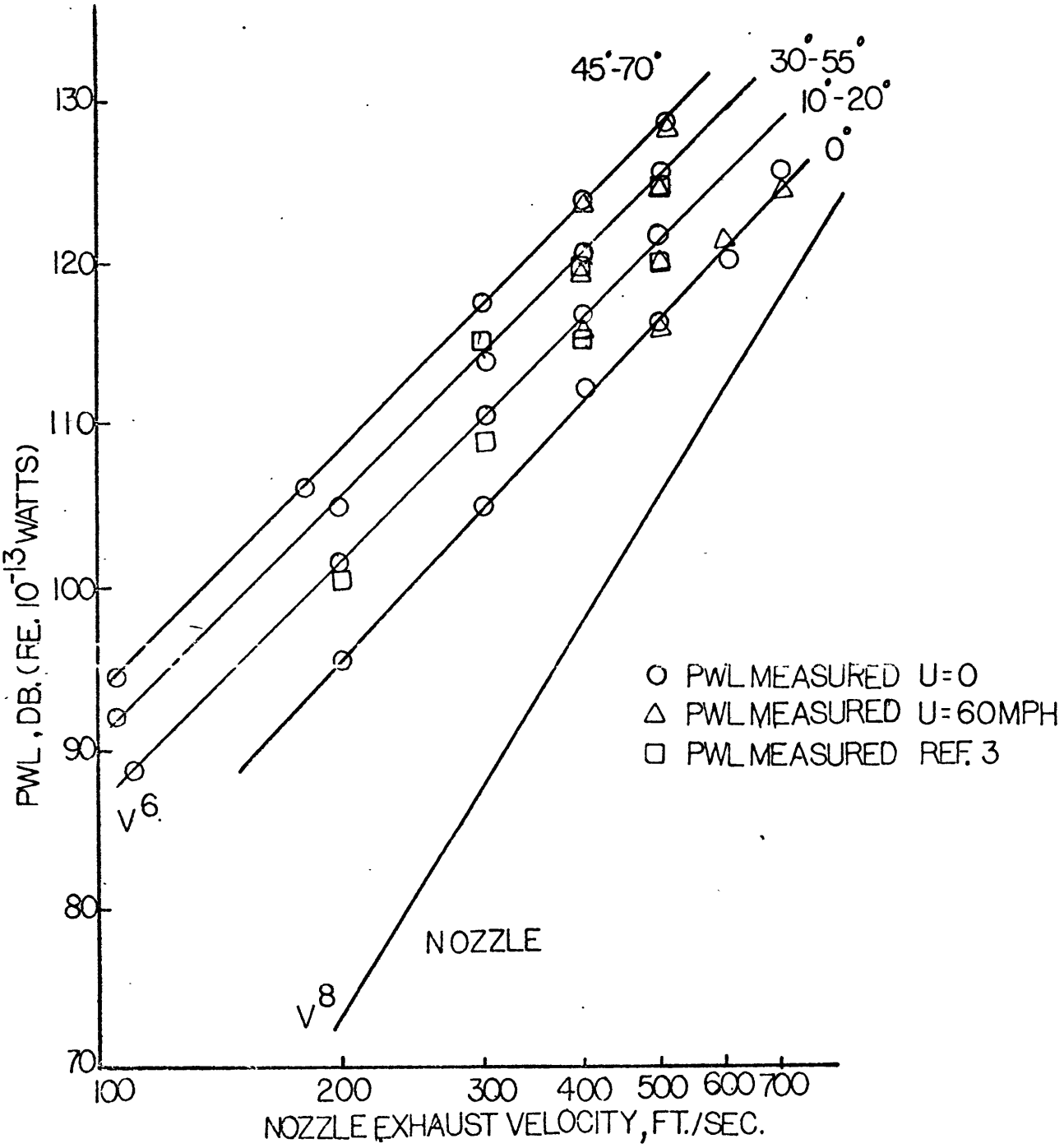

FIGURE 19. Comparison of the Power Radiated by the Five Test Configurations.

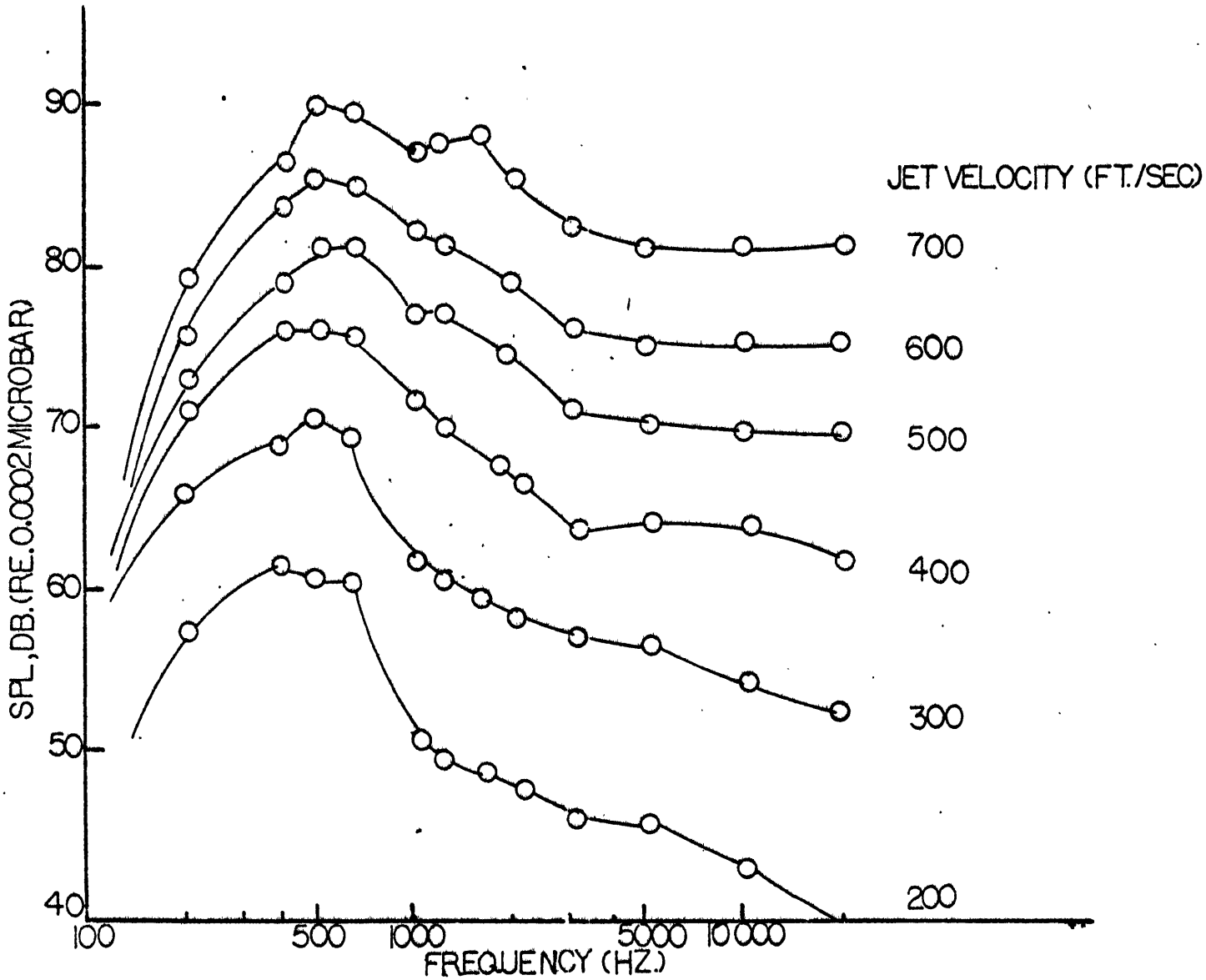

FIGURE 20. One-third Octave Sound Pressure Level Spectra for the Externally Blown Flap at the Flaps Retracted Position for the Various Jet Exhaust Velocities. Microphone location; $\theta = 90°$, $\phi = 0°$, R = 63.5 inches.

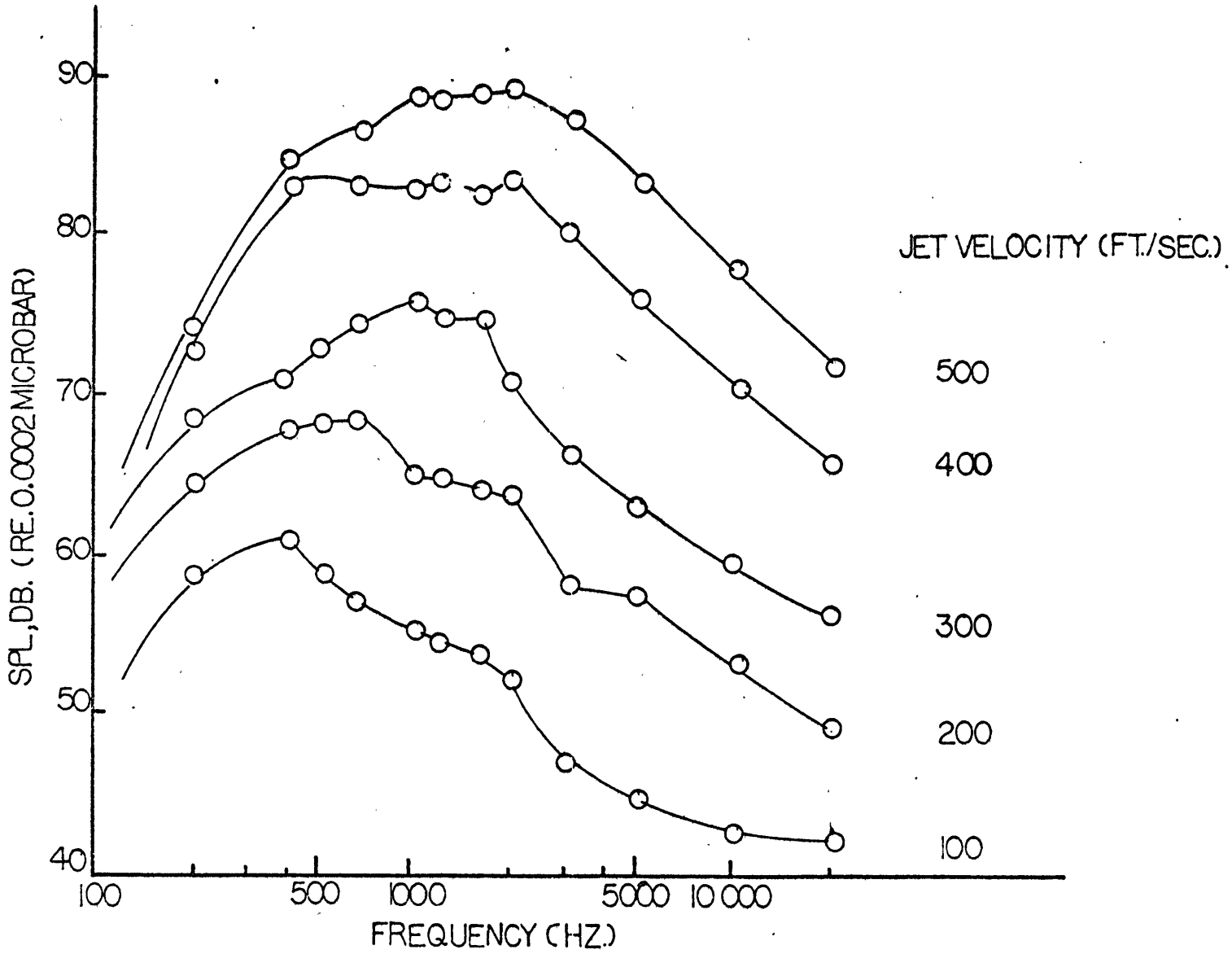

FIGURE 2]. One-third Octave Sound Pressure Level Spectra for the Externally Blown Flap at a 10°-20° Flap Angle for the Various Jet Exhaust Velocities. Microphone Location; $\theta = 90°$, $\phi = 0°$, R= 63.5inches.

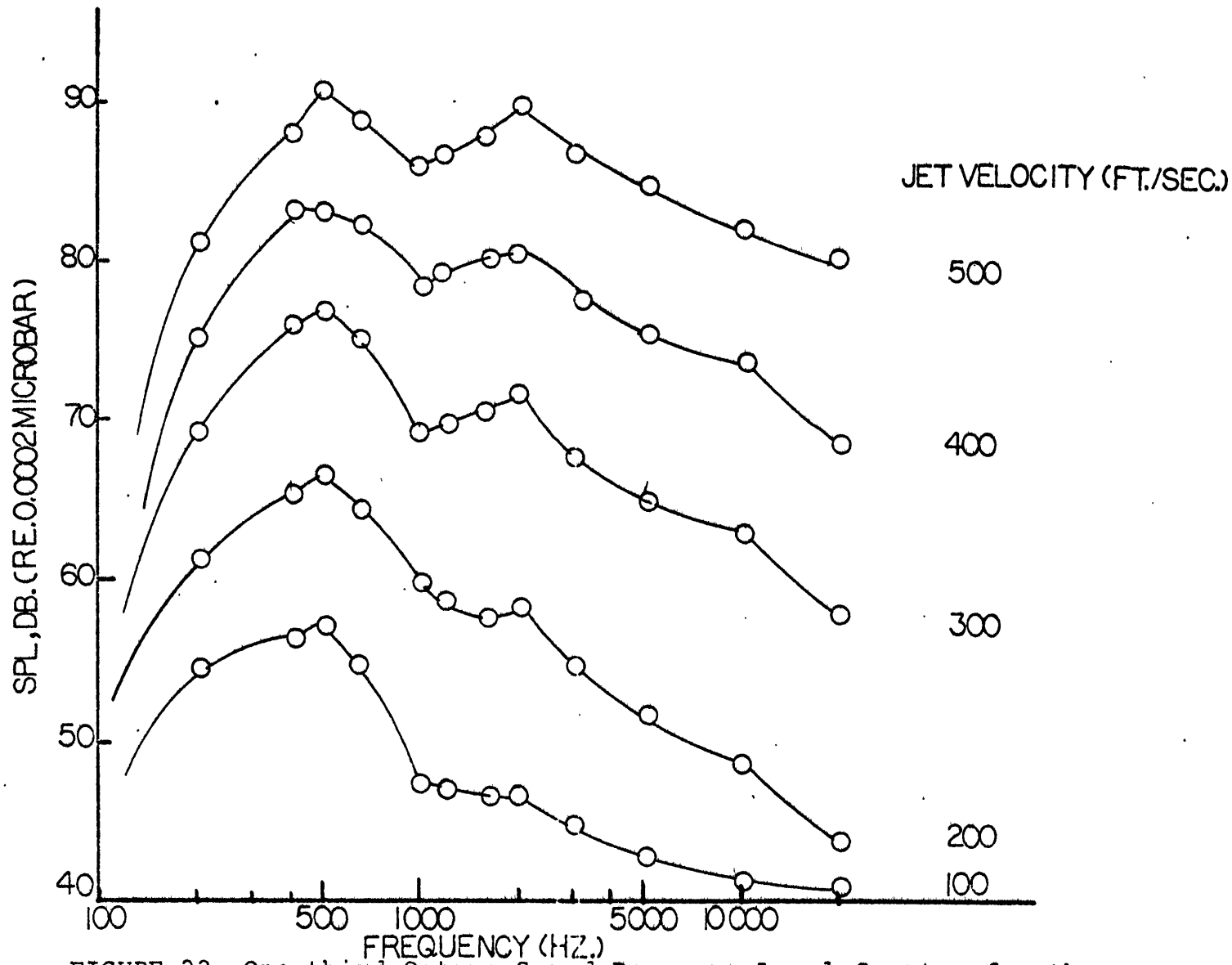

FIGURE 22. One-third Octave Sound Pressure Level Spectra for the Externally Blown Flap at a 30°-55° Flap Angle for the Various Jet Exhaust Velocities. MIcrophone Location; θ = 90°, ϕ = 0°, R = 63.5 inches.

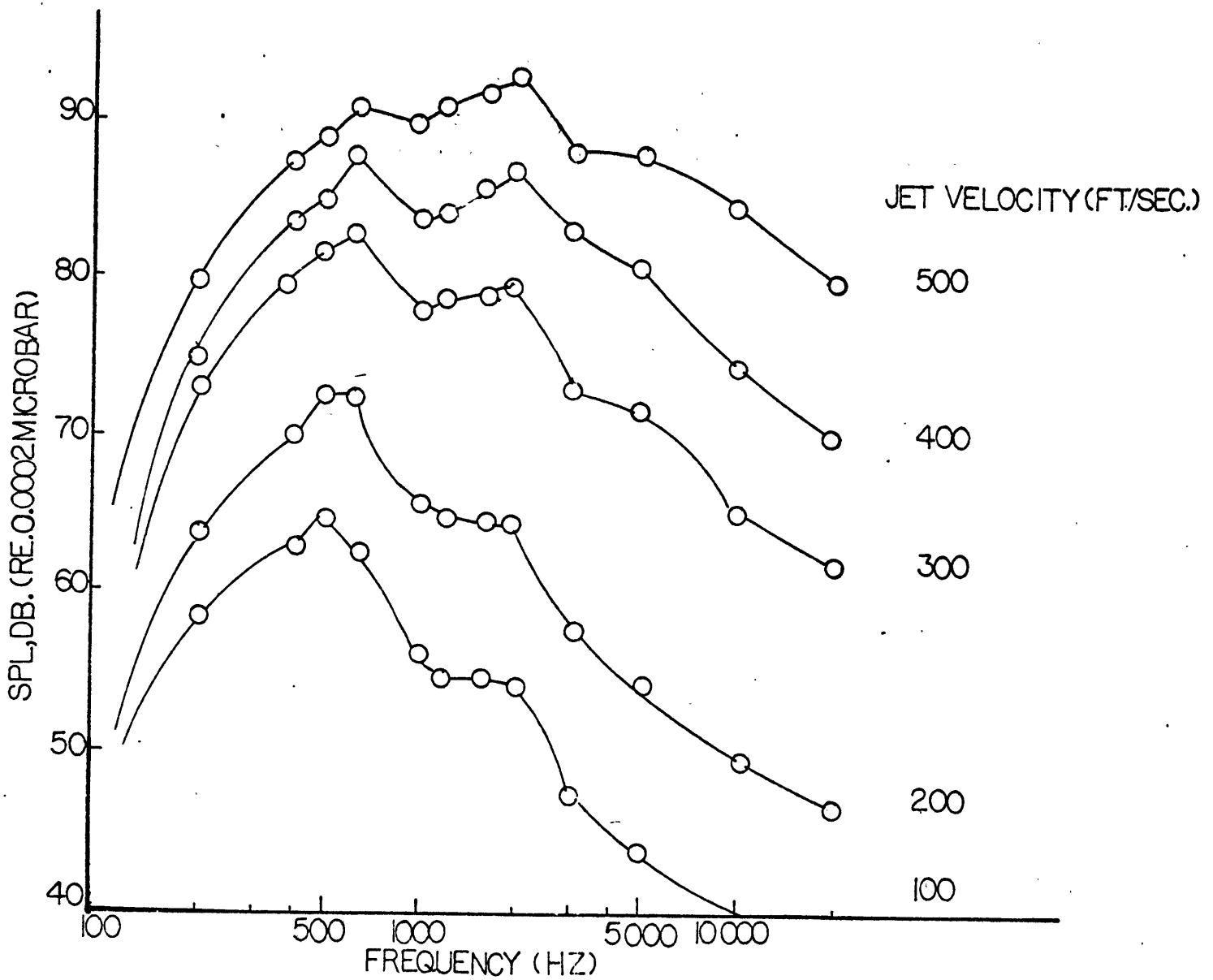

FIGURE 23. One-third Octave Sound Pressure Level Spectra for the Externally Blown Flap at a 45°-70° Flap Angle for the Various Jet Exhaust Velocities. Microphone Location; θ=90°, ϕ=0°, R=63.5 inches.

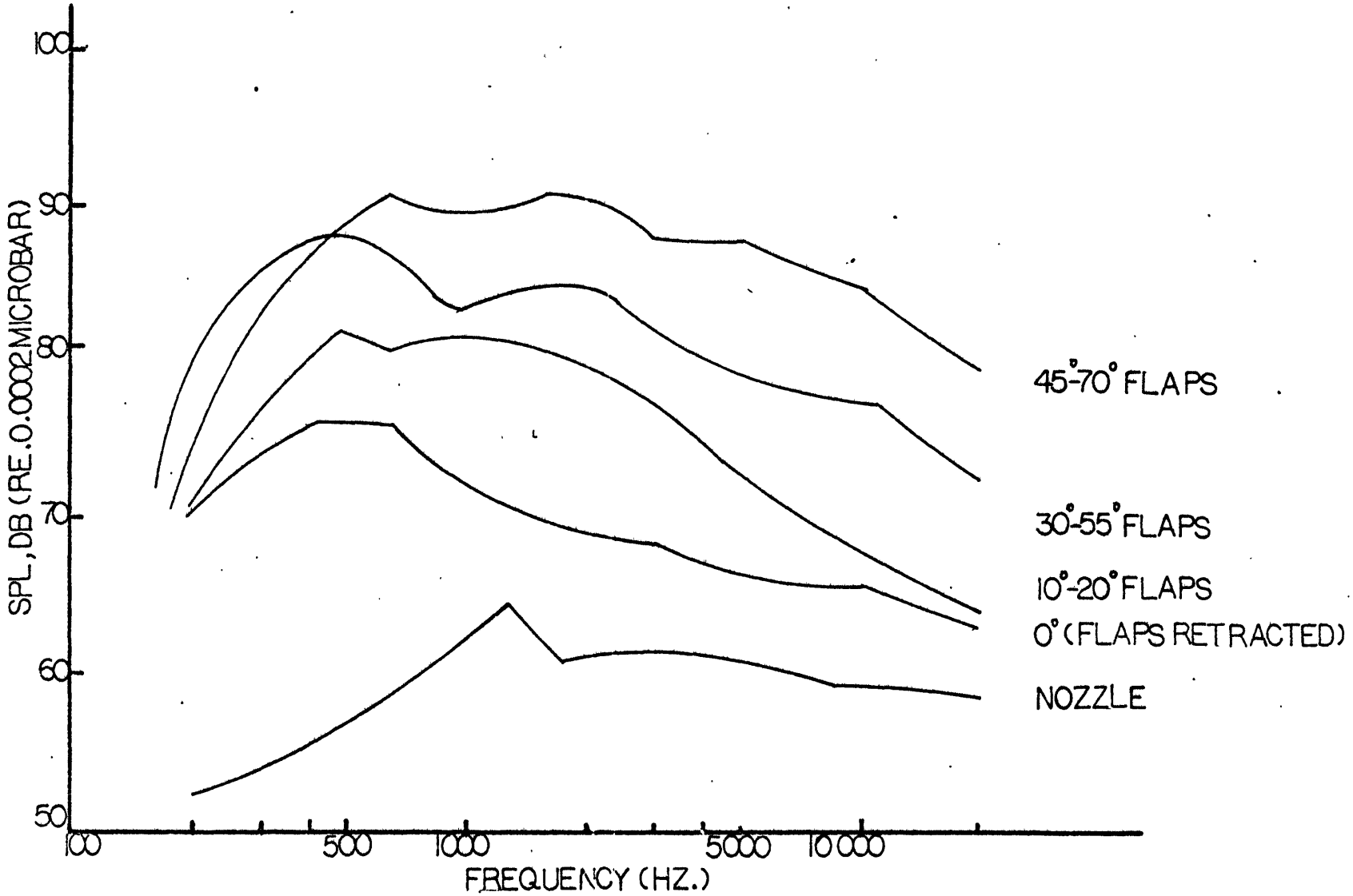

FIGURE 24. Typical Externally Blown Flap One-third Octave Spectra for the Different Flap Configurations Tested. Exhaust Velocity, 400 ft./sec. Microphone Position; θ = 90°, ϕ = 0°, R = 63.5 inches.

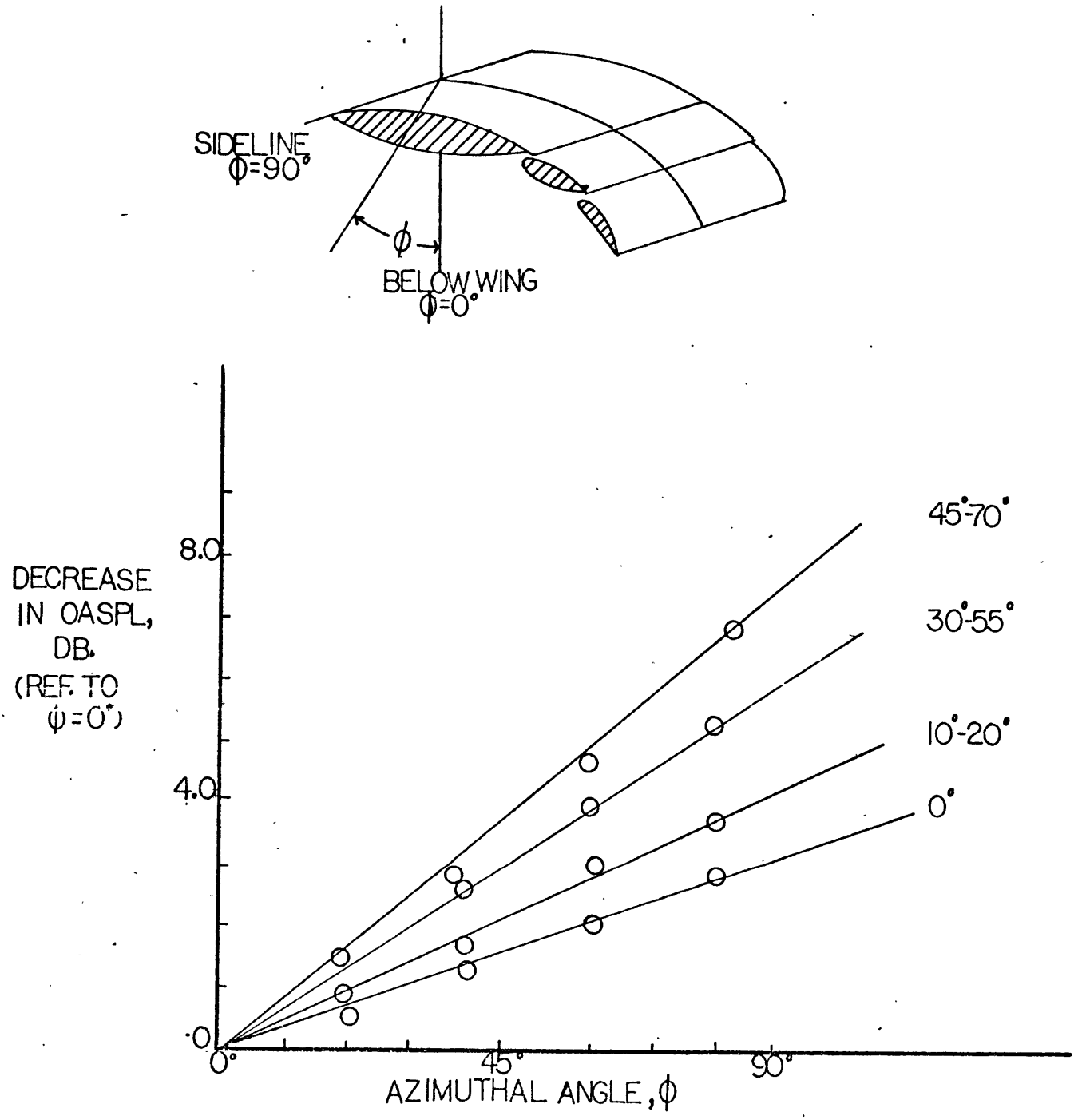

FIGURE 25. Decrease in Externally Blown Flap Noise with Azimuthal Angle, ϕ for each Flap Configuration Microphone Location; R = 63.5, θ = 90°. Jet Velocity, 400 feet/second.

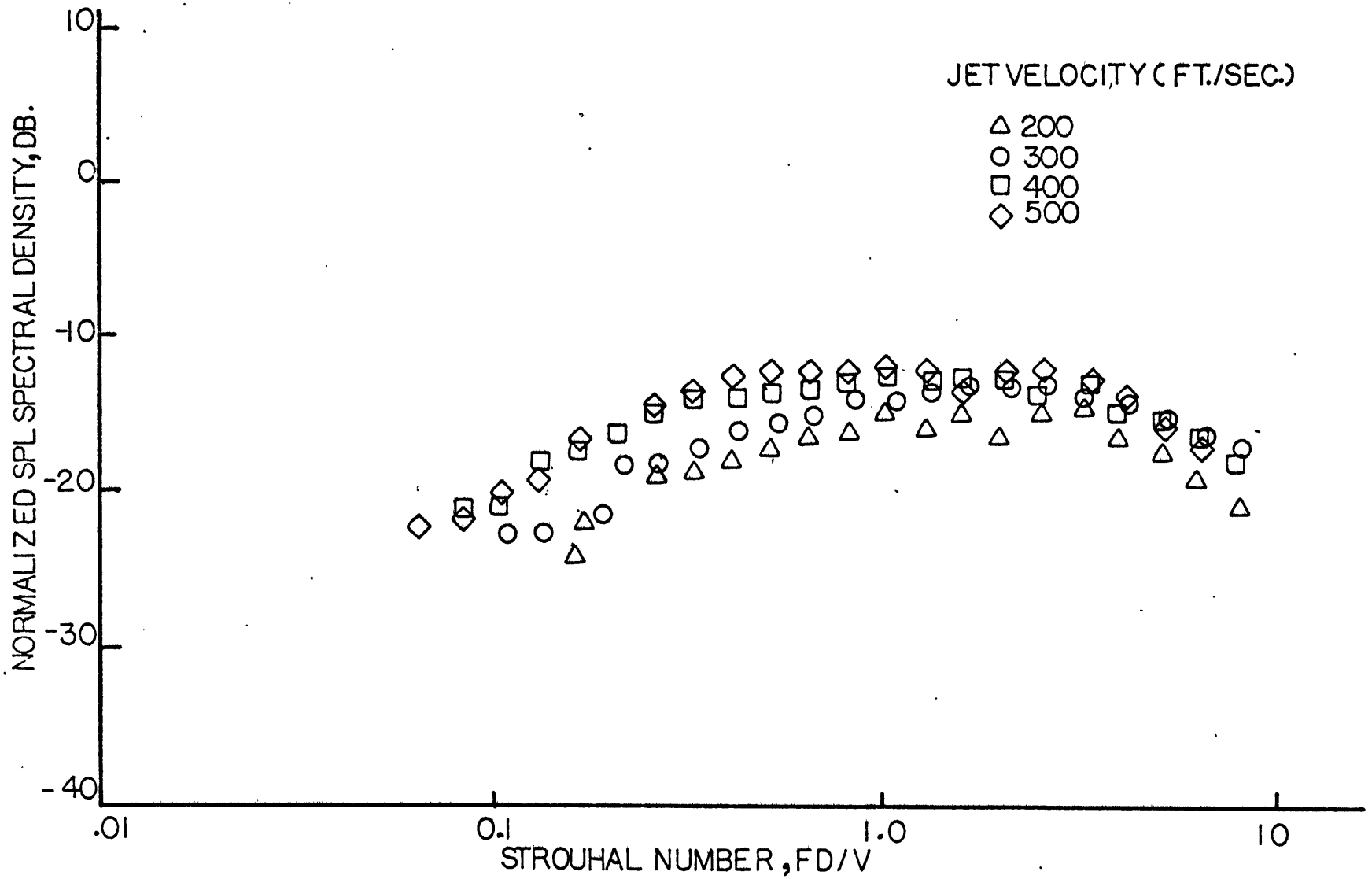

FIGURE 26. Normalized SPL - Spectral Density as a Function of the Nozzle Strouhal Number. Noise Generated by a 2 inch Diameter Nozzle. Microphone Angle, 90°.

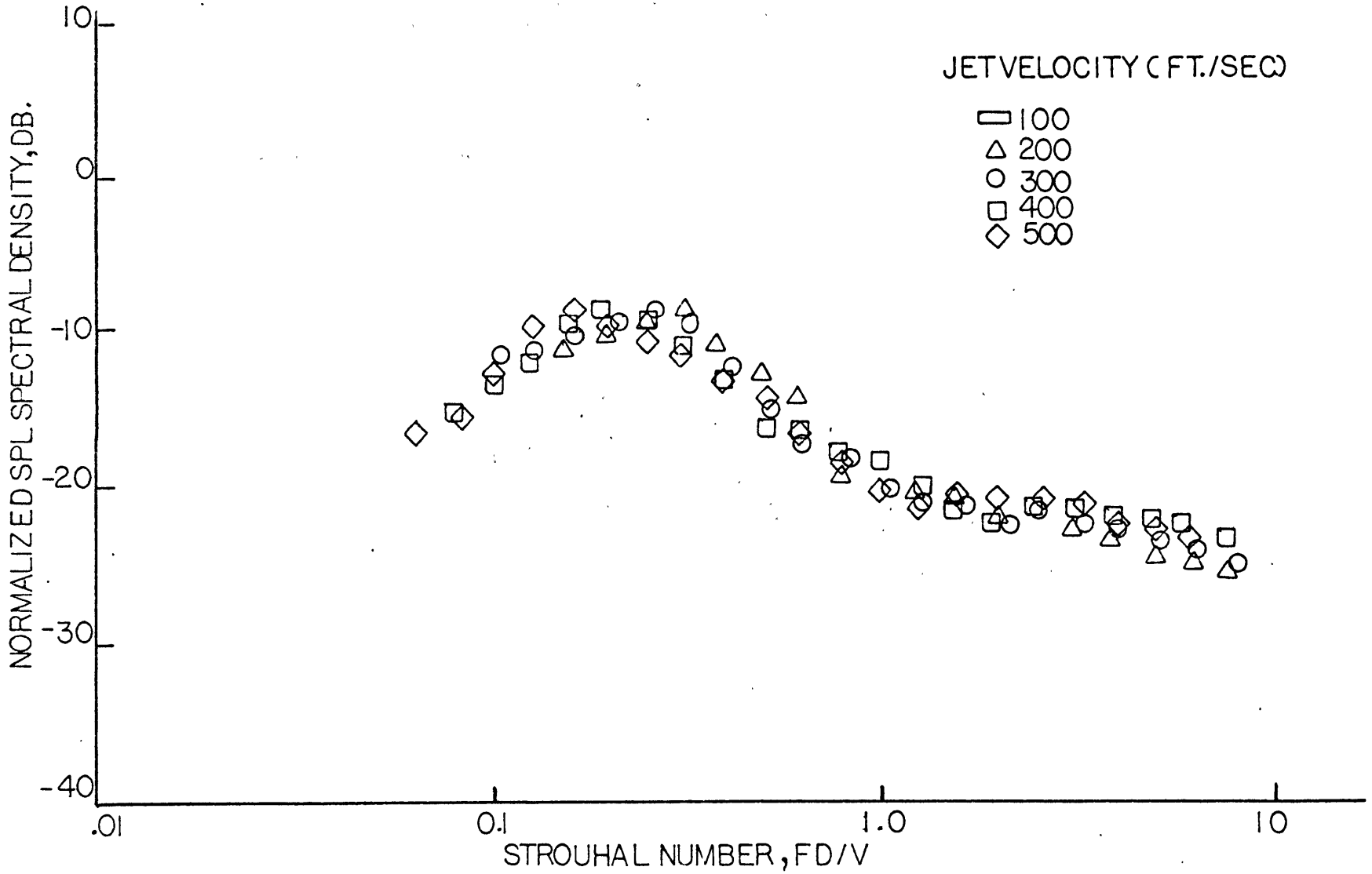

FIGURE 27. Normalized SPL - Spectral Density as a Function of the Nozzle Strouhal Number. Noise generated by Externally Blown Flap Model, Basic Configuration at 0° Flap POsition. Microphone Angle, 90°.

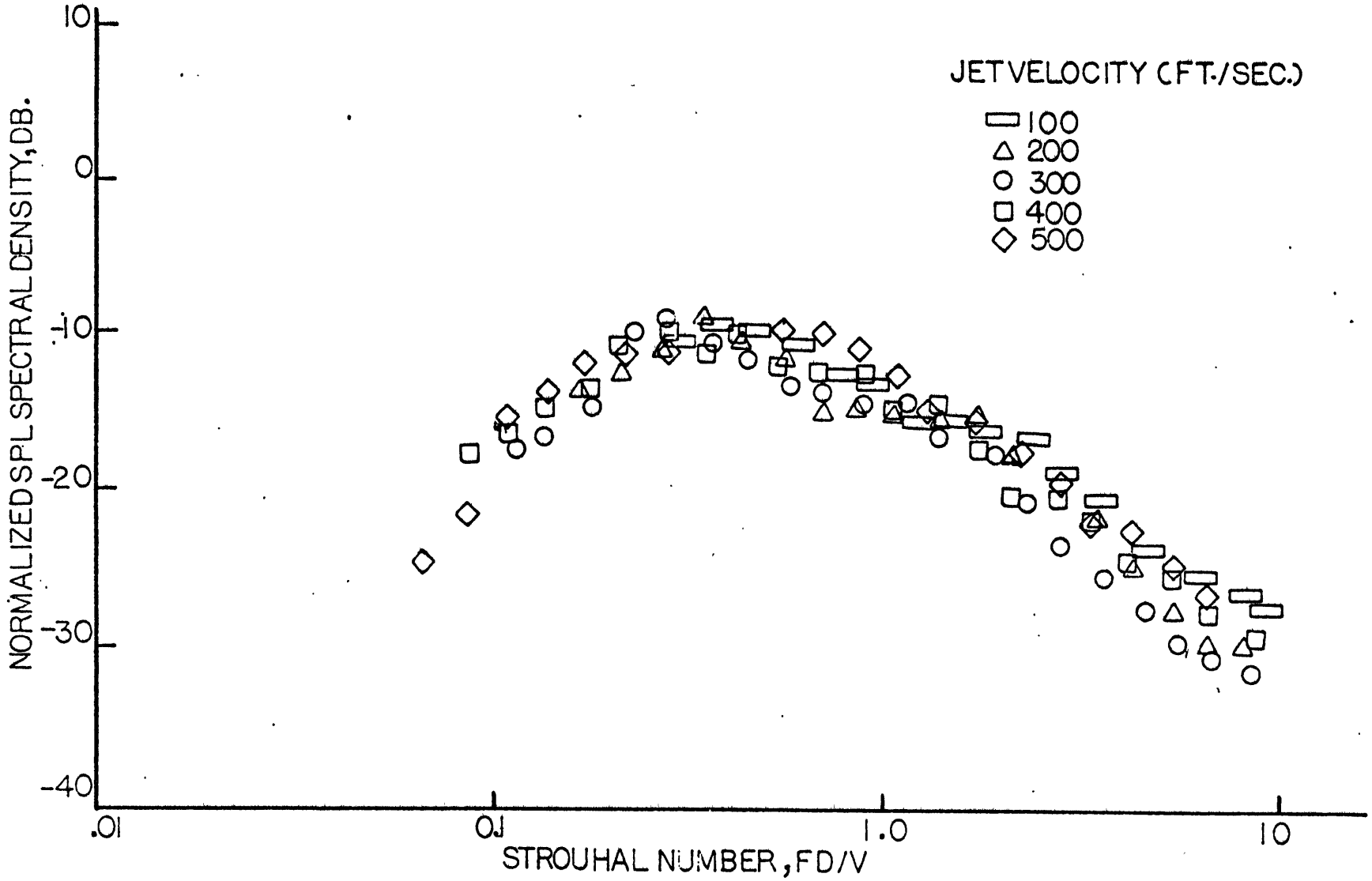

FIGURE 28. Normalized SPL Spectral Density as a Function of the Nozzle Strouhal Number. NOise Generated by the Externally Blown Flap Model, Basic Configuration at 10°-20° Flap Angle. Microphone Location, 0 = 90°.

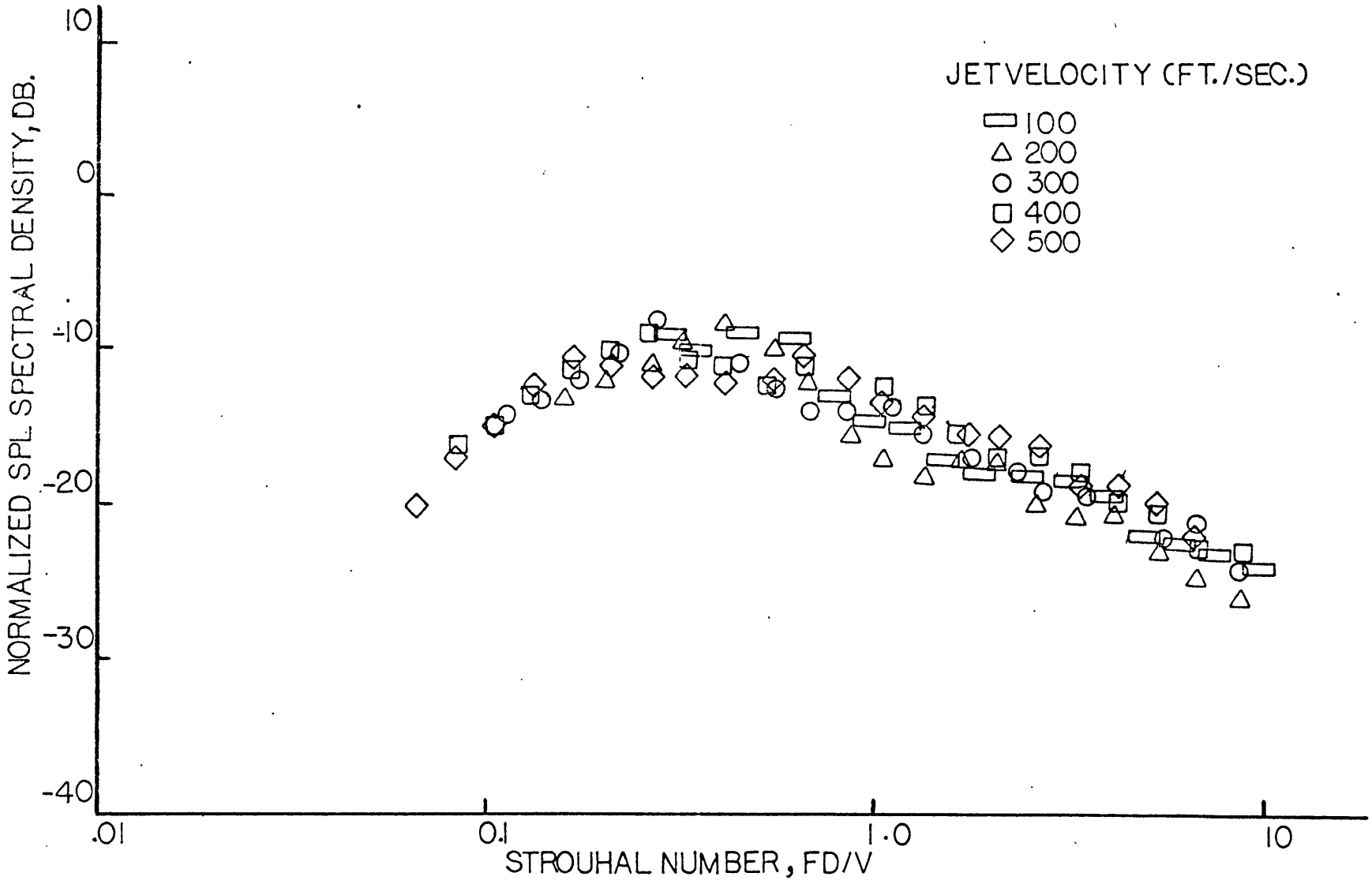

FIGURE 29. Normalized SPL Spectral Density as a Function of the Nozzle Strouhal Number. Noise Generated by the Externally Blown Flap Model, Basic Configuration at 30°÷55° Flap Angle. Microphone Angle, 90°.

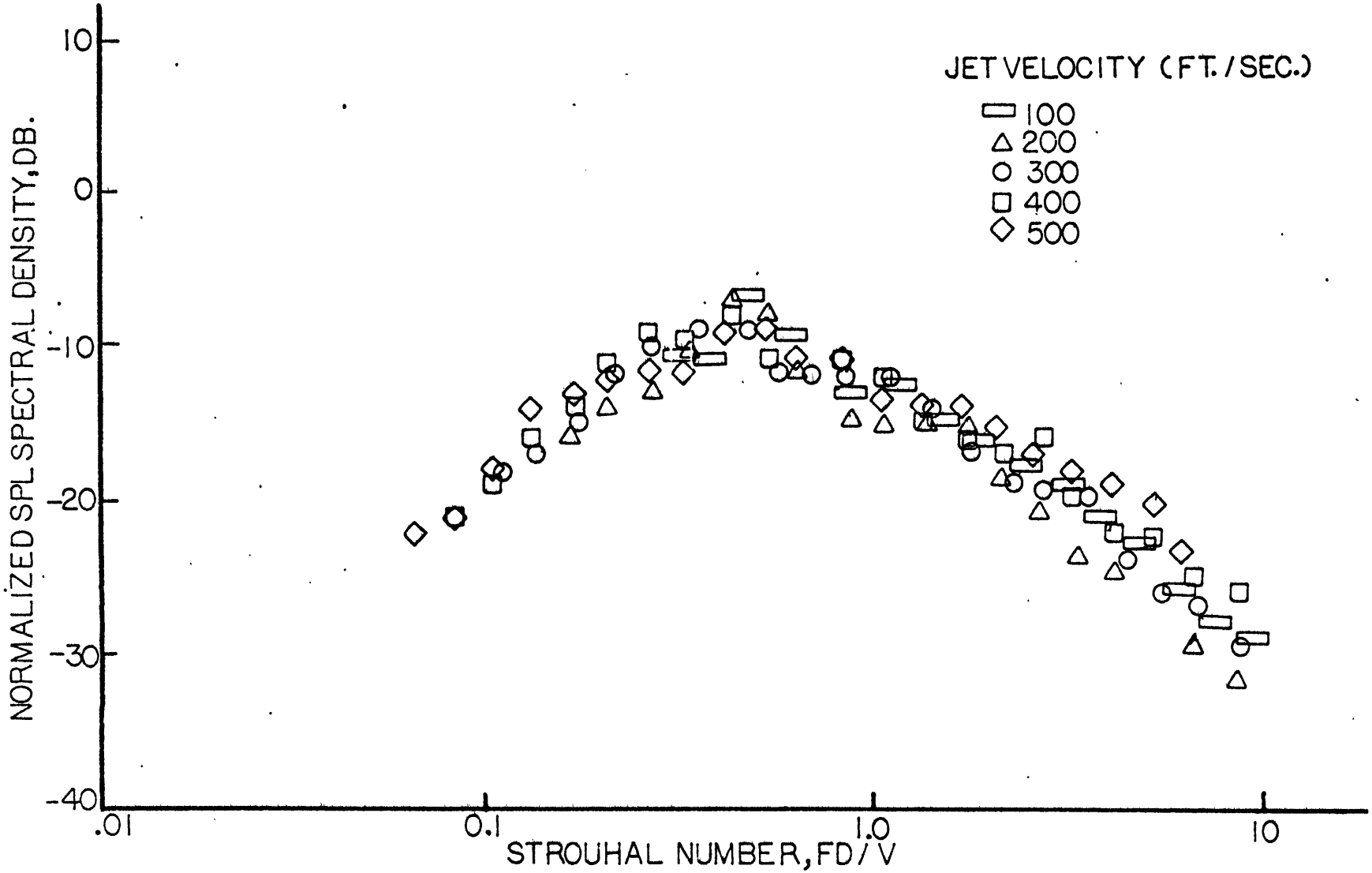

FIGURE 30. Normalized SPL Spectral Density as a Function of the Nozzle Strouhal Number. Noise Generated by the Externally Blown Flap Model , Basic Configuration at 45°-70° Flap Angle. Microphone Angle, 90°.

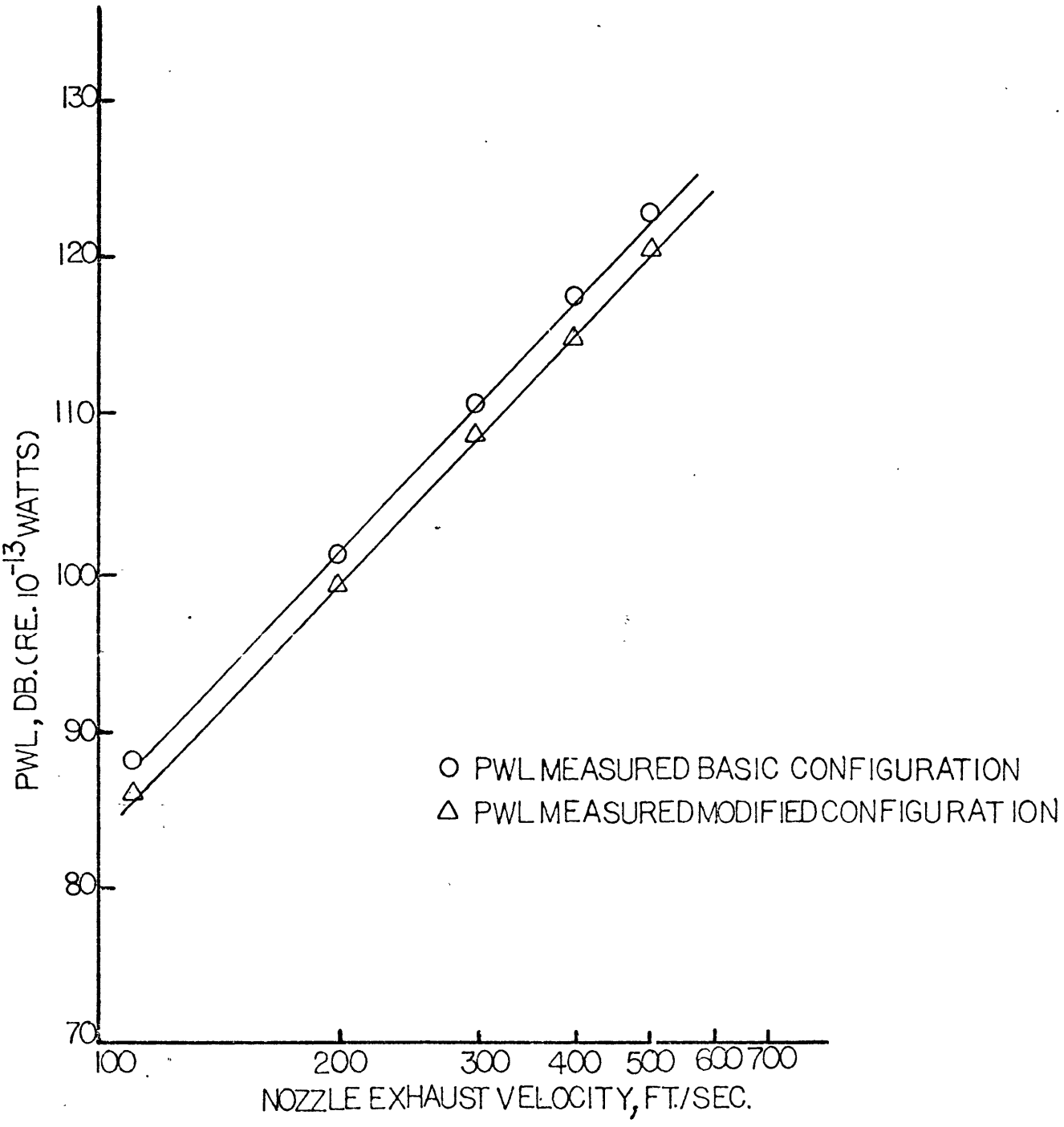

FIGURE 31. Comparison of the Power Radiated from the Basic and Modified Externally Blown Flap Configurations with a Flap Angle of 10°-20°.

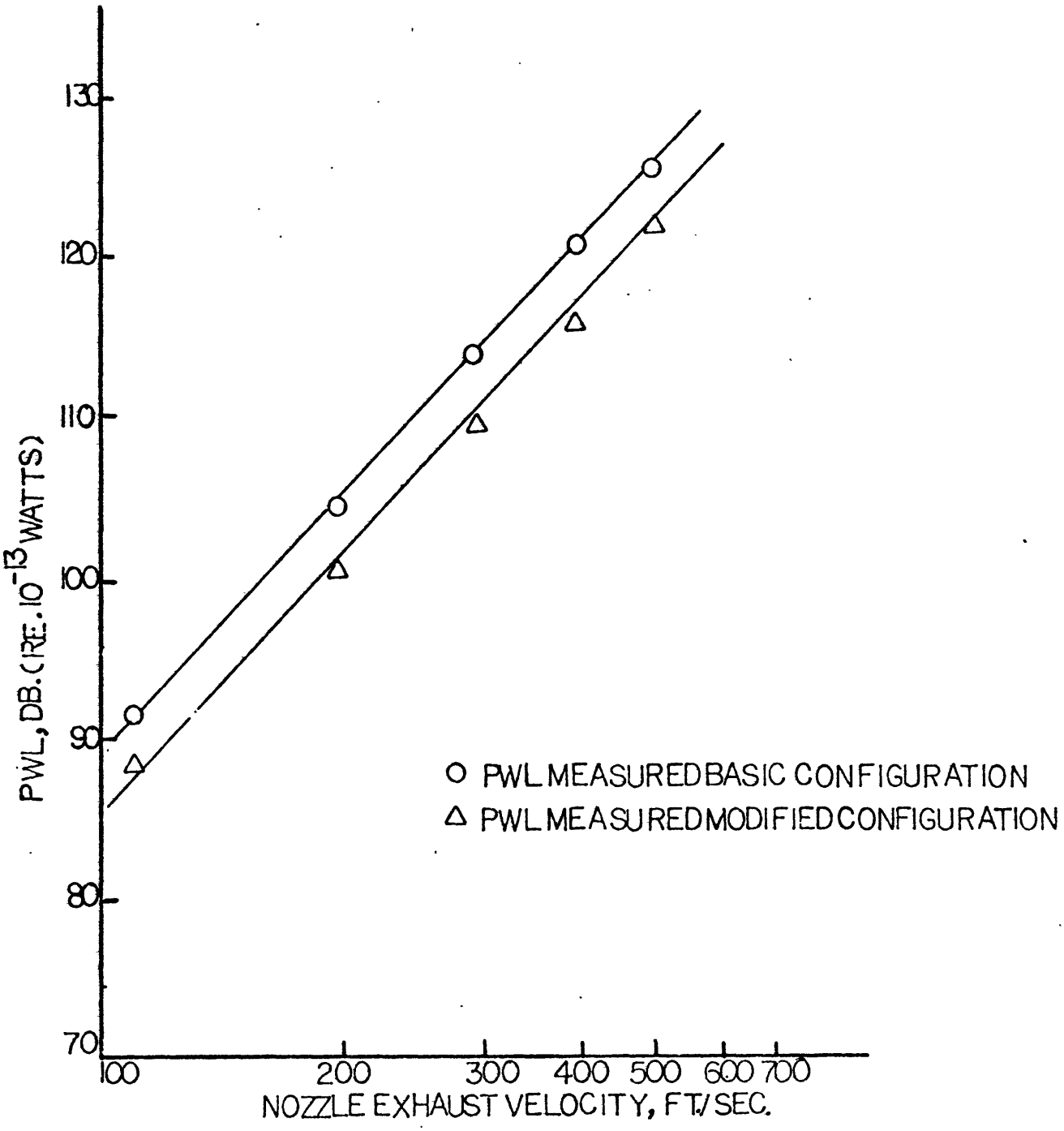

FIGURE 32. Comparison of the Power Radiated from the Basic and Modidied Externally Blown Flap Configuration with a Flap Angle of 30°-55°.

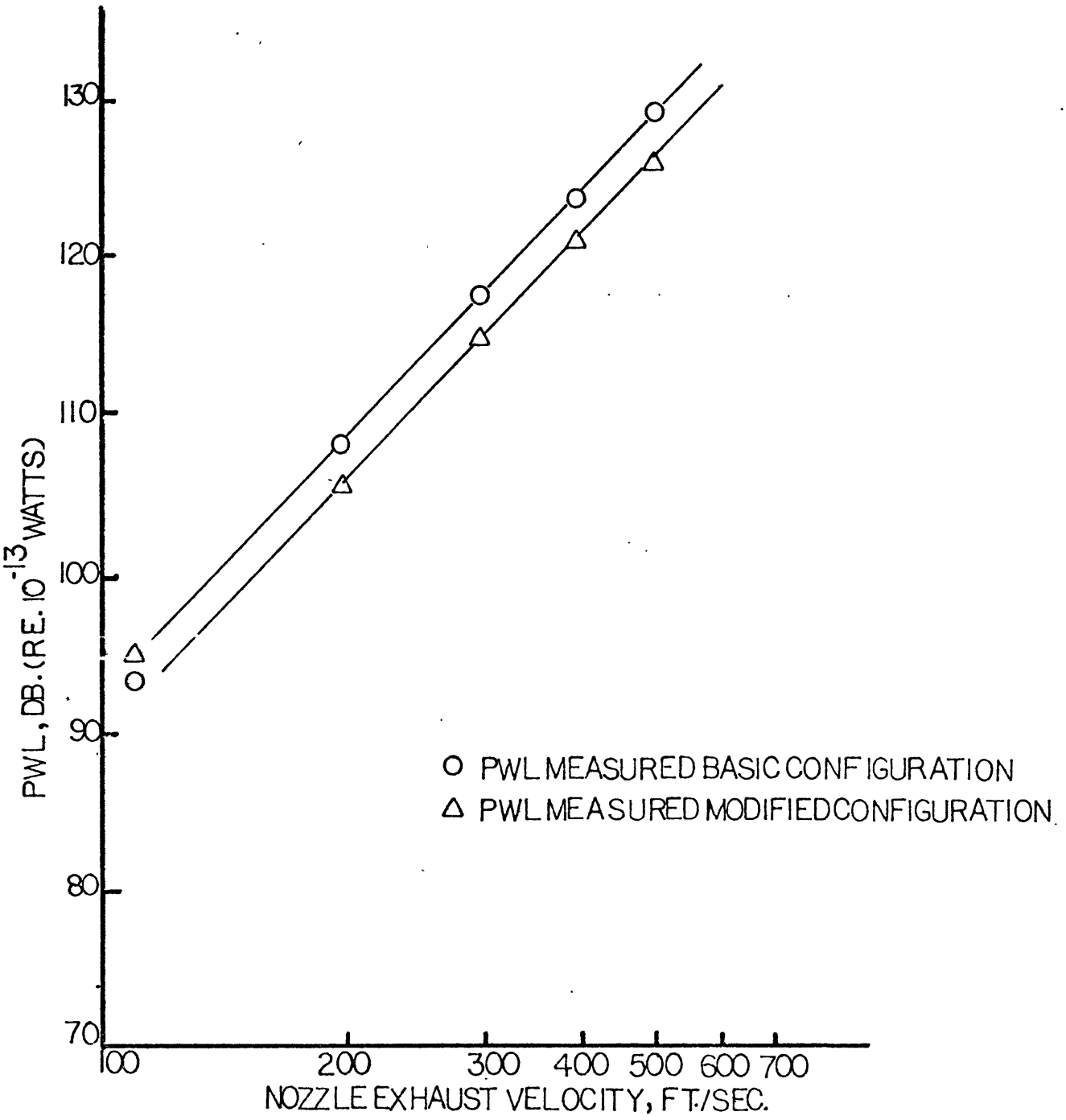

FIGURE 33. Comparison of the Power Radiated from the Basic and Modified Externally Blown Flap Configuration with a Flap Angle of 45°-70°.

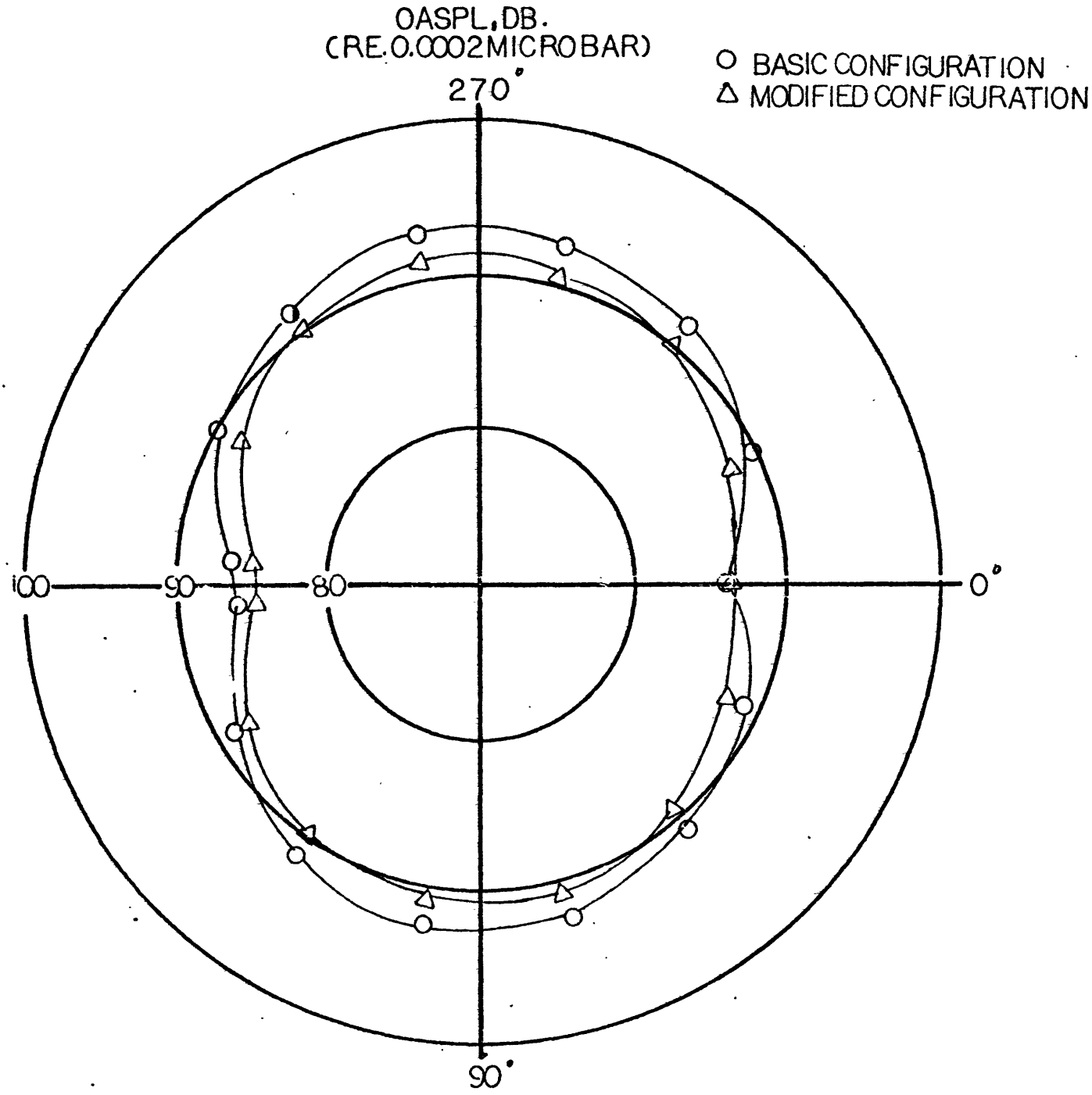

FIGURE 34. Comparison of the Directivity Patterns for the Basic and Modified Externally Blown Flap Configurations with a Flap Angle of 10°-20°. Microphone Location; R = 63.5 inches, ϕ = 0°. Blowing Velocity, 400 ft./sec.

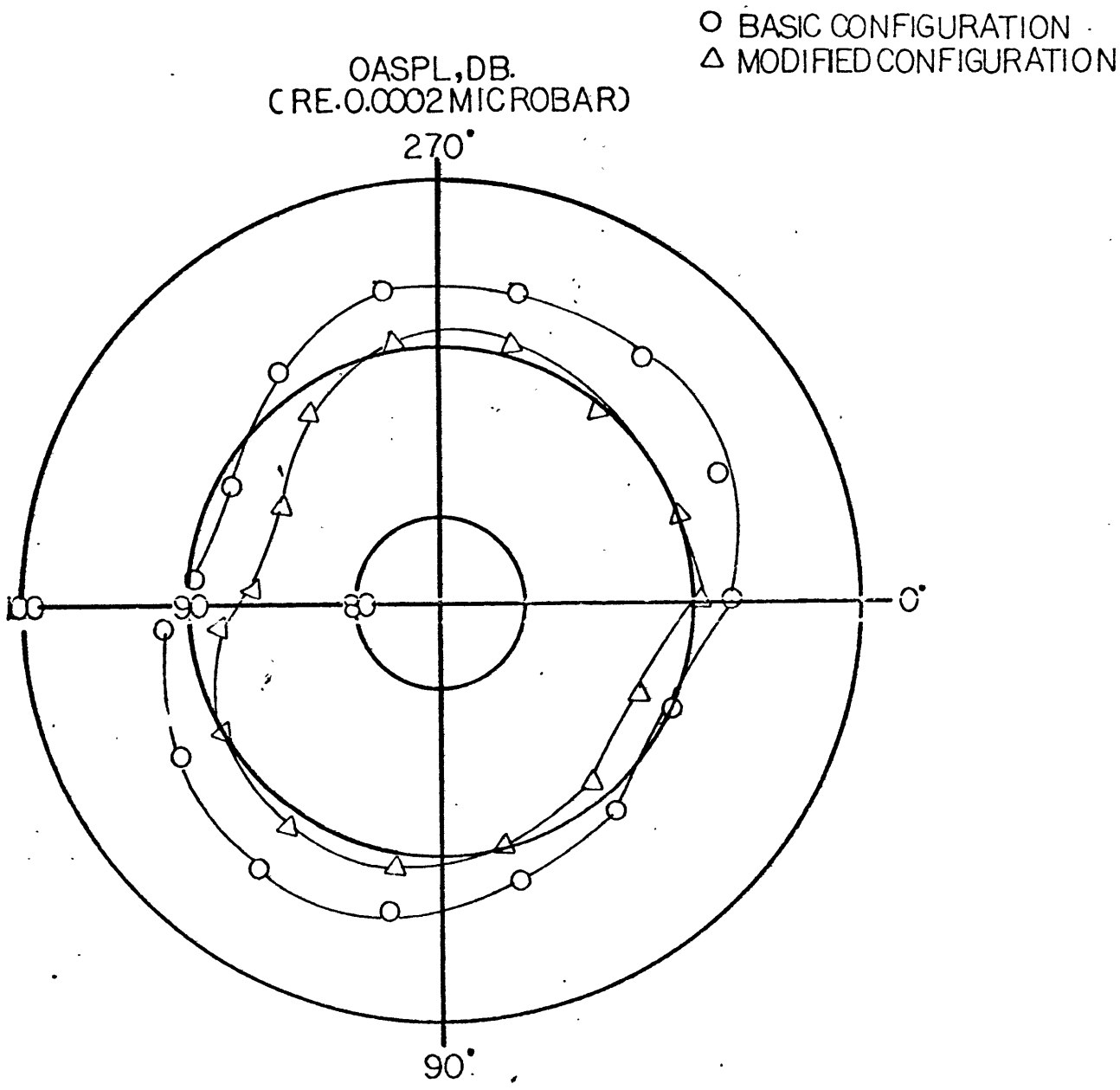

FIGURE 35. Comparison of the Directivity Patterns for the Basic and Modified Externally Blown Flap Configurations with a Flap Angle of 30°-55°. Microphone Location; R = 63.5 inches, ϕ = 0°. Blowing Velocity, 400 ft./sec.

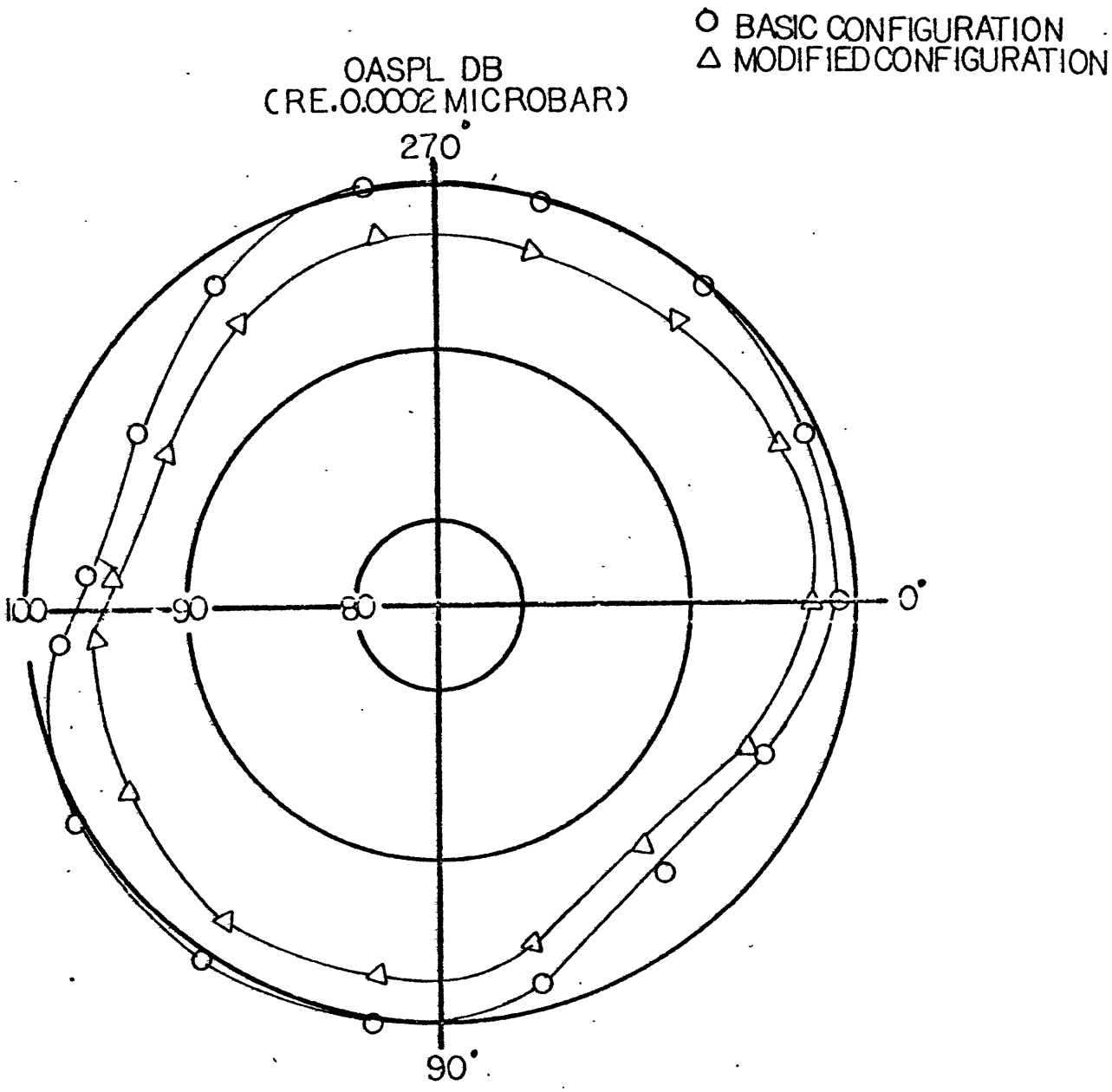

FIGURE 36. Comparison of the Directivity Patterns for the Basic and Modified Externally Blown Flap Configurations with a Flap Angle of 45°-70°. Microphone Location; ϕ = 0°, R = 63.5 inches. Blowing Velocity, 400 ft./sec.

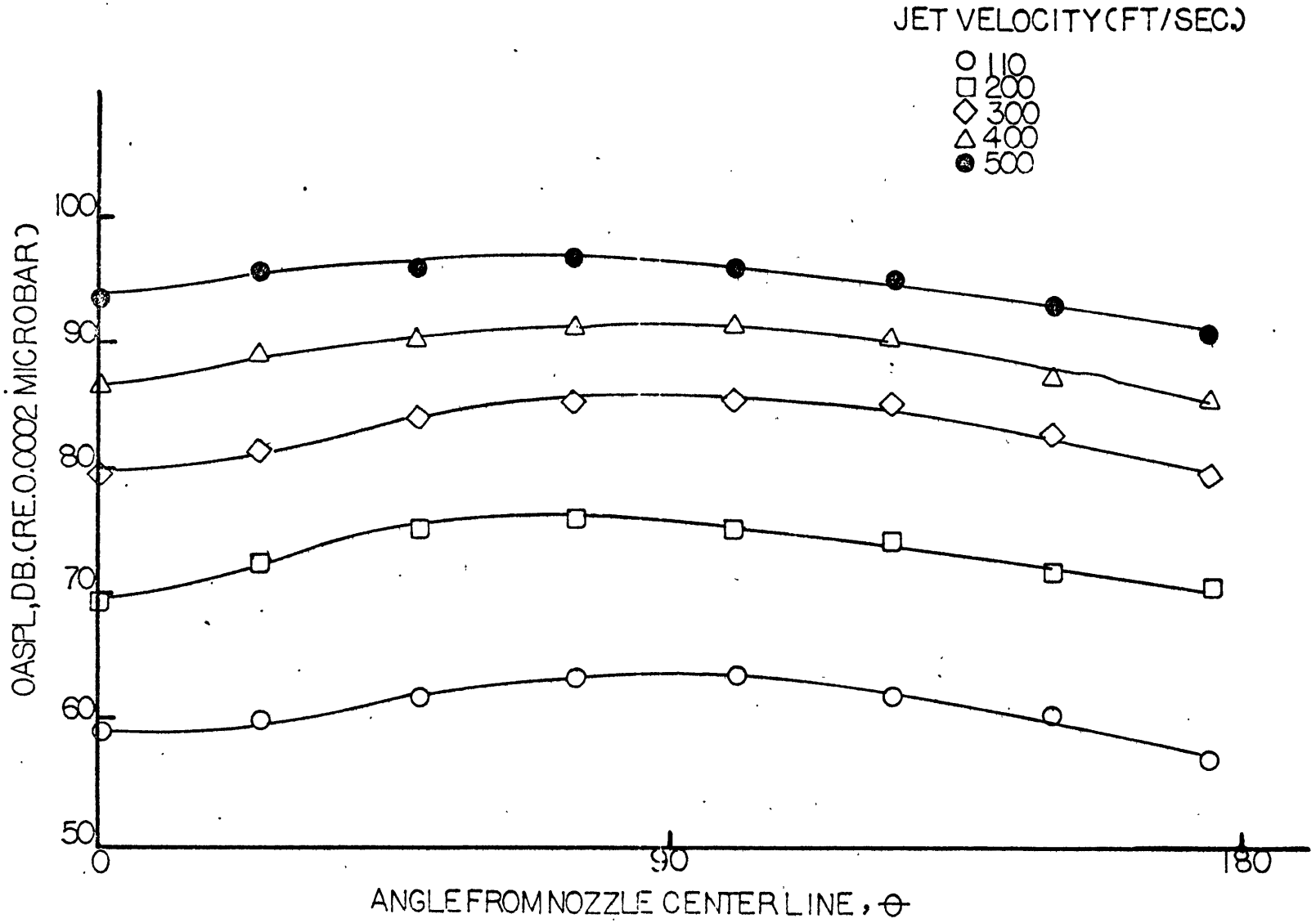

FIGURE 37. Effect of Jet Exhaust Velocity on the OASPL for the Modified Externally Blown Flap with a 10°-20° Flap Angle. Microphone Position; ϕ = 0°, R = 63.5 inches.

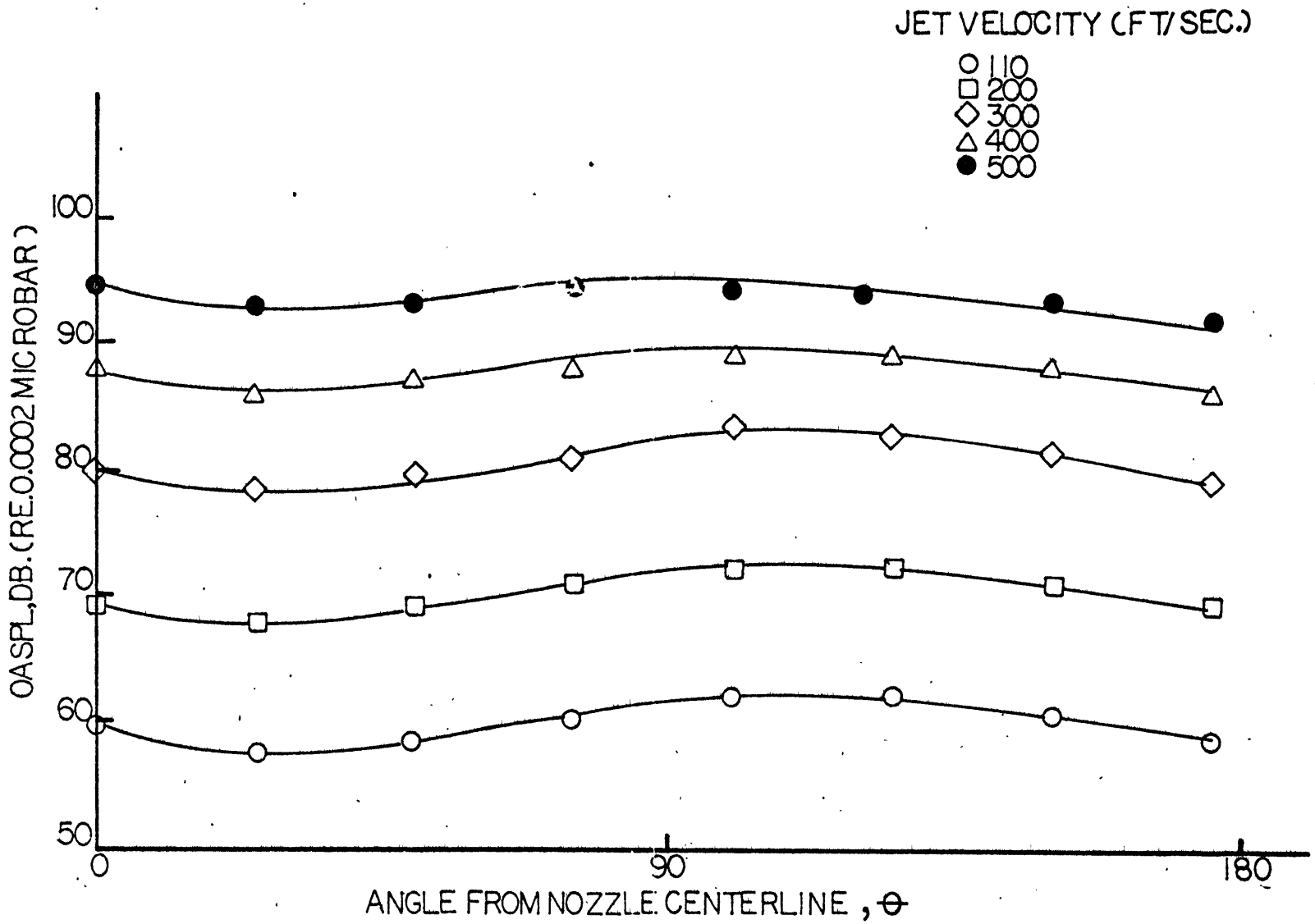

FIGURE 38. Effect of Jet Exhaust Velocity on the OASPL for the Modified Externally Blown Flap with a 30°-55° Flap Angle. Microphone Position; ϕ = 0°, R = 63.5 inches.

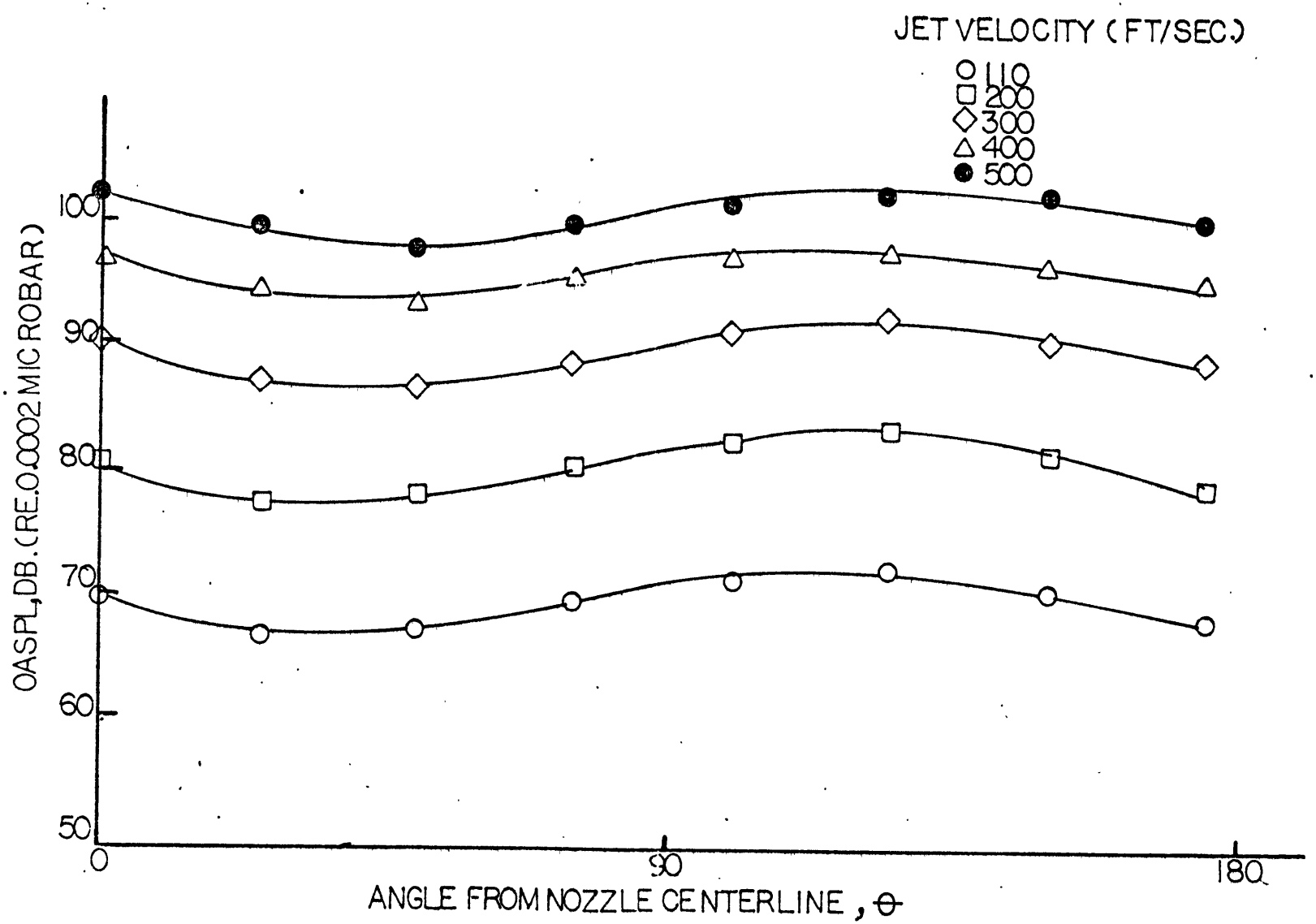

FIGURE 39. Effect of Jet Exhaust Velocity on the OASPL for the Modified Externally Blown Flap with a 45°-70° Flap Angle. Microphone Position; ϕ = 0°, R = 63.5 inches.

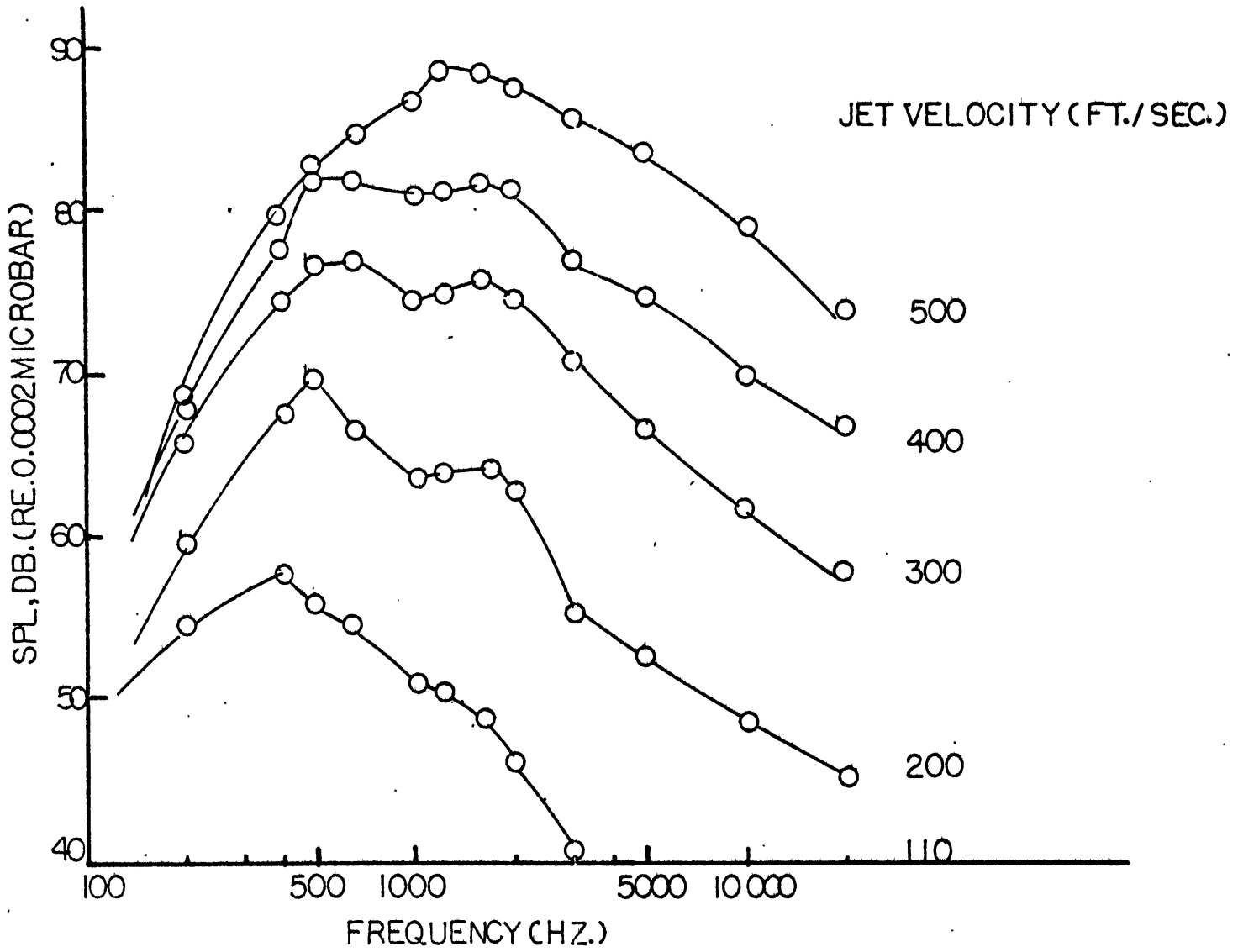

FIGURE 40. One-third Octave Noise Spectra for the Modified Externally Blown Flap at a 10°-20° Flap Angle. Microphone Position; θ = 90°, R = 63.5 inches, ϕ = 0°.

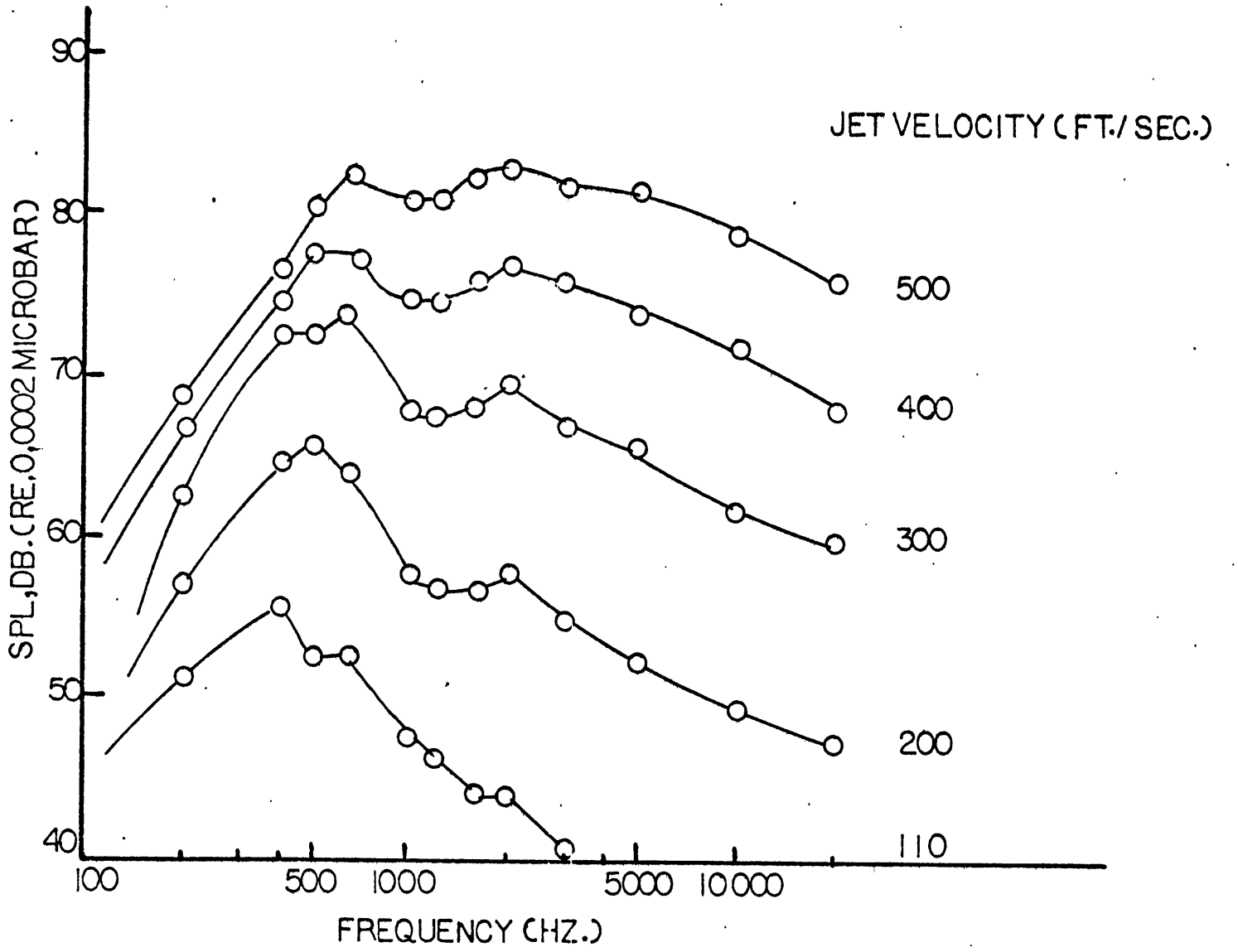

FIGURE 41. One-third Octave Noise Spectra for the Modified Externally Blown Flap at a 30°-55° Flap Angle. Microphone Position; θ = 90°, ϕ = 0°, R = 63.5 inches.

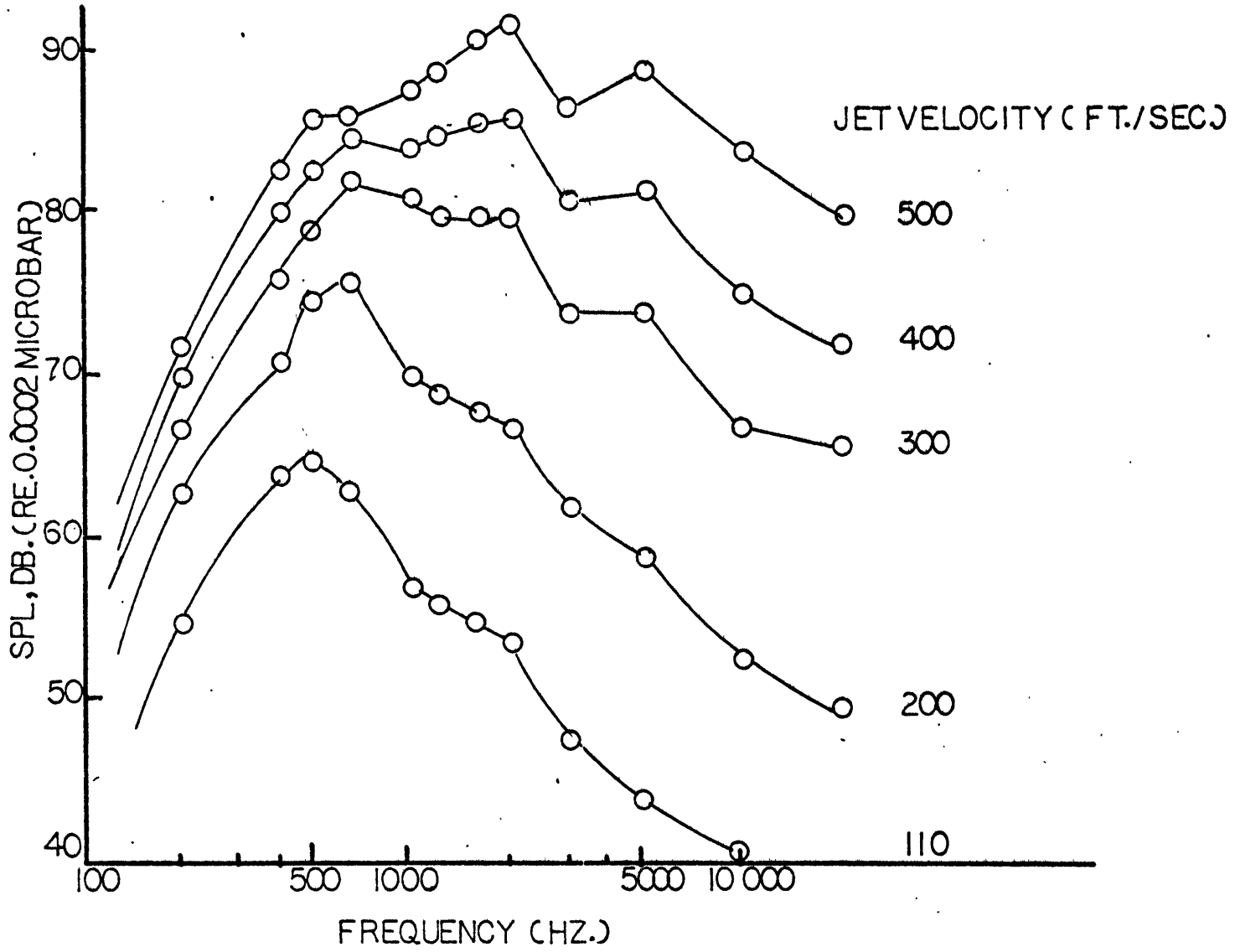

FIGURE 42. One-third Octave Noise Spectra for the Modified Externally Blown Flap at a 45°-70° Flap Angle. Microphone Position; θ = 90°, ϕ = 0°, R = 63.3 inches.

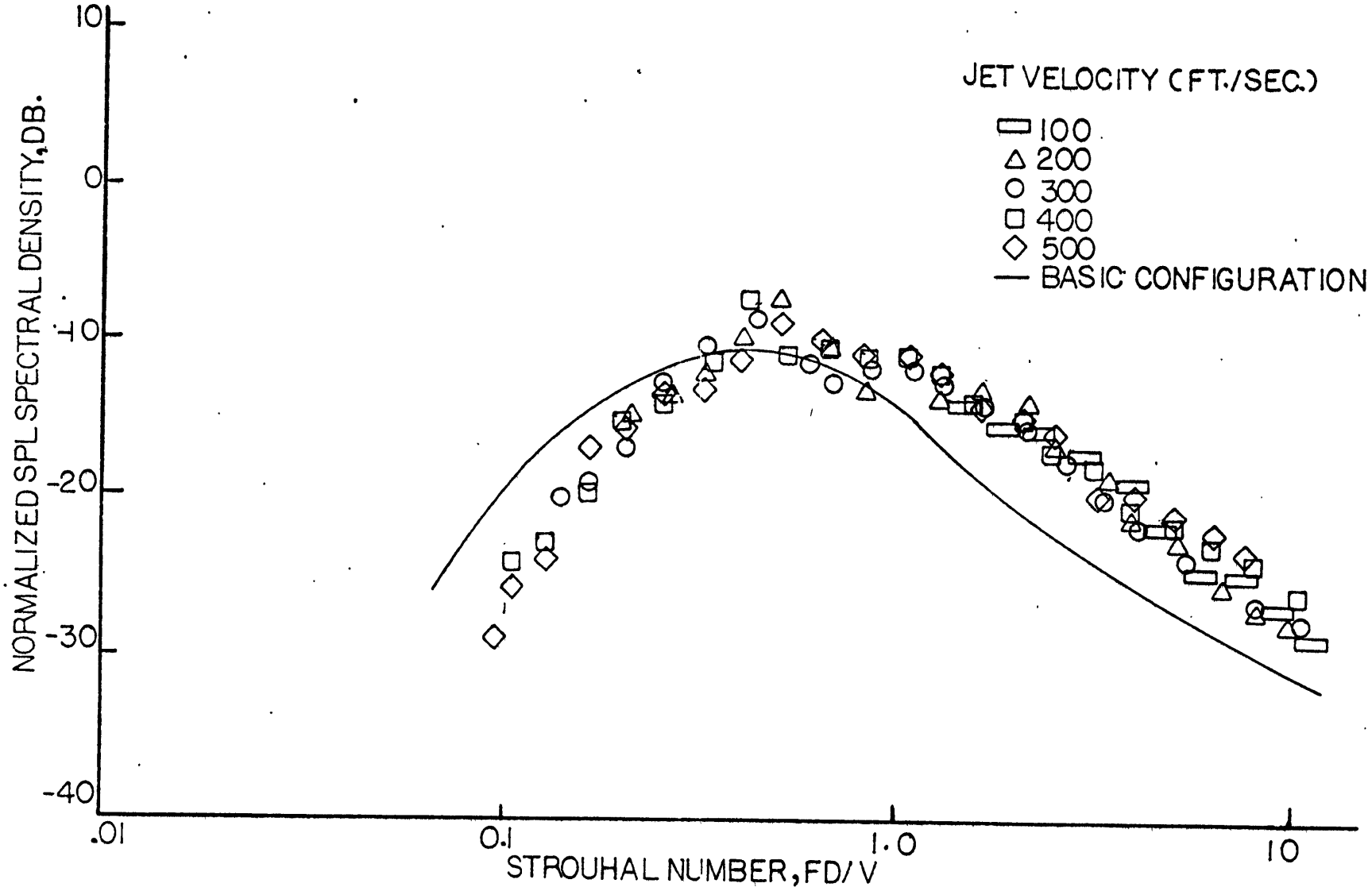

FIGURE 43. Normalized SPL Spectral Density Curve for the Noise Generated by the Modified Configuration at 10°-20° Flap Angle. Microphone Position; R = 63.5 inches, ϕ = 0°, θ = 90°.

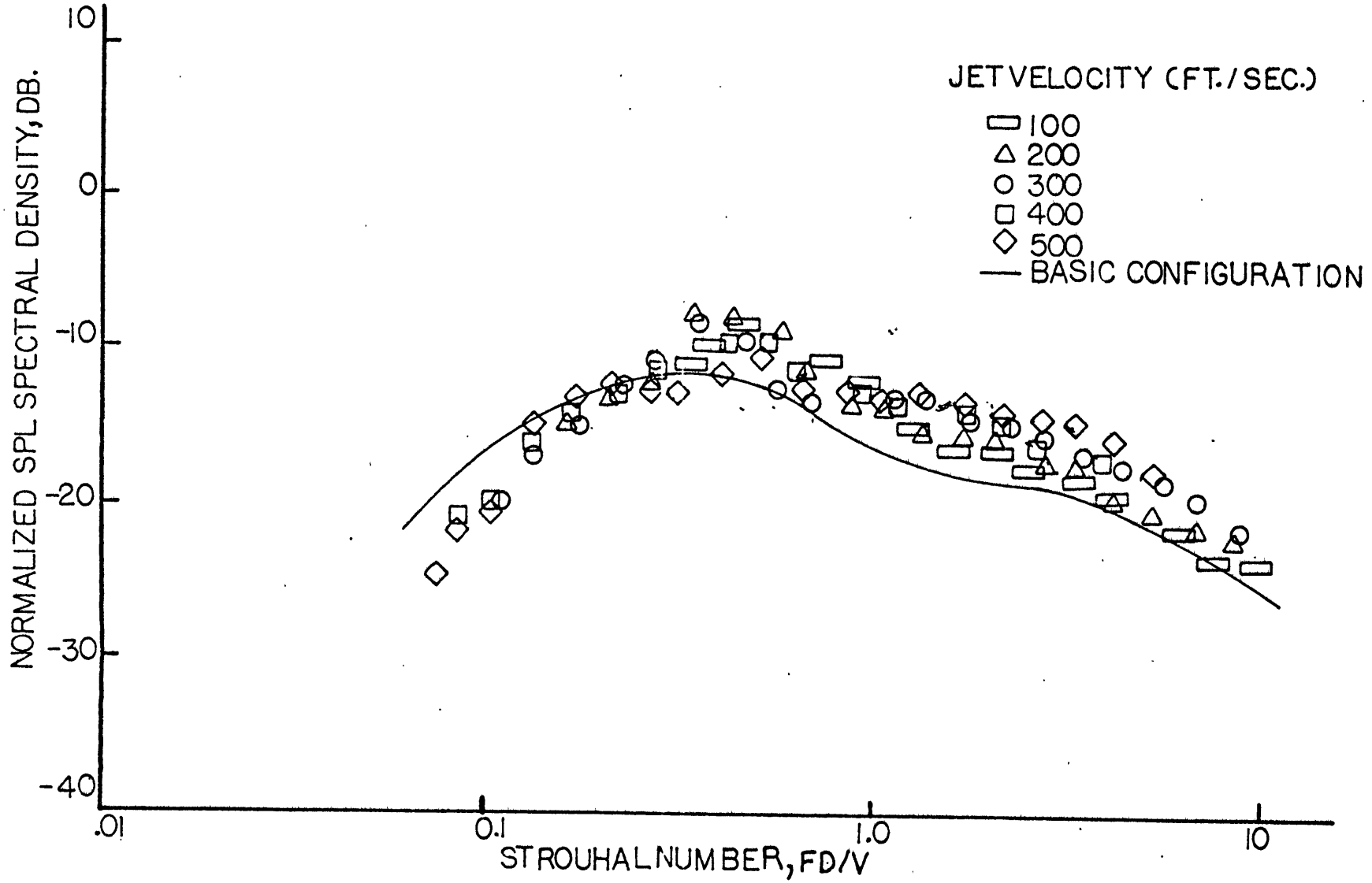

FIGURE 44. Normalized SPL Spectral Density Curve for the Noise Generated by the Modified Configuration at 30°-55° Flap Angle. Microphone Position: R = 63.5 inches, ϕ = 0°, θ = 90°.

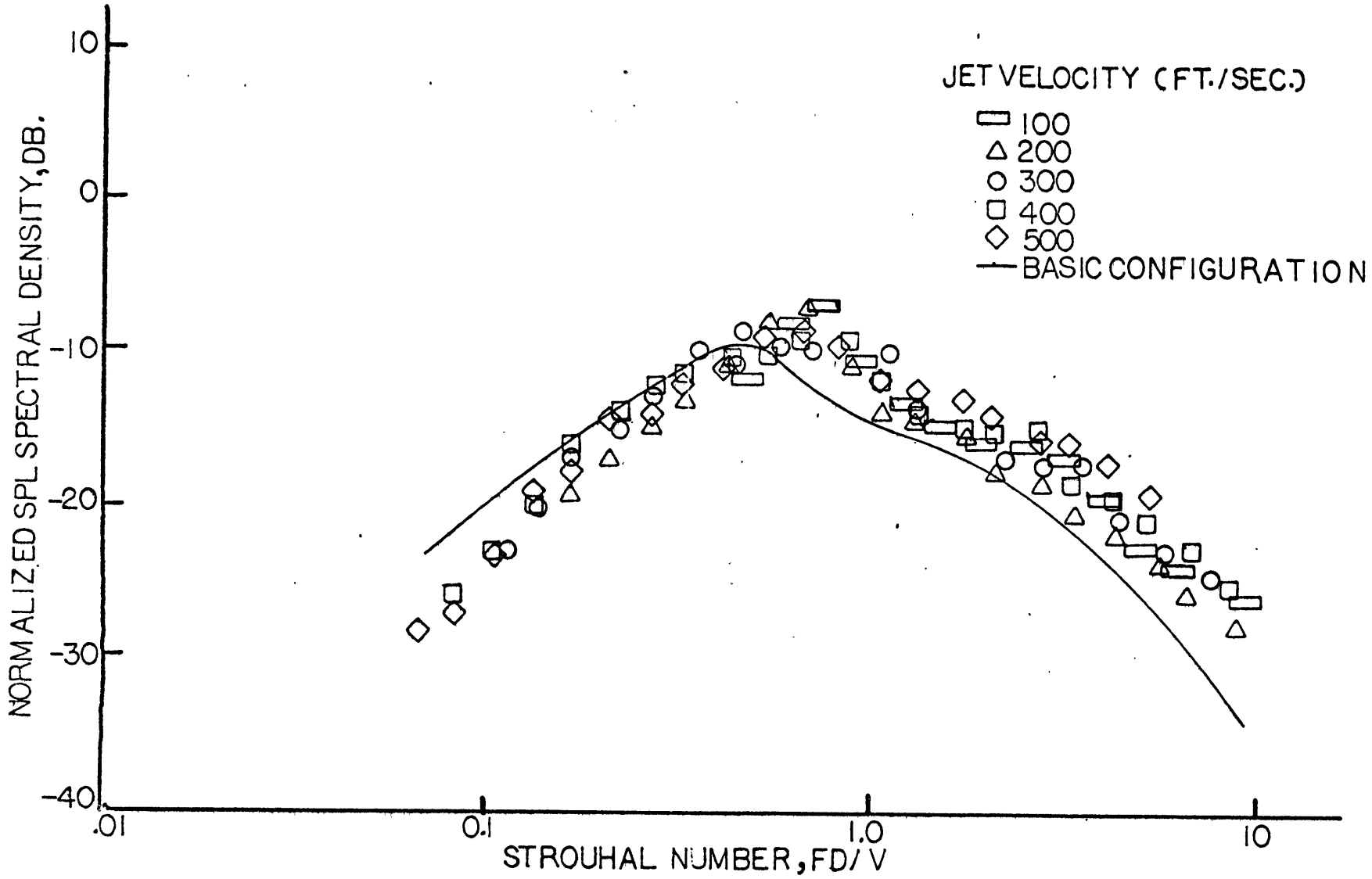

FIGURE 45. Normalized SPL Spectral Density Curve for the Noise Generated by the Modified Configuration at 45°- 70° Flap Angle. Microphone Position; R = 63.5 inches, ϕ = 0°, θ = 90°.

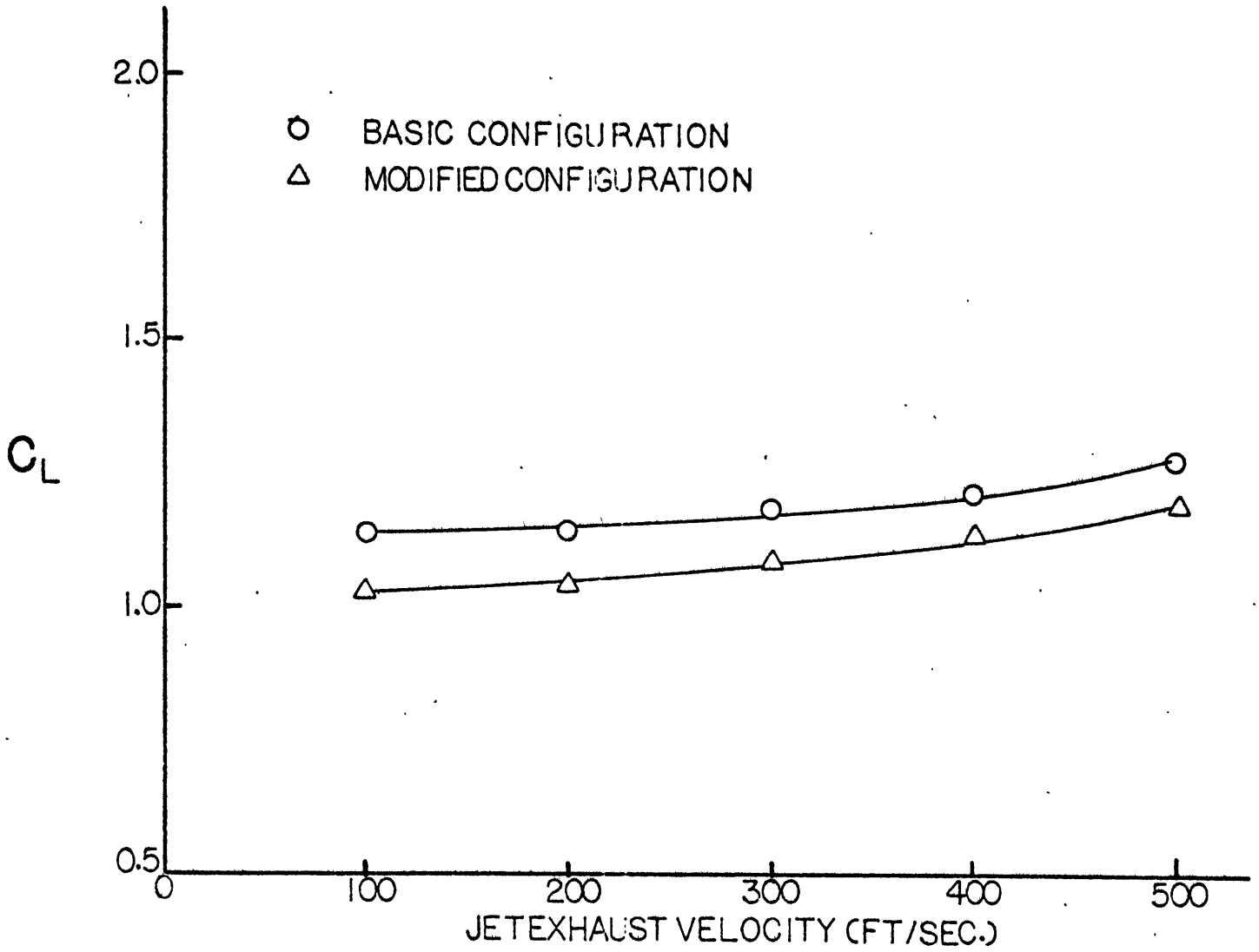

FIGURE 46. Lift Coefficient as a Function of Blowing Velocity for the 10°-20° Flap Angle.

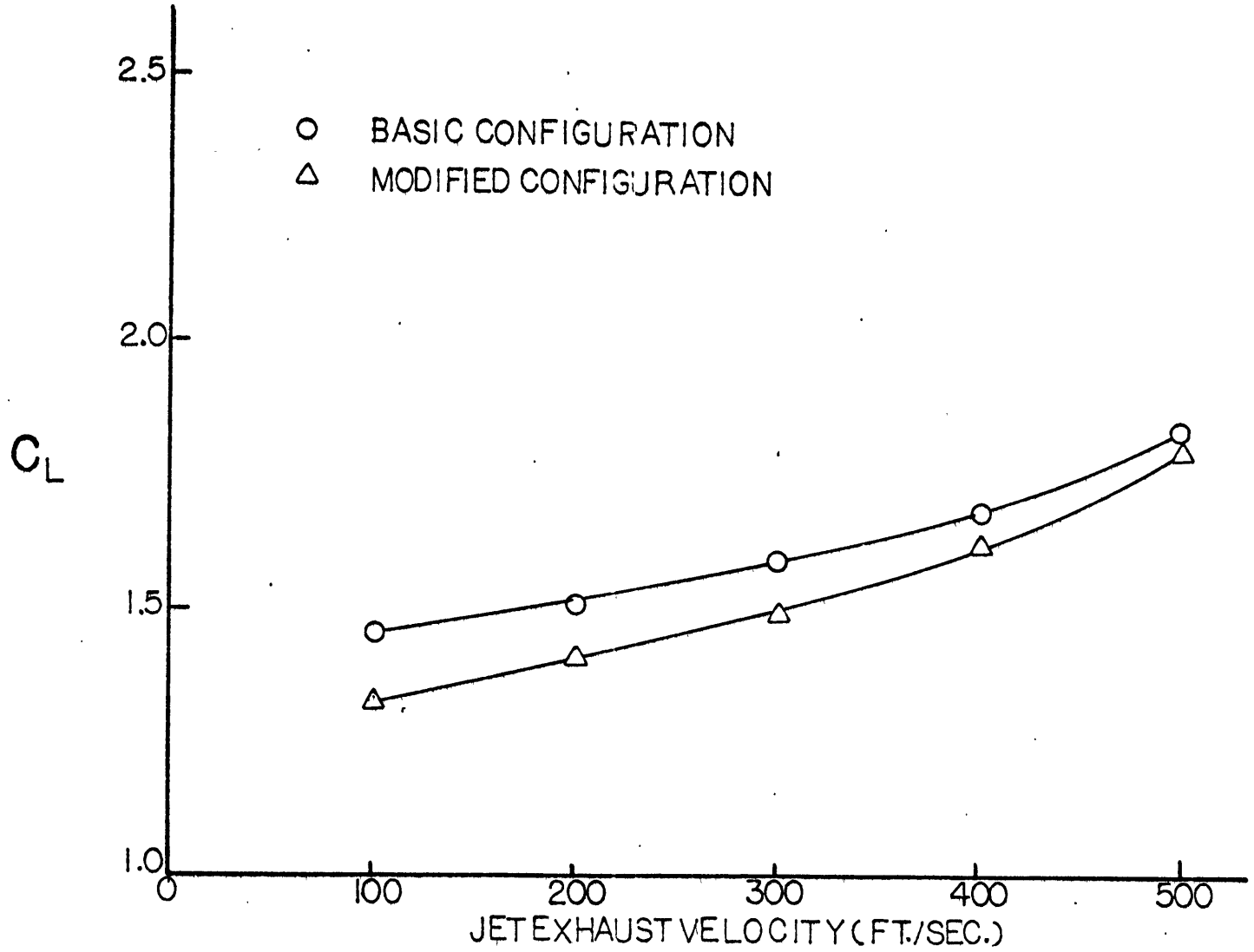

FIGURE 47. Lift Coefficient as a Function of Blowing Velocity for the 30°-55° Flap Angle

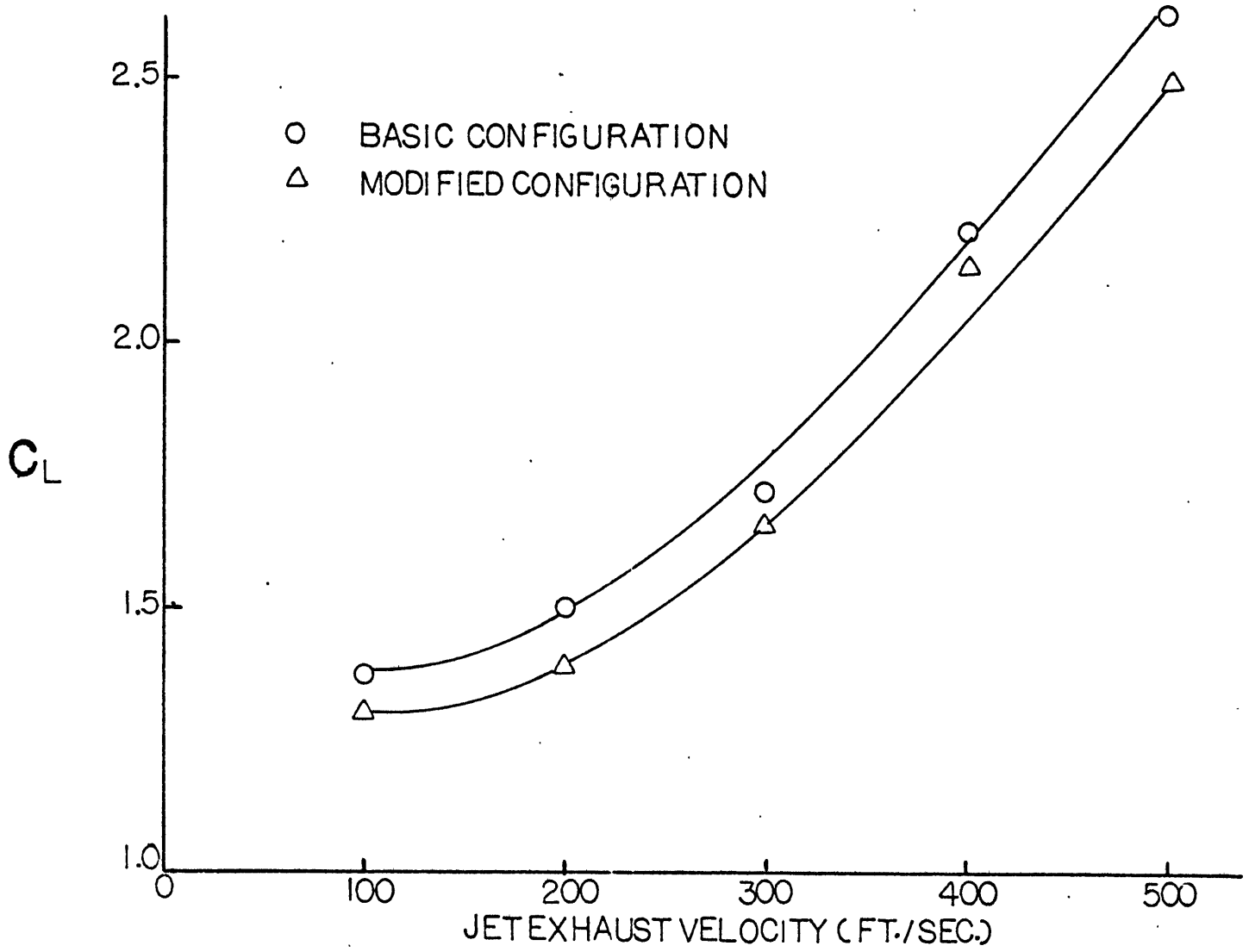

FIGURE 48. Lift Coefficient as a Function of Blowing Velocity for the 45°-70° Flap Angle.

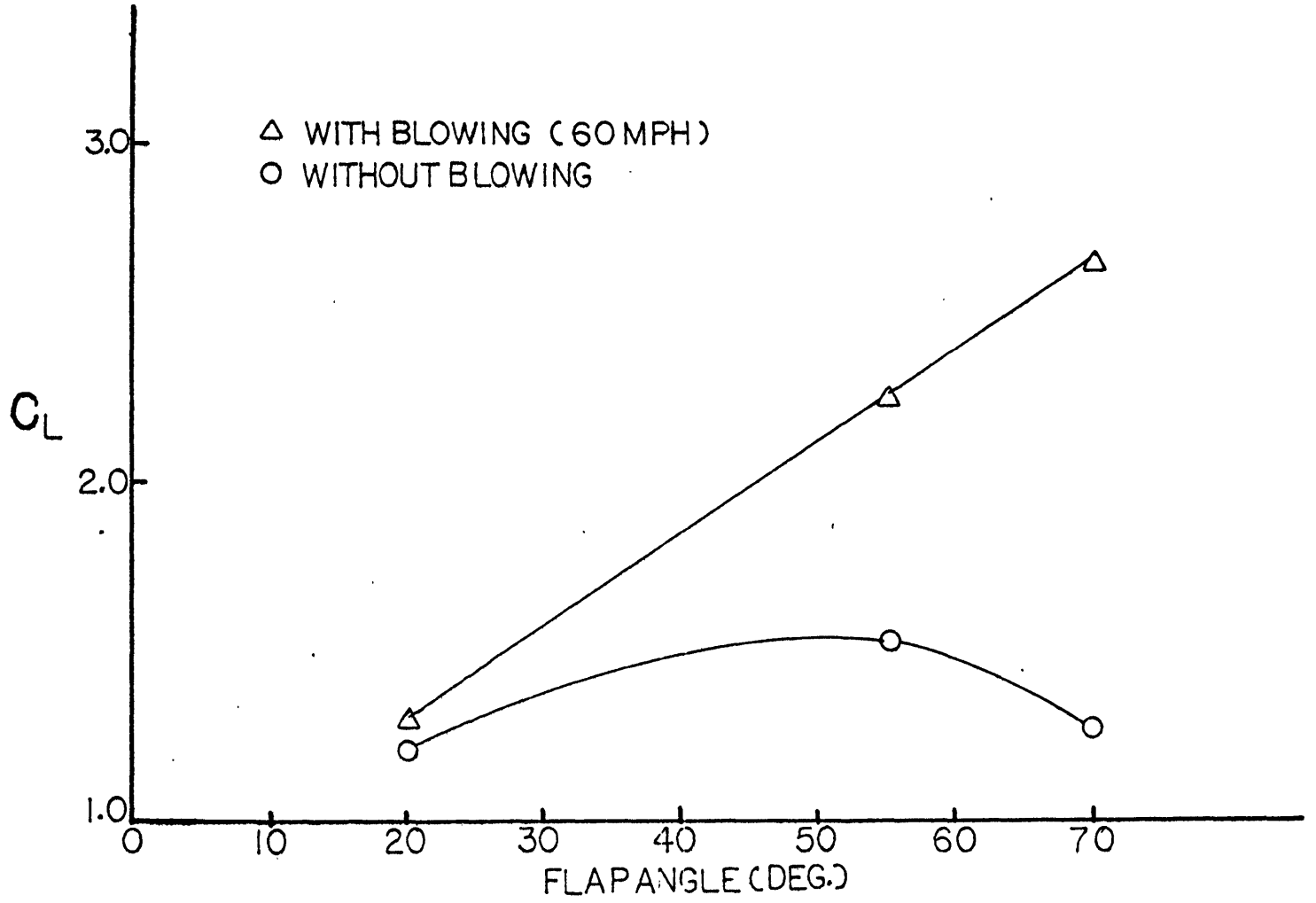

FIGURE 49. Comparison of Lift on a Externally Blown Flap with and without a Blowing Velocity of 500ft./sec. Tunnels Speed 60 MPH.

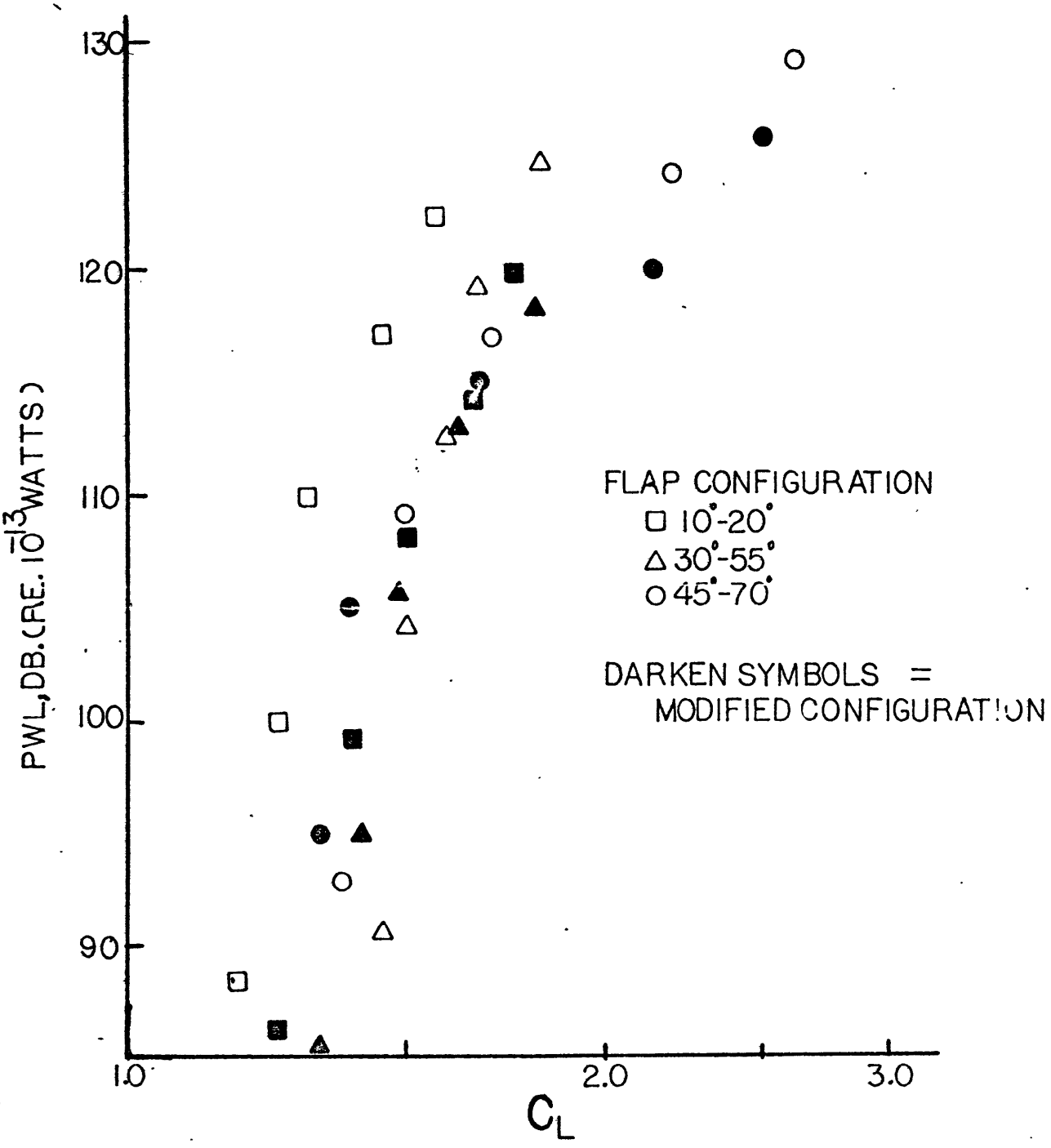

FIGURE 50. Correlation between Lift and Radiated Sound Power Level.

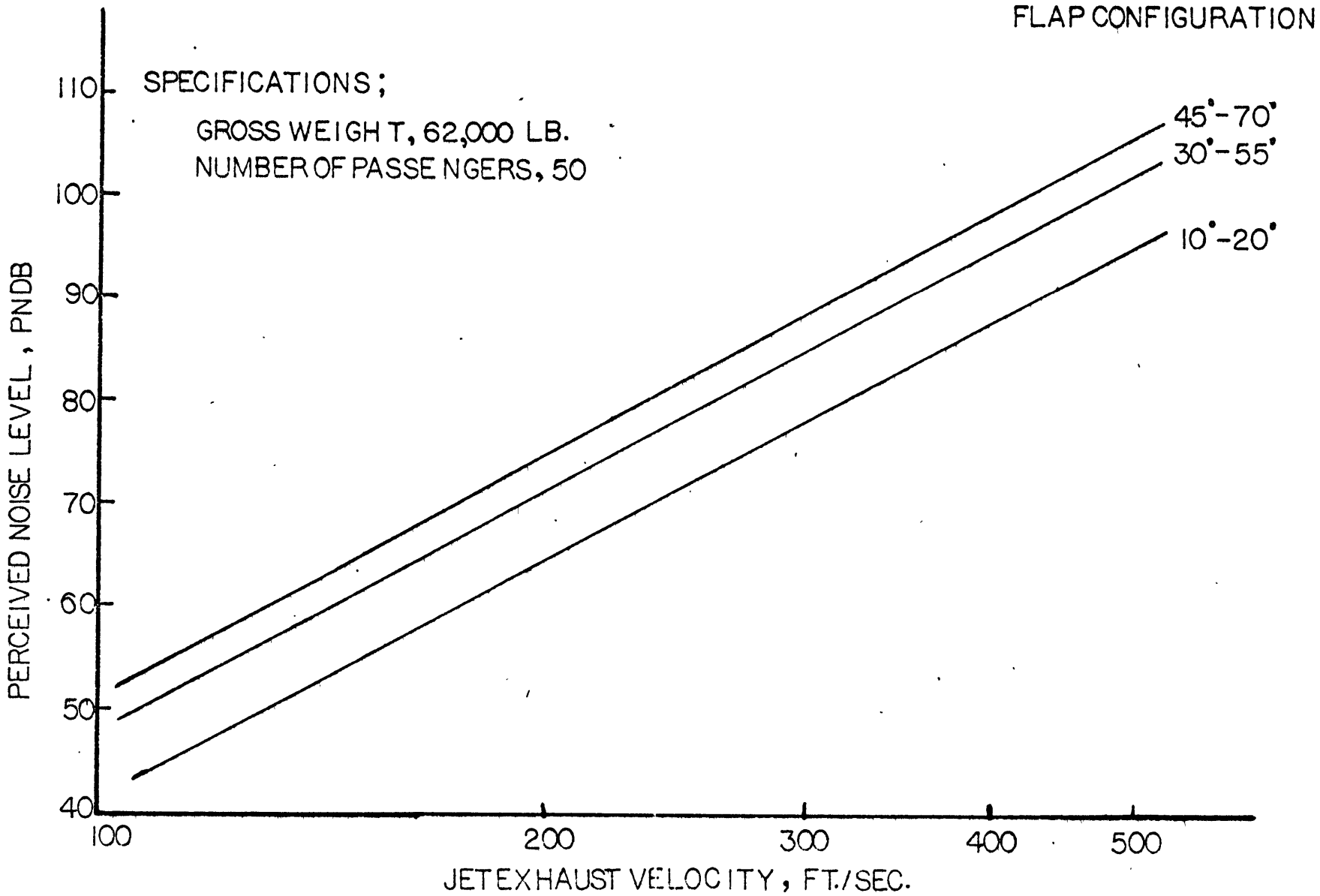

FIGURE 51. Perceived Noise Level as a Function of Jet Velocity for a 500 foot Flyover.

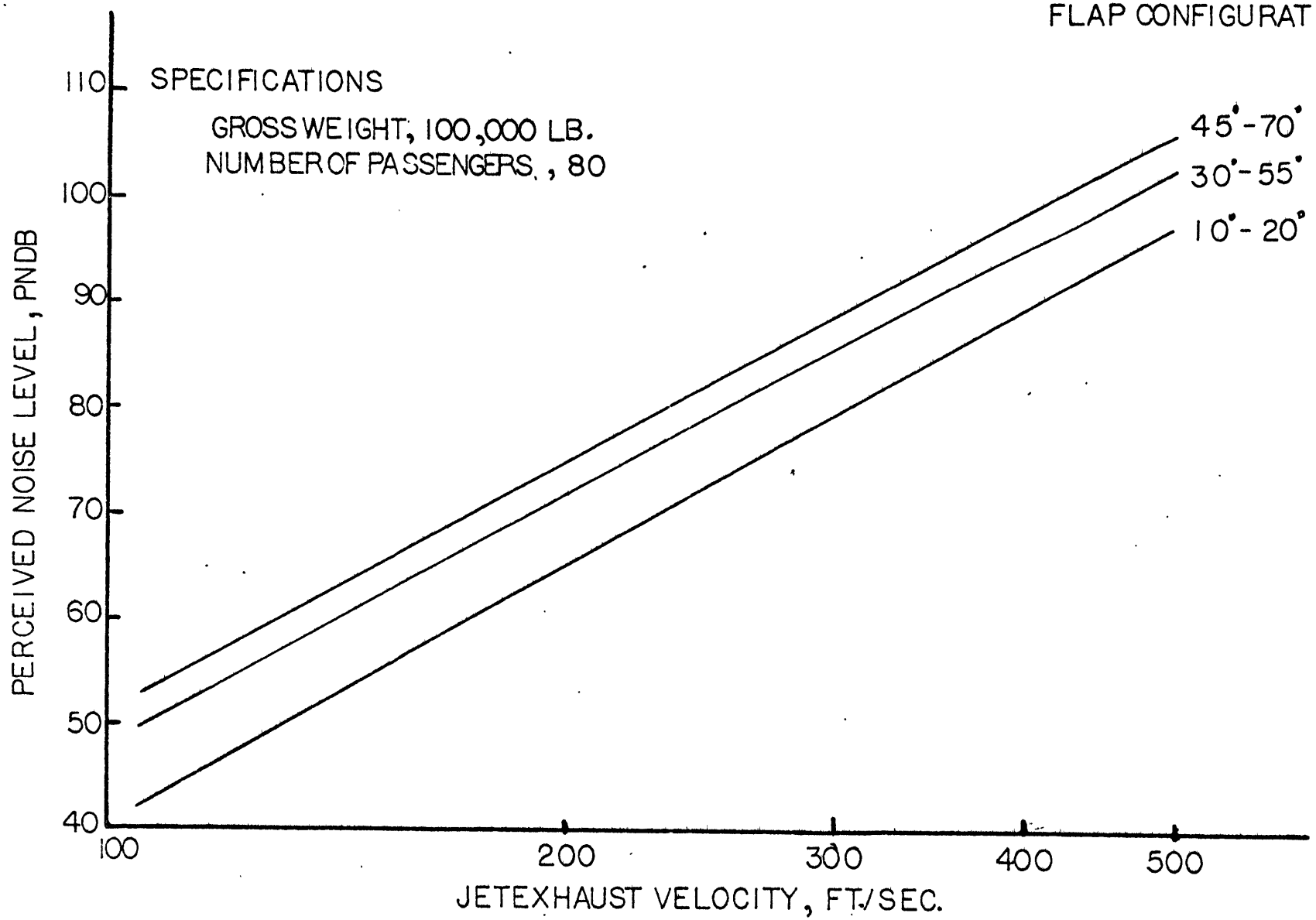

FIGURE 52. Perceived Noise Level as a Function of Jet Velocity for a 500 foot Flyover.

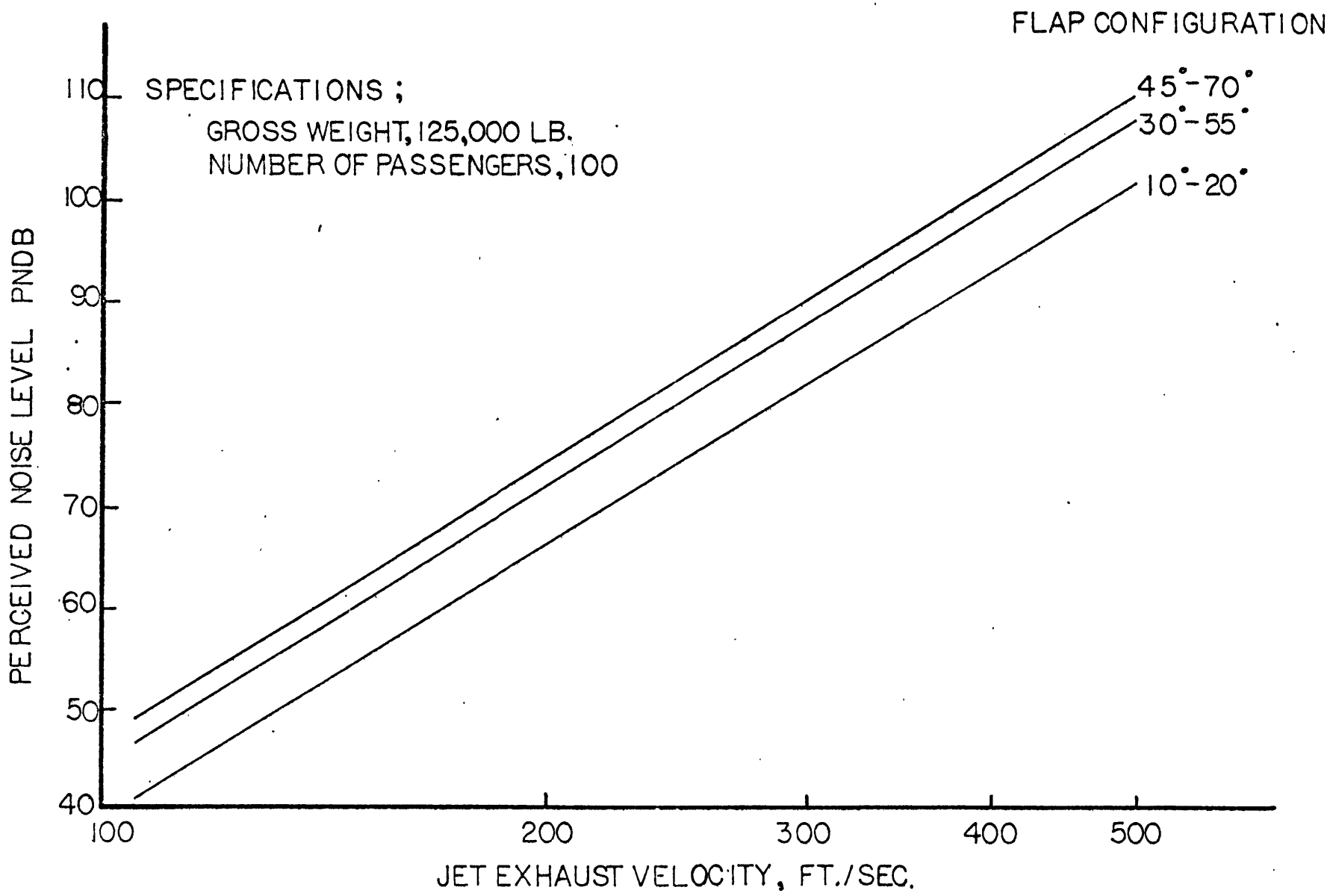

FIGURE 53. Perceived Noise Level as a Function of Jet Velocity for a 500 foot Flyover.

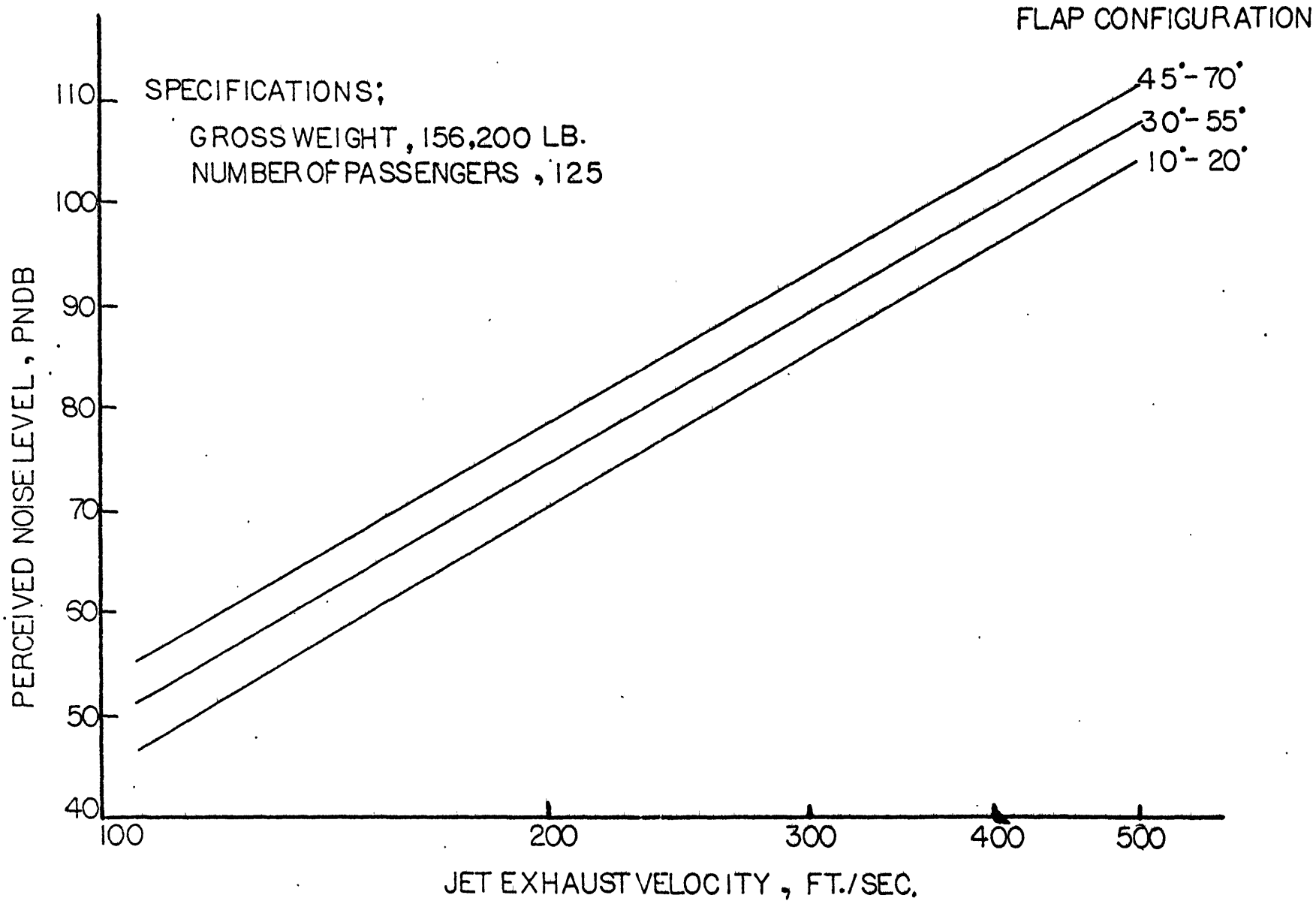

FIGURE 54. Perceived Noise Level as a Function of Jet Velocity for a 500 foot Flyover.

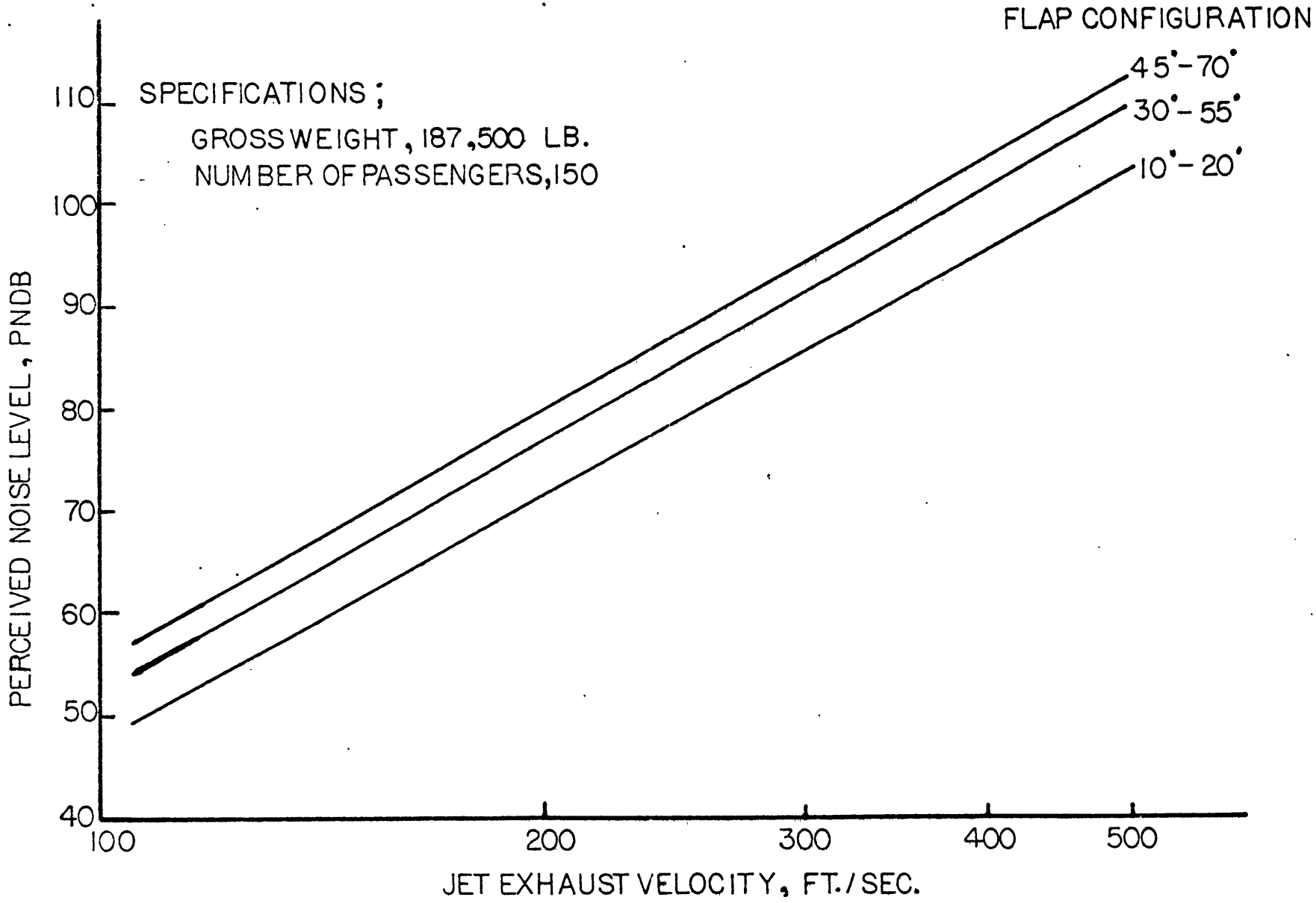

FIGURE 55. Perceived Noise Level as a Function of Jet Velocity for a 500 foot Flyover.

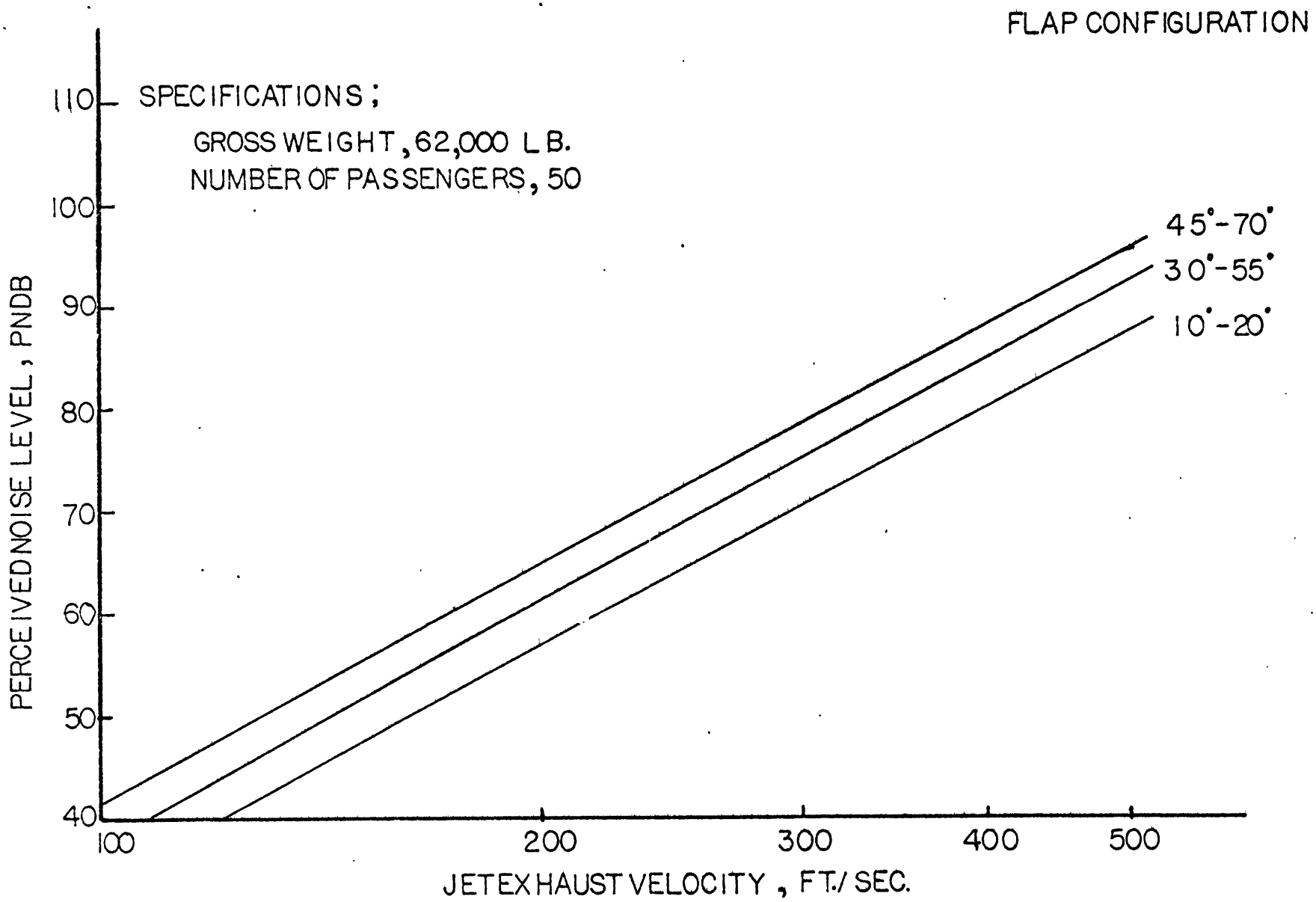

FIGURE 56. Perceived Noise Level at a 500 foot sideline as a Function of jet Exhaust Velocity.

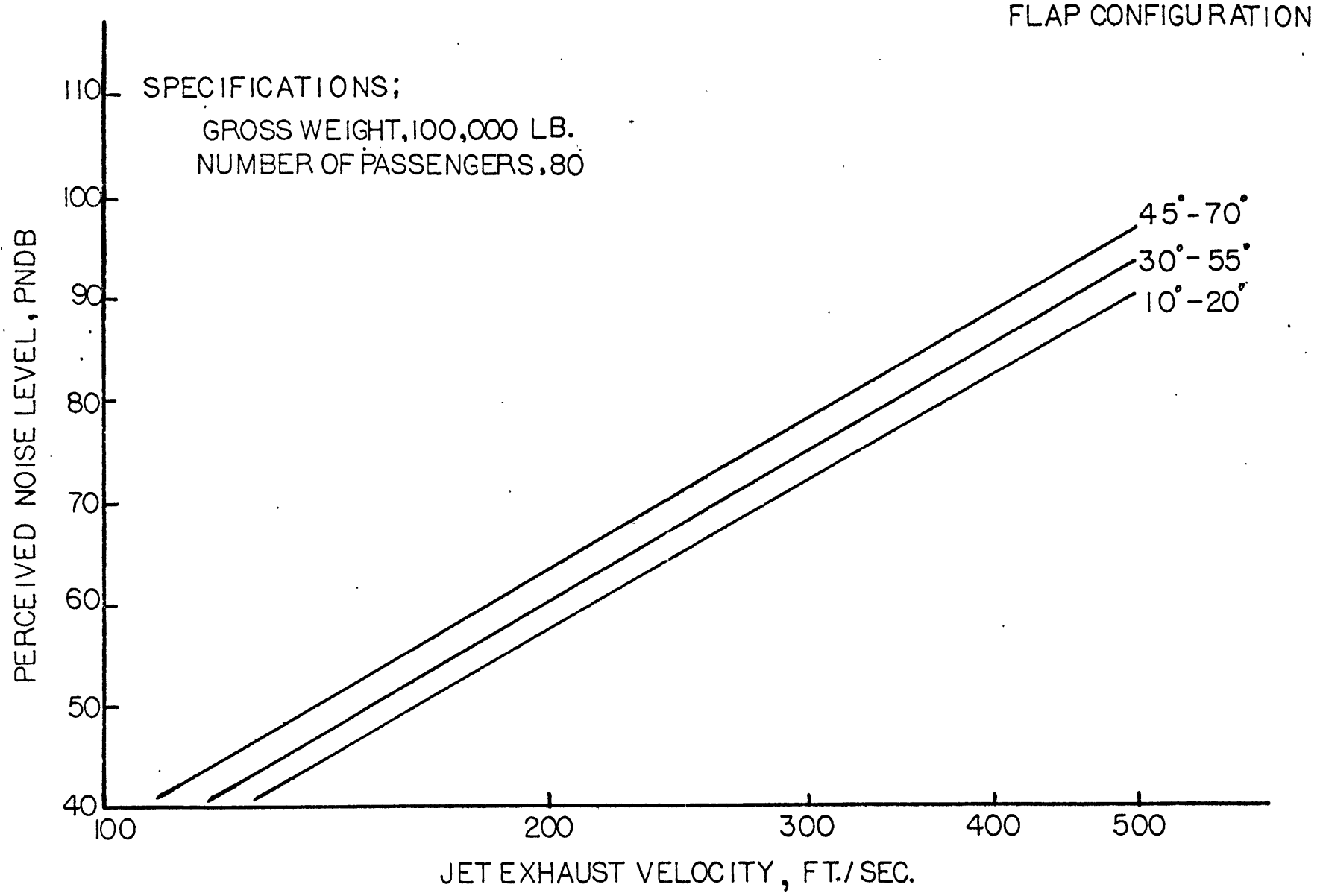

FIGURE 57. Perceived Noise Level as a Function of Jet Exhaust Velocity at a 500 foot Sideline.

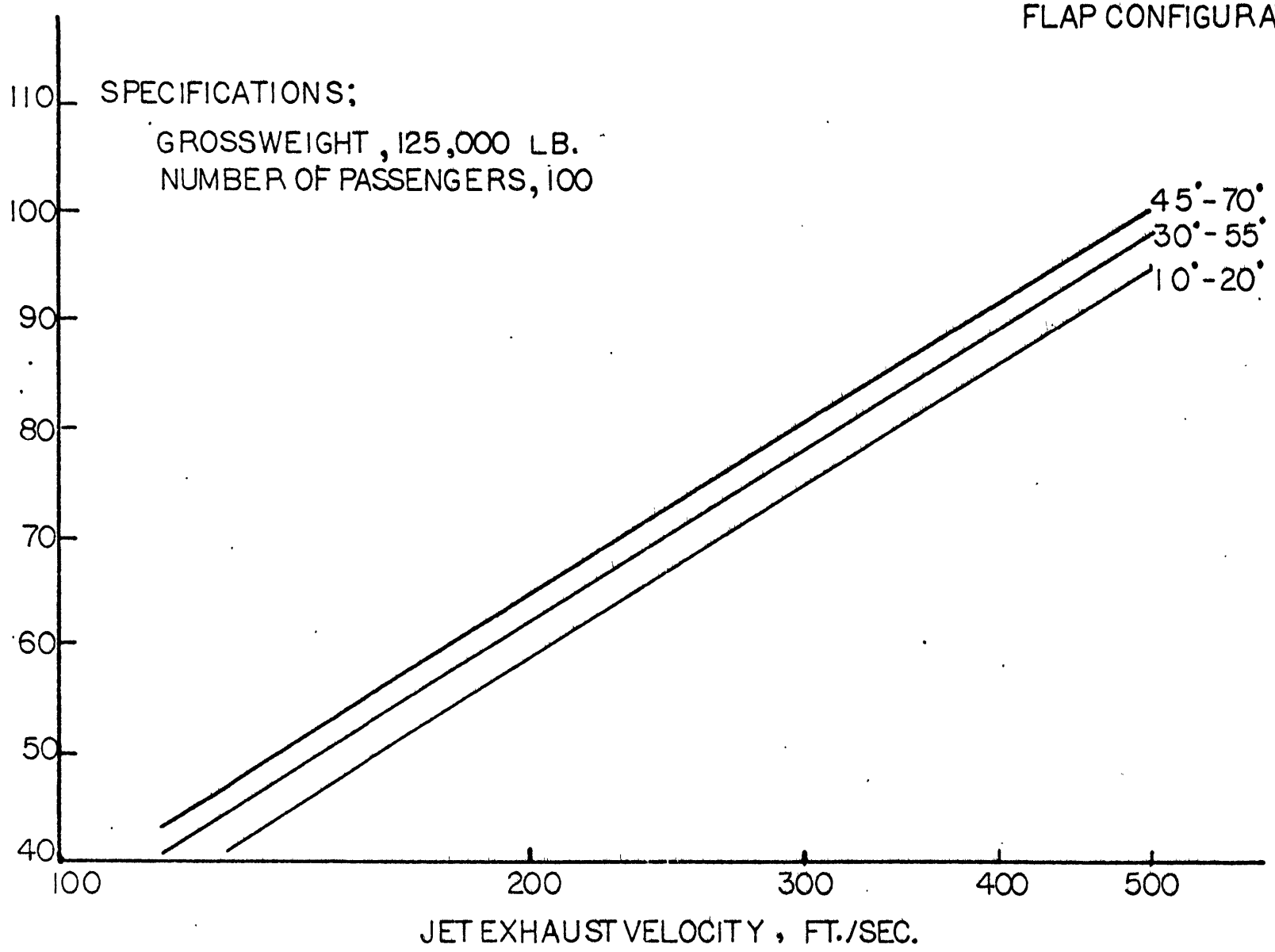

FIGURE 58. Perceived Noise Level as a Function of Jet Exhaust Velocity at a 500 foot Sideline.

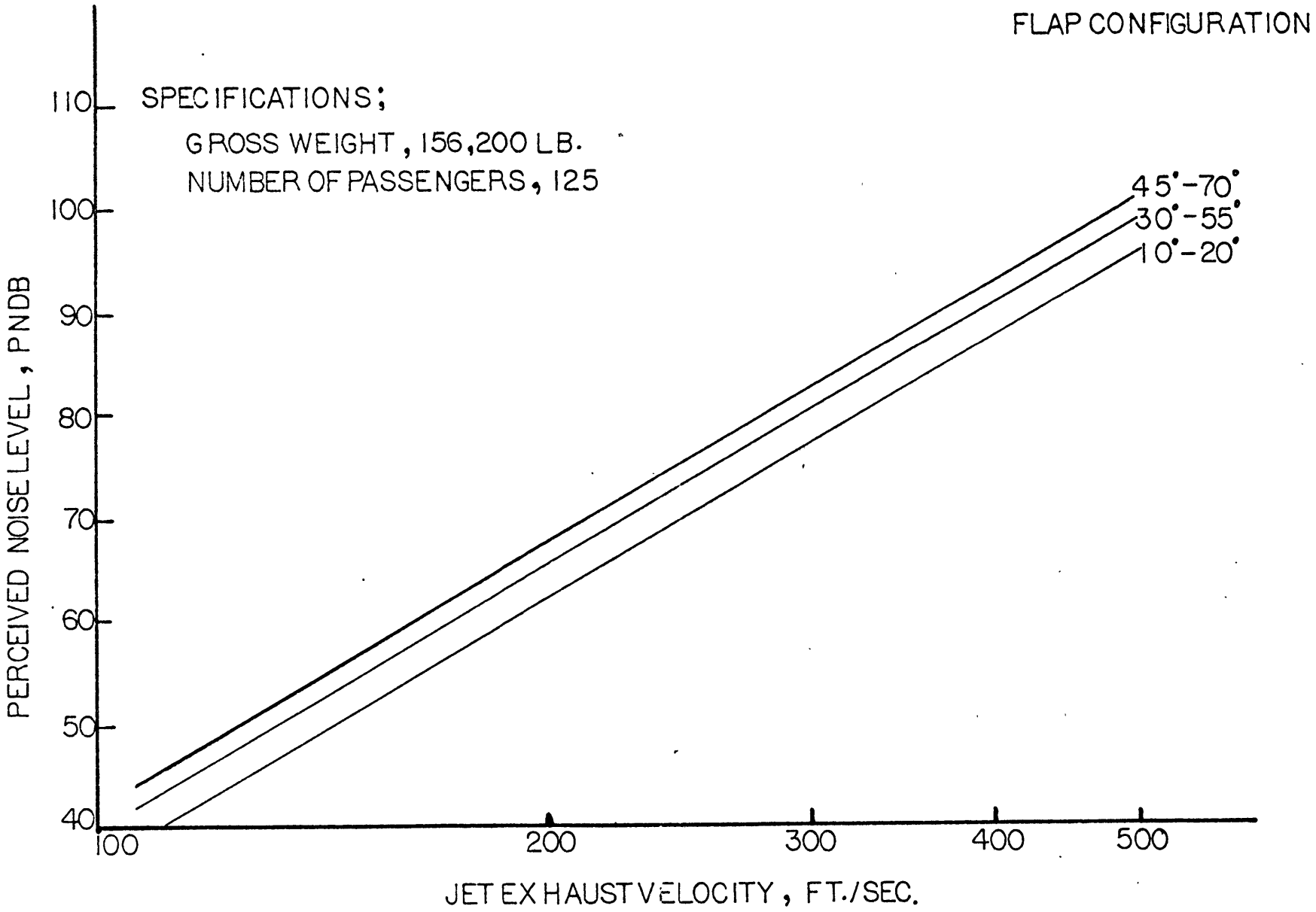

FIGURE 59. Perceived Noise Level as a Function of Jet Exhaust Velocity at a 500 foot Sideline.

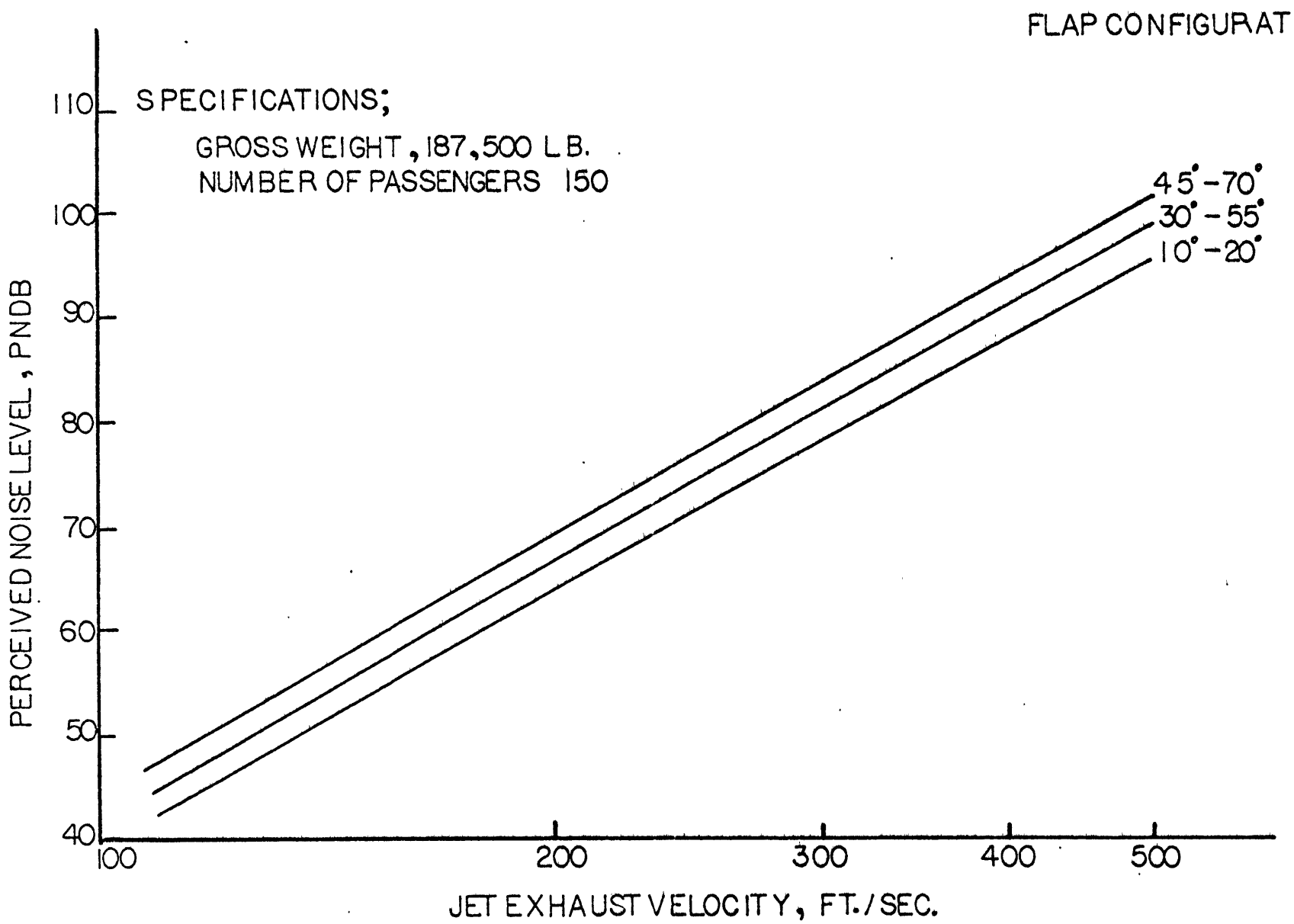

FIGURE 60. Perceived Noise Level as a Function of Jet Exhaust Velocity at a 500 foot Sideline.

REFERENCES

1. Lighthill, M. J. "On Sound Generated Aerodynamically I, General Theory" Proceedings of the Royal Society (London), Volume 211A, pp. 564-587, (1952).

2. Curle, N. "The Influence of Solid Boundaries Upon Aerodynamic Sound", Proceedings of the Royal Society (London), Volume 231A, pp. 505-514, (1955).

3. Dorsch, R. G., Krejsa, E., and Olsen, W. A., "Blown Flap Noise Research", American Institute of Aeronautics and Astronautics Paper No. 71-745, (June, 1971).

4. Olsen, W. A., Dorsch, R. G., and Miles, J. H. "Noise Production by A Small-Scale, Externally Blown Flap", National Aeronautics and Space Administration Technical Note D-6636 (March, 1972).

5. Dorsch, R. G., Kreim, W. J., and Olsen, W. A., "Externally Blown Flap Noise", American Institute of Aeronautics and Astronautics Paper Number 72-129, (January, 1972).

6. Rosen, G., "An Engine for Quiet STOL Propulsion", Journal of the American Institute of Aeronautics and Astronautics (December, 1971).

7. Granger, T. G., "Results of Prop-Fan/STOL Wing Acoustics Tests", National Aeronautics and Space Administration CR111956, (July, 1971).

8. Parlett, L., Fink, M., Freeman, D., "Wind Tunnel Investigation of a Larger Jet Transport Model Equipped with an External-Flow Jet Flap", National Aeronautics and Space Administration Technical Note D-4928, (December, 1968).

9. Vogler, R., "Wind Tunnel Investigation of a Four-Engine Externally Blowing Jet-Flap STOL Airplane Model", National Aeronautics and Space Administration Technical Note D-7034, (December, 1970).

10. Beranek, L. L., "Noise Reduction" (Chapters 3 and 7), McGraw-Hill Book Co., Inc., (1960).

11. Gordon, C. G., and Maidanik, G., "Influence of Upstream Flow Discontinuities On the Acoustic Power Radiated by a Model Air Jet", National Aeronautics and Space Administration Contractor Report 679, (January, 1967).

12. Widnall, S. E., "Helicopter Noise Due to Blade/Vortex Interaction", The Journal of the Acoustic Society of American Volume 50 No. 1, (1971).